3900 CSL

300: NO SUBJECT
INVENTION NOTED
DATE: LAW
30 Mar 64

300 RH

[redacted]

Coordinated Science Laboratory

UNIVERSITY OF ILLINOIS – URBANA, ILLINOIS

NONLINEAR OSCILLATIONS IN A SECOND ORDER SYSTEM

Peter James Ponzo

REPORT R-193 **JANUARY, 1964**

COORDINATED SCIENCE LABORATORY
UNIVERSITY OF ILLINOIS
URBANA, ILLINOIS

Contract DA-36-039-AMC 02208(E)
DA Project 3A-99-25-004

The research reported in this document was made possible by support extended to the University of Illinois, Coordinated Science Laboratory, jointly by the Department of the Army, Department of the Navy (Office of Naval Research), and the Department of the Air Force (Office of Scientific Research) under Department of Army Contract DA-36-039-AMC 02208(E).

Report R-193: Nonlinear Oscillations in a Second Order System

ERRATA

Page	Line	Should Read:
1	19	$F(x(\tau), \dot{x}(\tau), \tau)$
18	14	$y > F(-a)$
18	22	$y > F(-a)$
20	16	$A^{+} = \max(x_p(t))$
20	21	$B = \frac{7}{4}(\cdots)$
27	1	$F(b) - y_o$
27	17	$(g(b)/(f'(b))^2)^{1/3}$
46	23	Figure 21
89	5	$2\eta\dot{\eta}$
95	16-17	$y^2(B') - y^2(A') < y^2(B) - y^2(A).$
96	14	omit line 14
96	16	$y^2(B'') - y^2(A'') < y^2(B) - y^2(A)$
96	21	$y^2(B'') - y^2(A'') = y^2(B) - y^2(A)$

NONLINEAR OSCILLATIONS IN A SECOND ORDER SYSTEM

Peter James Ponzo, Ph.D.
Department of Electrical Engineering
University of Illinois, 1964

ABSTRACT

Relaxation oscillations as described by the equation $\ddot{x} + \mu f(x)\dot{x} + g(x) = 0$, $\mu \gg 1$, are investigated in the plane defined by $\dot{x} = \mu(y - F(x))$, $\mu\dot{y} = -g(x)$ where $F(x) = \int_0^x f(u)du$. A number of analytic curves are obtained which serve as upper and lower bounds on solution trajectories in this plane. In many cases, piecewise connection of such bounding curves provide annular regions within which periodic orbits lie. The number, location, stability and amplitude bounds of periodic solutions may be determined in this manner. When the method is applied to the equation of van der Pol, the upper and lower bounds obtained for the amplitude of the unique periodic solutions compare favourably with the known asymptotic expansion of the amplitude in terms of μ.

Forced oscillations described by the equation $\ddot{x} + \mu f(x)\dot{x} + g(x) = p(t)$, $\mu \gg 1$, are investigated in the plane defined by $\dot{x} = \mu(y - F(x)) + P(t)$, $\mu\dot{y} = -g(x)$, where $P(t) = \int^t p(\tau)d\tau$ is bounded for all t. It is found that forced solution trajectories may be confined to lie between the trajectories of two associated autonomous systems. In some cases, both associated systems admit periodic orbits whose limit cycles serve to define the boundaries of annular regions in the plane. These annuli, when they exist, confine forced trajectories in their interior. Some of the analytic properties of such confined trajectories are discussed and numerical solutions presented.

ACKNOWLEDGMENT

The author wishes to thank Dr. Nelson Wax for his constant guidance and stimulation during the course of this investigation. Thanks, too, go to Dr. Richard M. Brown for making the computer so readily available.

TABLE OF CONTENTS

		Page
CHAPTER I.	Introduction	1
CHAPTER II.	Free Oscillations in a Second Order System	9
	2.1 Introduction	9
	2.2 The van der Pol Type of Equation	11
	2.3 The Inner Boundary	13
	2.4 The Outer Boundary	21
	2.5 Generalizations	28
	2.6 Summary	30
CHAPTER III.	Forced Oscillations in a Second Order System	41
	3.1 Introduction	41
	3.2 The First Auxiliary System (FAS)	43
	3.3 The Second Auxiliary System (SAS)	48
	3.4 General Systems	50
	3.5 Some Properties of Solutions within an Annulus	53
	3.6 Summary	59
CHAPTER IV.	Numerical Results	70
	4.1 Introduction	70
	4.2 Numerical Solutions	70
	4.3 Conclusions	72
APPENDIX		82
BIBLIOGRAPHY		99

CHAPTER I

INTRODUCTION

We are concerned in this study with the equation

$$\ddot{x} + f(x)\dot{x} + g(x) = p(t), \tag{1.1}$$

where $(\cdot) = d/dt$ and $f(x)$, $g(x)$, $p(t)$ are sufficiently smooth to guarantee the existence and uniqueness of a solution with prescribed initial conditions.

By far the largest part of the literature on nonlinear differential equations is devoted to quasi-linear, conservative systems described by the equation

$$\ddot{x} + \omega^2 x = \varepsilon F(x,\dot{x},t) \tag{1.2}$$

where ε, a small parameter, is a measure of the degree of nonlinearity. For such equations, methods of solution involving successive approximations have been employed with considerable success. We will briefly describe some of the analytical tools available for the approximate integration of (1.2), where ε is small. For $\varepsilon = 0$ the equation is linear and a solution $x_o(t) = a \cos(\omega t + \theta)$ exists, where a, θ are constants. For $\varepsilon \neq 0$, but small, one supposes that solutions differ little from $x_o(t)$. To lend strength to this supposition we may rewrite (1.2) as an integral equation

$$x(t) = x_o(t) + \frac{\varepsilon}{\omega}\int_{t_o}^{t} F(x(\tau),\dot{x}(\tau)) \sin \omega(t-\tau)\, d\tau \tag{1.3}$$

or $x(t) = x_o(t) + \varepsilon z(t)$ where $x_o(t)$ is the solution to the linear equation with $\varepsilon = 0$, and $z(t)$ is the correction due to the nonlinearity.

Note that

$$z(t) = \frac{1}{\omega}\int_{t_o}^{t} F(x,\dot{x},\tau)\sin\omega(t-\tau)d\tau$$

satisfies $z(t_o) = \dot{z}(t_o) = 0$ so that the initial conditions prescribed for the solution to (1.2) or (1.3) are contained entirely in $x_o(t)$.

Poisson's method of solution involves direct substitution into (2) of the assumed power series solution $x = x_o + \epsilon z_1 + \epsilon^2 z_2 + \ldots$, and equating like powers of ϵ to obtain a set of linear equations which may be solved recursively for the unknown functions $z_1(t), z_2(t), \ldots$. Since the initial conditions are contained in $x_o(t)$, the $z_i(t)$ are required to satisfy $z_i(t_o) = \dot{z}_i(t_o) = 0$. In practice one usually considers only first or second order corrections to the approximate solution $x_o(t)$.

Although the solution obtained by Poisson's method is valid for $\epsilon(t - t_o)$ sufficiently small, the presence of terms such as $t \sin \omega t$, called secular terms, completely disguises the true nature of the solution. For example, bounded, periodic solutions may appear to be unbounded and nonperiodic.

The secular terms arise whenever "resonance" occurs. That is, in the equations for the $z_i(t)$, which take the form

$$\ddot{z}_i + \omega^2 z_i = G(x_o, z_1, z_2, \ldots, z_{i-1}, t),$$

the function G may contain a periodic term of frequency ω. Lindstedt's method was designed to avoid the secular terms which arise in this manner by admitting the possibility of a frequency correction to the generating solution $x_o(t)$. One then assumes a modified frequency $\Omega = \omega + \epsilon\omega_1 + \epsilon^2\omega_2 + \ldots$ where $\omega_1, \omega_2, \ldots$ are frequency corrections

to be determined. Setting $\Omega t = \theta$ in (1.2) and assuming a solution $x(\theta) = x_o(\theta) + \epsilon z_1(\theta) + \epsilon^2 z_2(\theta) + \ldots$ as before, one is able to eliminate the secular terms as they arise by a suitable choice of $\omega_1, \omega_2, \ldots$. Poincare has shown, however, that the solution series obtained may diverge in some cases.

Perhaps the most satisfactory method of treating quasi-linear, conservative systems analytically, is the method of variation of parameters used with great success by Krylov and Bogoliubov, and B. van der Pol. If the integral equation (1.3) is written in the form

$$x = a \cos \omega t + b \sin \omega t + \frac{\epsilon}{\omega} \int_{t_o}^{t} F(x,\dot{x},\tau) \sin \omega (t - \tau) d\tau$$

and $\sin \omega(t - \tau)$ expanded; $\sin \omega(t - \tau) = \sin \omega t \cos \omega\tau - \cos \omega t \sin \omega\tau$, one obtains

$$x(t) = A(t) \cos \omega t + B(t) \sin \omega t \tag{1.4}$$

where

$$A(t) = a - \frac{\epsilon}{\omega} \int_{t_o}^{t} F(x,\dot{x},\tau) \sin \omega\tau d\tau$$

and

$$B(t) = b + \frac{\epsilon}{\omega} \int_{t_o}^{t} F(x,\dot{x},\tau) \cos \omega\tau \, d\tau .$$

Noting that $\dot{A} \cos \omega t + \dot{B} \sin \omega t = 0$, it is seen that

$$\dot{x} = -\omega A \sin \omega t + \omega B \cos \omega t. \tag{1.5}$$

Indeed, (1.4) and (1.5) alone will serve to define A(t) and B(t). This formulation, in terms of A(t), B(t), was used by van der Pol to discuss the forced oscillations of a triode oscillator.

The problem of solution then involves solving the following equations for the "slowly varying" quantities A(t) and B(t):

$$\dot{A}(t) = -\frac{\varepsilon}{\omega}F(A\cos\omega t + B\sin\omega t, -\omega A\sin\omega t + \omega B\cos\omega t, t)\sin\omega t$$
$$\dot{B}(t) = \frac{\varepsilon}{\omega}F(A\cos\omega t + B\sin\omega t, -\omega A\sin\omega t + \omega B\cos\omega t, t)\cos\omega t \tag{1.6}$$

Use is now made of the fact that $\dot{A}(t) = 0(\varepsilon)$ and $\dot{B}(t) = 0(\varepsilon)$, in the approximation called the "method of averaging". The right hand side of (1.6) are expanded in a Fourier series of the form

$$F\sin\omega t = F_o(A,B) + F_1(A,B)\cos\omega t + \ldots$$
$$F\cos\omega t = G_o(A,B) + G_1(A,B)\cos\omega t + \ldots$$

where

$$F_o(A,B) = \omega/2\pi\int_o^{2\pi/\omega} F\sin\omega\tau\, d\tau$$

and

$$G_o(A,B) = \omega/2\pi\int_o^{2\pi/\omega} F\cos\omega\tau\, d\tau.$$

In these expansions the Fourier coefficients are determined by integration over the explicit time, so that A, B are held constant during the integration. Observe then, that $F_o(A,B)$ and $G_o(A,B)$ are the result of "averaging" the right hand side of (1.6) over a time interval $2\pi/\omega$, during which A(t) and B(t) are assumed to remain constant. If these Fourier expansions are substituted into (1.6), and only the first terms retained, there results the "averaging equations":

$$\dot{A}(t) = -\frac{\varepsilon}{\omega}F_o(A,B)$$
$$\dot{B}(t) = \frac{\varepsilon}{\omega}G_o(A,B). \tag{1.7}$$

The solutions of (1.7) provide a first order approximation to the solutions of (1.6). Higher order approximations may be obtained

by using more terms in the Fourier expansions.

It is enlightening to derive (1.7) somewhat differently in order to reveal more clearly the nature of the approximation involved. If the exact equations (1.6) are integrated over a time interval $2\pi/\omega$ we obtain

$$\frac{A(t + 2\pi/\omega) - A(t)}{2\pi/\omega} = -\frac{\varepsilon}{\omega} \cdot \frac{\omega}{2\pi} \int_t^{t+2\pi/\omega} F \sin \omega\tau \, d\tau$$

$$\frac{B(t + 2\pi/\omega) - B(t)}{2\pi/\omega} = \frac{\varepsilon}{\omega} \cdot \frac{\omega}{2\pi} \int_t^{t+2\pi/\omega} F \cos \omega\tau \, d\tau$$

Observe now that the left hand sides are just the time derivatives of the averages of A(t) and B(t) over the interval $(t, t + 2\pi/\omega)$. That is

$$(A(t + 2\pi/\omega) - A(t))/\frac{2\pi}{\omega} = \frac{d}{dt}\left(\frac{\omega}{2\pi}\int_t^{t+2\pi/\omega} A(\tau)d\tau\right)$$

and similarly for B(t).

The approximation employed is in the right hand sides, where it is assumed that A(t), B(t) vary little over $(t, t + 2\pi/\omega)$; they may be replaced, in the integrands, by their averages over this interval. The equations (1.7) result, where we now interpret A(t), B(t) as averages over the time interval $(t, t + 2\pi/\omega)$.

It has been noted that (1.4) and (1.5) will serve to define the variables A(t), B(t). It is clear, however, that one may write $x(t) = a(t) \cos(\omega t + \theta(t))$, $\dot{x}(t) = -\omega a(t)\sin(\omega t + \theta(t))$ and thereby obtain equations for the slowly varying amplitude a(t) and phase $\theta(t)$, as:

$$\dot{a}(t) = -\frac{\epsilon}{\omega}F(a\cos\Phi, -\omega a\sin\Phi, t)\sin\Phi$$

$$\dot{\theta}(t) = -\frac{\epsilon}{a\omega}F(a\cos\Phi, -\omega a, \sin\Phi, t)\cos\Phi$$

where $\Phi(t) = \omega t + \theta(t)$. It is this formulation which has been employed by Krylov and Boboliubov.

The methods described above are analytic in nature and serve to produce approximations with any required degree of accuracy, provided the sequence of approximations converges. Unless ϵ is sufficiently small the methods fail either because the series do not converge or converge very slowly.

If the parameter associated with the nonlinearity is large, as for example with the equation $\ddot{x} + \mu f(x)\dot{x} + x = 0$ where $\mu \gg 1$, one might expect that a solution may be obtained as a power series in μ^{-1} such as: $x = x_o + z_1/\mu + z_2/\mu^2 + \ldots$. In general, however, such series do not converge.

Dorodnytsin has attempted this method of solution for the equation of van der Pol, $\ddot{x} + \mu(x^2 - 1)\dot{x} + x = 0$, where $\mu \gg 1$; he finds it necessary to assume four different asymptotic expansions of the solution, each valid over some region of the phase plane defined by: $x = v, \dot{v} = -\mu(x^2 - 1)v - x$. Dorodyntsin is able to obtain four analytic expressions for the periodic half-orbit, each having an asymptotic nature in four overlapping regions. By matching the expansions in the areas of common asymptotic convergence, Dorodyntsin obtains information concerning the asymptotic amplitude and period of the unique periodic solution to van der Pol's equation.

The technique employed by Dorodyntsin involves a detailed

investigation of the various solution expansions so as to determine the regions over which they possess the proper asymptotic character. No precise information is available concerning the error in truncating the expansions, for moderate values of μ.

In Chapter II we describe a method of investigating periodic solutions of autonomous differential equations which is in some sense a geometrical analogue of the technique of Dorodnytsin. We are able to obtain quite accurately the location of the periodic orbit, in the phase or Lienard planes, for a class of equations which includes the equation of van der Pol.

In the case of forced oscillations described by $\ddot{x} + \mu f(x)\dot{x} + g(x) = p(t)$, $\mu \gg 1$, perhaps the most prominent work has been done by M. L. Cartwright and J. E. Littlewood, who prove some remarkable properties of the harmonically forced van der Pol equation:

$$\ddot{x} + \mu(x^2 - 1)\dot{x} + x = A \sin \omega t.$$

This equation may be replaced by the equivalent system

$$\begin{aligned} \dot{x} &= \mu(y - F(x) - \gamma \cos \omega t) \\ \dot{y} &= -x/\mu \end{aligned} \tag{1.8}$$

where $F(x) = x^3/3 - x$; the quantity $\gamma = A/\mu\omega$, an important parameter, is a measure of the forcing amplitude.

Cartwright and Littlewood show that for "most" γ in the range $(1/100, 2/3 - 1/100)$, stable subharmonic solutions of odd integral order exist. The significance of "most" is that there are narrow critical subintervals in the range $(1/100, 2/3 - 1/100)$ which are transition regions. Except for these, the only stable solutions are odd subharmonics of large order, $0(\mu)$. In fact as γ increases in this range (jumping the critical subintervals) the stable subharmonics which occur have orders $2n+1$, $2n\pm1$,

$2n-1$, $2n-2\pm1$, etc. That is, there are successively one, then two, then one, etc. stable odd subharmonic solutions. The transition between regimes occurs in the critical subintervals of the γ range.

A further result of their researches is that a first subharmonic (of order one, with period $2\pi/\omega$) exists, and for γ in (1/100, 2/3 - 1/100) it is completely unstable.

N. Levinson has considered a piece-wise linear version of the above equation, namely:

$$\ddot{x} + \mu f(x)\dot{x} + x = A \sin t$$

where $f(x) = +1$ for $x^2 > 1$ and $f(x) = -1$ for $x^2 < 1$. This equation (which can evidently be solved exactly) exhibits the same behavior as encountered by Cartwright and Littlewood. Here, however, the unstable first harmonic can be obtained explicitly as $x_1 = \frac{A}{\mu} \cos t = \gamma \cos t$.

The range of interest for γ is $0 < \gamma < 1$. It is clear that $x_1(t)$ lies entirely in the region of negative damping, $x^2 < 1$, which accounts for the instability.

In Chapter III we investigate the geometrical properties of the solutions to (1.8) and obtain, for γ in some restricted range, annular regions in the (x,y) plane with the property that solutions which enter these regions remain therein. The methods we apply are geometrical in nature and the annular regions we obtain are the "smallest" possible, in the sense that no sub region will possess the property of confinement for all interior trajectories. The annuli we obtain contain the periodic solutions mentioned by the above authors for the particular equations they consider. However, the methods we apply have applications to a wider class of equations.

CHAPTER II

FREE OSCILLATIONS IN A SECOND ORDER SYSTEM

2.1 INTRODUCTION

We will be concerned in this chapter with the class of equations

$$\ddot{x} + \mu f(x)\dot{x} + g(x) = 0, \tag{2.1}$$

where μ is a large parameter and $f(x)$, $g(x)$ are sufficiently smooth to guarantee the existence and uniqueness of solutions with prescribed initial conditions.

We do not consider the "generalized Lienard equation" (2.1) directly, but rather the following equivalent pair of first order equations:

$$\dot{x} = y_1 - \mu F(x), \quad \dot{y}_1 = -g(x) \quad \text{where } F(x) = \int_0^x f(u)du.$$

These equations define the Lienard plane. It is convenient, however, for large μ, to set $y_1 = \mu y$ and work in the scaled Lienard plane, namely:

$$\dot{x} = \mu(y - F(x)), \quad \dot{y} = -g(x)/\mu. \tag{2.2}$$

Any initial condition $x(t_o)$, $\dot{x}(t_o)$ prescribed for the solution to (2.1) will define a unique point $x(t_o)$, $y(t_o) = \dot{x}(t_o)/\mu + F(x(t_o))$ in the scaled Lienard plane. The subsequent development in time of $x(t)$, $\dot{x}(t)$ corresponds to a motion of the point $(x(t),y(t))$ in the plane. Such motions will be referred to as trajectories or orbits.

It is our purpose to investigate the geometrical properties of these trajectories in the plane (2.2), and in particular to locate periodic orbits, which are manifested as simple closed curves.

Our methods, which are topological, result in a set of curves that define an annular region in the plane. The annular region has the property that once trajectories enter this region they must remain therein.

A crude but suggestive way of discussing (2.2) geometrically is to write $(y - F(x))dy/dx = -g(x)/\mu^2$. Hence, when $\mu \gg 1$ one has either (a) $y = F(x)$ or (b) $dy/dx = 0$, very nearly. That is, one might expect that the motion would consist of arcs which "follow" the curve $y = F(x)$, together with almost horizontal line segments. This expectation is fulfilled. Indeed we note that for $y > F(x)$, say $y = F(x) + C (C > 0)$, then $\dot{x} = \mu C = 0(\mu) > 0$, so that the trajectory has a large positive x-velocity. The rapid motion to the right will continue until $y = F(x)$ is reached, whereupon $\dot{x} = 0$. In the half-plane $x > 0$, $\dot{y}$ has the sign of $-g(x)$ and we shall always assume that $g(x)$ is "restoring", that is, $xg(x) > 0$ for $x \neq 0$. Then $\dot{y} < 0$ in $x > 0$. It is clear then that the general motion of trajectories is clockwise in the plane. Figure 1 illustrates two typical trajectories which begin at P and Q, for $t = t_o$ say.

Note that the Q-trajectory will eventually converge to the origin (which is a solution of (2.2) for $g(x)$ continuous and restoring), whereas the P-trajectory will not. In fact the P-trajectory will converge to a closed periodic orbit. If, however, the local minimum of $F(x)$ at $x = -a$ were lowered somewhat, then the P-trajectory would intersect $y = F(x)$ near $x = -a$ as does the Q-trajectory and so converge to the origin as well. A small change in the geometry of the curve $y = F(x)$ in the neighborhood of $x = -a$ would completely eliminate the possibility

of a periodic orbit. We will refer to such a periodic solution as "structurally unstable", if small changes in the nature of $F(x)$ or $g(x)$ produce qualitative changes in the periodic solution, or eliminate it entirely.

In cases where the equations (2.2) admit a structurally stable periodic orbit we will in general be able to obtain an annular region within which the periodic orbit will lie. The method may be aptly illustrated by application to a particular type of generalized Lienard equation. We will refer to this particular class of equations as the van der Pol type of equation, it being a natural generalization of the equation of van der Pol, namely

$$\ddot{x} + \mu(x^2 - 1)\dot{x} + x = 0.$$

2.2 THE VAN DER POL TYPE OF EQUATION

We assume the following conditions:

(a) $f(x)$ and $g(x)$ possess continuous first derivatives,

(b) $xg(x) > 0$ for $x \neq 0$ and $G(x) = \int_0^x g(u)du$ satisfies $G(\pm\infty) = \infty$,

(c) $f(x)$ has one positive and one negative zero, so $f(-a) = 0 = f(b)$, and $f(x) < 0$ in $(-a,b)$, $f(x) > 0$ outside $(-a,b)$,

(d) $F(x) = \int_0^x f(u)du$ satisfies $F(\pm\infty) = \pm\infty$,

and (e) $g(x)/f(x)$ is monotone decreasing outside $(-a,b)$.

These conditions are sufficient (but not necessary) to assure the existence of a unique periodic orbit to which all trajectories (other than $x = y = 0$) will converge. We proceed to the location of this stable closed orbit, or limit cycle.

Consider the function $\Phi(x,y) = y^2/2 + G(x)/\mu^2$ which is proportional to the energy associated with the point (x,y) in the plane (2.2). The family of contours $\Phi(x,y) = C$ (C = constant > 0) are closed and nested orals enclosing the origin, larger ovals corresponding to greater values of C. If x(t), y(t) is a solution to (2.2) and we compute the time rate of change of $\Phi(x,y)$ along this trajectory we obtain $\dot{\Phi} = y\dot{y} + g(x)\dot{x}/\mu^2 = -g(x)F(x)/\mu$, substituting from (2.2). Observe that $\dot{\Phi}$ is just the scalar product of the velocity vector defined by (1.2), and the vector grad (Φ) which gives the direction of maximum increase in $\Phi(x,y)$. Consequently, a solution trajectory which crosses a member of the family $\Phi(x,y) = C$, in a region R where $\dot{\Phi} = \frac{-g(x)F(x)}{\mu} \geq 0$, does so in a direction of increasing $\Phi(x,y)$; that is, toward the exterior of the oval. Such an oval effectively bounds exterior trajectories away from the origin and we will call such a contour an "inner bound" in the region R. Conversely, if $\dot{\Phi} \leq 0$, in some region R', then Φ ovals will be crossed toward their interior and we will call such a contour an "outer bound" in R'.

For example, if we let $-\alpha$ and β be the two nonzero roots of $F(x) = 0$, and assume that $G(\beta) \leq G(-\alpha)$, then the oval Φ_β: $y^2/2 + G(x)/\mu^2 = G(\beta)/\mu^2$ lies entirely in $-\alpha \leq x \leq \beta$ and $-g(x)F(x)/\mu \geq 0$ throughout this region, so that $\dot{\Phi} \geq 0$.

Hence Φ_β may only be crossed by solution trajectories from within; that is, Φ_β excludes exterior trajectories from its interior and thus provides an inner bound on these trajectories.

If we denote the unique stable periodic orbit by $y_p(x)$, then it is clear from the fact that all trajectories (other than x = y = 0)

converge to $y_p(x)$ that the periodic orbit lies exterior to Φ_β as indicated in Figure 2.

2.3 THE INNER BOUNDARY

Since our objective is to construct an annular region containing $y_p(x)$, we might for example adopt Φ_β as the inner boundary for this region. Indeed, Φ_β is the best inner bound known, valid for all values of $\mu>0$. For $\mu \gg 1$, however, a considerable improvement may be obtained. We now proceed to affect this improvement on Φ_β.

Consider the family of "shifted" ovals defined by $\psi(x,y) = \frac{(y-K)^2}{2} + \frac{G(x)}{\mu^2}$ = constant, where K is a constant at our disposal. Then $\psi(x,y)$ will change along a solution trajectory according to

$$\dot{\psi}(x,y) = (y-K)\dot{y} + g(x)\dot{x}/\mu^2 = -g(x)(F(x) - K))/\mu.$$

We will use a particular set of ψ ovals in the construction of our inner bound, namely the one parameter family defined by

$$\psi_u: \quad \tfrac{1}{2}(y - F(u))^2 + G(x)/\mu^2 = G(u)/\mu^2 \qquad (2.3)$$

where the parameter u is to assume values $u > b$.

For the moment we will confine ourselves to the half-plane $x \geq 0$. Then the ψ_u ovals satisfy $\dot{\psi}_u = g(x)(F(u) - F(x))/\mu \geq 0$ wherever $F(x) \leq F(u)$.

Note that the maximum x-excursion of a ψ_u oval occurs at $x = u$, where $y = F(x) = F(u)$. Note also that for $u = \beta$ then $F(u) = F(\beta) = 0$, and this particular ψ_u oval reduces to the contour Φ_β.

Consider now a trajectory which begins (at some $t = t_o$) at a point P_o on $x = 0$ (Figure 3). We will assume that P_o is exterior to Φ_β as indicated. If we now choose a ψ_u oval which passes through P_o, the

appropriate value of u_o will satisfy $u_o > \beta$. Then in $0 \leq x \leq u_o$, we have $F(x) \leq F(u_o)$ for this value of u, so that $\dot{\psi}_u \geq 0$, and the ψ_u oval through P_o will be an inner bound on the trajectory through P_o.

Let us call $(x_1, F(x_1))$ the point of intersection of the trajectory through P_o with $y = F(x)$; then $x_1 > u_o$. We now consider the trajectory subsequent (in time) to this intersection.

Observe then that the trajectory through P_o will lie exterior not only to the ψ_u oval chosen above, but to all ψ_u ovals which provide inner bounds for the trajectory. Note that all these ovals project somewhat below the curve $y = F(x)$, so that the trajectory we are considering will lie below these projections, in $x > b$. In particular the trajectory will lie below the <u>envelope</u> to the family (2.3) in $x > b$ (Figure 4).

Parametric equations for the ψ_u envelope may be obtained from (2.3) together with the equation resulting from the partial differentiation of (2.3) with respect to u. If we denote the envelope by E, we obtain

$$E: \quad y = F(u) - g(u)/\mu^2 f(u) \tag{2.4}$$

$$G(x) = G(u) - \frac{1}{2\mu^2}(g(u)/f(u))^2$$

For a given value of the parameter u, equations (2.4) furnish a point Q_u on the envelope E. Figure 5 illustrates the geometrical significance of equations (2.4). The point Q_u is the appropriate solution to (2.4) for a given u. The locus of points Q_u is the envelope E. The curve marked Γ in Figure 5 is defined by Γ: $y = F(x) - g(x)/\mu^2 f(x)$. It will play an important role when we come to construct the outer

boundary of our annulus.

Note that E is an inner bound wherever the ψ_u ovals exclude exterior trajectories. However, these ovals possess the excluding property only where $F(x) \leq F(u)$. Consequently, for each value of u there is defined a ψ_u oval, an "excluding interval" where $F(x) \leq F(u)$, and a point Q_u on the envelope E. Only for points Q_u which lie within the excluding interval will E provide an inner bound. This is the case, for example, in Figure 5.

Now if U_m is the minimum value of the parameter u for which Q_u lies in the excluding interval, then E will be an inner bound only for $u \geq U_m$. Figure 6 depicts the situation. The point Q_m, associated with $u = U_m$, lies on the edge of the excluding interval ($F(x) \leq F(U_m)$). For $u < U_m$, the envelope will not be an inner bound.

The coordinates of Q_m, (x_m, y_m) may be obtained by solving (2.4) together with $F(x_m) = F(U_m)$. Clearly $x_m < b < U_m$.

Let us obtain the asymptotic form of the equation for E.

From $G(x) = G(u) - \frac{1}{2\mu^2} (g(u)/f(u))^2$, it is clear that $x \doteq u$ wherever $\mu f(u) \gg 1$, that is, for $u - b \gg \mu^{-1}$. For this portion of the envelope we may determine the relation between x and u by putting $u = x + \Delta$ and expanding;

$$G(u) = G(x) + g(x)\Delta + 0(\Delta^2)$$

$$g(u)/f(u) = g(x)/f(x) + 0(\Delta)$$

There results

$$\Delta = g(x)/2\mu^2 f(x) + 0(\Delta^2) + 0(\Delta/\mu^2)$$

so that $\Delta = 0(\mu^{-2})$. Then

$$u = x + g(x)/2\mu^2 f(x) + 0(\mu^{-4}).$$

Substituting into $y = F(u) - g(u)/\mu^2 f(u)$ gives

$$E: \quad y = F(x) - g(x)/2\mu^2 f(x) + 0(\mu^{-4}).$$

This equation for the envelope is valid for $x - b >> \mu^{-1}$. In particular it applies to the region $x \geq b + 0(\mu^{-2/3})$.

We now compute the coordinates (x_m, y_m) of Q_m, where E ceases to be an inner bound, from the equations:

$$y = F(u) - g(u)/\mu^2 f(u), \quad G(x) = G(u) - \frac{1}{2\mu^2}(g(u)/f(u))^2, \quad F(x) = F(u).$$

As mentioned previously, the solutions x_m, u_m satisfy $x_m < b < U_m$. Putting $x = x_m = b - \Delta$ and $u = U_m = b + \delta$ into the last equation we have

$$F(b) + f'(b)\Delta^2/2 + 0(\Delta^3) = F(b) + f'(b)\delta^2/2 + 0(\delta^3)$$

(Note that $f(b) = 0$). Then $\Delta = \delta + 0(\delta^2) + 0(\Delta^2)$.

We perform the same expansion about $x_m = U_m = b$ in the middle equation and obtain:

$$-\Delta = \delta - g(b)/2\mu^2 f'(b)\delta^2 + 0(\Delta^2) + 0(\delta^2) + 0(1/\delta\mu^2).$$

Substituting $\Delta = \delta + 0(\delta^2) + 0(\Delta^2)$ yields

$$\delta = (g(b)/4(f'(b))^2)^{1/3}\mu^{-2/3} + 0(\mu^{-4/3})$$

so that $\Delta = \delta + 0(\mu^{-4/3})$, where we have set $\Delta = 0(\mu^{-2/3})$ and $\delta = 0(\mu^{-2/3})$ in the terms neglected in the expansions.

We now have

$$x_m = b - (g(b)/4(f'(b))^2)^{1/3}\mu^{-2/3} + 0(\mu^{-4/3})$$

$$U_m = b + (g(b)/4(f'(b))^2)^{1/3}\mu^{-2/3} + 0(\mu^{-4/3})$$

and from $y_m = F(U_m) - g(U_m)/\mu^2 f(U_m)$ we obtain

$$y_m = F(b) - \frac{7}{4}(g^2(b)/2f'(b))^{1/3}\mu^{-4/3} + 0(\mu^{-2}).$$

The point Q_m at which we terminate the inner bound E, lies $0(\mu^{-2/3})$ to the left and $0(\mu^{-4/3})$ below the point (b,F(b)) where y = F(x) attains its minimum. We now continue the inner bound from Q_m to the negative y-axis.

Let us select the member of the family $\Phi(x,y) = y^2/2 + G(x)/\mu^2$ = constant which passes through Q_m. As we have seen, $\dot{\Phi}(x,y)$ $= -g(x)F(x)/\mu \geq 0$ in $-\alpha \leq x \leq \beta$ so that the oval we select, namely $y^2/2 + G(x)/\mu^2 = y_m^2/2 + G(x_m)/\mu^2$, will provide a continuation of the inner bound from Q_m. We will denote this particular oval by Φ_m, then:

$$\Phi_m: \quad y = -(y_m^2 + 2(G(x_m) - G(x))/\mu^2)^{1/2}$$

$$= y_m - 0(\mu^{-2}) \text{ in } 0 \leq x \leq x_m.$$

That is, Φ_m is a horizontal line segment, to within $0(\mu^{-2})$ and will intersect the y-axis at $y = y_m - 0(\mu^{-2})$. We will call this ordinate $\bar{y}_m$, so that

$$\bar{y}_m = F(b) - \frac{7}{4}(g^2(b)/2f'(b))^{1/3}\mu^{-4/3} + 0(\mu^{-2}).$$

At this point we might proceed into the half-plane $x \leq 0$ with a contour through $(0,\bar{y}_m)$ which is analogous to the ψ_u oval described in connection with the trajectory through P in Figure 3. By repeating the construction in $x \leq 0$, as we have done for $x \geq 0$, a complete inner bound may be obtained as in Figure 7. However, we choose to replace that portion of the inner bound covered by ψ_u in $x \geq 0$ (and the analogous contour in $x \leq 0$), with another curve which will yield an improved inner bound. The reason for not using ψ_u is the following: if we choose, in

$x \geq 0$ for example, the appropriate value of u in the equation (2.3) for ψ_u, we obtain $y = F(u) + (2(G(u) - G(x)))^{1/2}/\mu$, where we have selected the upper branch. At $x = 0$ we have $y = F(u) + (2G(u))^{1/2}/\mu$, and at $x = u$, $y = F(u)$, so that the decrement in y is $0(\mu^{-1})$ along ψ_u, which is significantly larger than the y-decrement for the trajectories (such as the trajectory through P in Figure 3). We will show below that in this region of the plane, the decrement in y is no greater than $0(\log\mu/\mu^2)$.

The inner bound illustrated in Figure 7 has a positive y-axis intercept $\bar{y}_m'$, (obtained as was done for $\bar{y}_m$, the negative y-axis intercept) where

$$\bar{y}_m' = F(-a) + \frac{7}{4}(g^2(-a)/2|f'(-a)|)^{1/3}\mu^{-4/3} + 0(\mu^{-2}).$$

We continue from this point into $x \geq 0$ as follows.

Solution trajectories satisfy $dy/dx = -g(x)/\mu^2(y - F(x))$, and for $x \geq 0$ and $y < F(-a)$ we have

$$\mu^2 dy/dx \geq -g(x)/(F(-a) - F(x)).$$

Observe that $F(-a) - F(x)$ has a simple zero at $x = x_o$ (Figure 8) so we may write

$$F(-a) - F(x) = h(x)(x_o - x)$$

where $h(x) > 0$ in $x \geq 0$.

The trajectories satisfy

$$\mu^2 dy/dx > \frac{-g(x)}{h(x)} \left(\frac{-1}{x - x_o}\right)$$

in $0 \leq x \leq x_o$ and $y \leq F(-a)$. If we set $\max (g(x)/h(x)) = m$, $0 \leq x \leq x_o$, then we have $\mu^2 dy/dx > \frac{-m}{x_o - x}$ for trajectories in $0 \leq x \leq x_o$, $y > F(-a)$.

We choose as inner bound, the solution to $\mu^2 dy/dx = \frac{-m}{x_o - x}$ which passes through $(0, \bar{y}_m')$. This gives

$$y = \bar{y}_{m'} + \frac{m}{\mu^2}\log\left(\frac{x_o - x}{x_o}\right).$$

Since this function has a logarithmic singularity at $x = x_o$, we use it only to $x = x_1$ where $x_1 < x_o$ (see Figure 8). We will continue from x_1 with a ψ_u oval. In fact, we choose the ψ_u oval such that it is tangent to the function obtained above. If we call this point of tangency (x_1, y_1) then x_1, y_1 and the appropriate parameter value u must satisfy:

$$y_1 = \bar{y}_{m'} - (m/\mu^2)\log(x_o/(x_o - x_1)) = F(u) + (2(G(u) - G(x_1)))^{\frac{1}{2}}/\mu$$

and

$$\frac{-m}{\mu^2}\left(\frac{1}{x_o - x_1}\right) = -g(x_1)/\mu(2(G(u) - G(x_1)))^{\frac{1}{2}}$$

where we have equated the coordinate values and the slope of the tangent at (x_1, y_1), of both curves.

Since it is clear that $x_1 \doteqdot x_o$ and $u \doteqdot x_o$ we will put $x_1 = x_o - \Delta$ and $u = x_o + \delta$ in order to estimate the solution to the above equations. We will assume here that $\Delta = 0(\mu^{-5/3})$ and $\delta = 0(\mu^{-2/3})$ in order to simplify the algebra. The validation of this assumption will follow from the consistency of the final result. We also have

$$\bar{y}_{m'} - F(x_o) = 0(\mu^{-4/3}).$$

From the last equation we obtain

$$\delta = g(x_o)\mu^2\Delta^2/2m^2 + 0(\mu^{-5/3})$$

and from the ordinate equation:

$$\delta = (\bar{y}_{m'} - F(x_o))/f(x_o) - (2g(x_o)\delta)^{\frac{1}{2}}/\mu + 0(\log\mu/\mu^2)$$

where the term $0(\log\mu/\mu^2)$ is due to $\frac{-m}{\mu^2}\log\left(\frac{x_o}{x_o - x_1}\right)$.

Solving for Δ gives

$$\Delta^2 = (2m^2/g(x_o)f(x_o))\left(\frac{\bar{y}_m' - f(x_o)}{\mu^2}\right) + O(\mu^{-11/3})$$

or

$$\Delta = \{2m^2(\bar{y}_m' - F(x_o))/\mu^2 g(x_o)f(x_o)\}^{1/2} + O(\mu^{-2}) = O(\mu^{-5/3}).$$

Substitution into the second δ equation above yields

$$\delta = (y_m' - F(x_o))/f(x_o) - \{2g(x_o)(\bar{y}_m' - F(x_o))/\mu^2 f^3(x_o)\}^{1/2} + O(\log\mu/\mu^2).$$

Note that the first term here is $O(\mu^{-4/3})$ and the second term is $O(\mu^{-5/3})$; then $\delta = O(\mu^{-4/3})$.

If we write $\bar{y}_m' = F(-a) + B\mu^{-4/3} + O(\mu^{-2})$ where $B = \frac{7}{4}(g^2(-a)/2|f'(-a)|)^{1/3}$, and set $F(x_o) = F(-a)$, we obtain the parameter value $u = x_o + \delta$ as

$$u = x_o + \frac{B}{f(x_o)}\mu^{-4/3} - (2g(x_o)B/f^3(x_o))^{1/2}\mu^{-5/3} + O(\log\mu/\mu^2).$$

Our inner bound is now complete and we may use it to compute a lower bound on the amplitude of the periodic solution to $\ddot{x} + \mu f(x)\dot{x} + g(x) = 0$. If we define $A^+ = \max(x_o(t))$ where $x_p(t)$ is the periodic solution, then A^+ is the maximum positive value attained by $x_p(t)$ and satisfies $A^+ \geq u$. That is,

$$A^+ \geq x_o + B\mu^{-4/3}/f(x_o) - (2g(x_o)B/f^3(x_o))\mu^{-5/3} + O(\log\mu/\mu^2)$$

where

$$F = \frac{7}{4}(g^2(-a)/2|f'(-a)|)^{1/3}.$$

In a similar manner we may define the maximum negative value

attained by $x_p(t)$ as $A^- = \min(x_p(t))$ and so obtain a lowerbound on $|A^-|$. With an obvious change in notation this lower bound on $|A^-|$ will take the form given above.

We will apply this inequality to the equation of van der Pol:

$$\ddot{x} + \mu(x^2 - 1)\dot{x} + x = 0.$$

Here $a = b = 1$, $F(-a) = 2/3 = F(x_o)$ and $x_o = 2$, and $B = \frac{7}{4}(\frac{1}{4})^{1/3}$. Since the periodic orbit is symmetrical about the origin, $A^+ = |A^-| = A$ say, and

$$A \geq 2 + \frac{7}{12}(\frac{1}{4})^{1/3}\mu^{-4/3} - (\frac{7}{27\cdot 4^{1/3}})^{1/2}\mu^{-5/3} + 0(\log\mu/\mu^2)$$

or

$$A \geq 2 + .367\mu^{-4/3} + 0(\mu^{-5/3}).$$

The asymptotic expansion obtained by Dorodyntsin for the amplitude of the periodic solution is:

$$A = 2 + .7794\mu^{-4/3} + 0(\log\mu/\mu^2).$$

It can be seen that our inner bound provides quite a good lower bound for the amplitude. Further we may note that the lower bounds we obtain always have the form $x_o + 0(\mu^{-4/3})$. We will compute an upper bound on the amplitude when the construction of the outer boundary for our annulus is complete, and will find that it too has the form $x_o + 0(\mu^{-4/3})$. Let us proceed now to the outer boundary.

2.4 THE OUTER BOUNDARY

Consider the contour Γ: $y = F(x) - g(x)/\mu^2 f(x)$ introduced previously in connection with the envelope E of the ψ_u ovals. In the scaled phase plane defined by $\dot{x} = \mu v$, $\dot{v} = -\mu f(x)\, v - g(x)/\mu$, we note

that Γ is just the isocline of zero slope; that is, the locus of points where $d\nu/dx = -f(x) - g(x)/\mu^2\nu = 0$. This gives $\nu = -g(x)/\mu^2 f(x)$ which becomes $y = F(x) + \nu = F(x) - g(x)/\mu^2 f(x)$ in the scaled Lienard plane.

Figure 9(a) illustrates the nature of Γ in the (x,ν)-plane, as well as typical velocity directions for solution trajectories. Due to the assumed monotonic nature of $g(x)/f(x)$ it is clear that trajectories in $x > b$, for example may not cross Γ from above. In this region then, Γ provides confinement of trajectories on the origin side of Γ. That is, Γ is an outer bound in $x > b$. A similar statement holds in $x < -a$.

In the (x,y) -plane Γ takes the form indicated in Figure 9(b). The nature of Γ in $-a < x < b$ will not concern us.

Note that Γ lies $0(\mu^{-2})$ below $y = F(x)$ in $x > b$ (or more precisely, in $x > b + 0(1)$) and will provide an outer bound for trajectories which cross $y = F(x)$ in this region. In particular it will serve as a portion of the outer boundary of the annulus for the periodic orbit $y_p(x)$. Recall that the inner boundary in this region is the envelope E which has the equation E: $y = F(x) - g(x)/2\mu^2 f(x) + 0(\mu^{-4})$.

That is, E lies midway between $y = F(x)$ and Γ. It is clear that trajectories such as $y_p(x)$, lie precisely $0(\mu^{-2})$ below $y = F(x)$ here.

We will again confine ourselves to the half-plane $x \geq 0$ in computing the outer boundary of the annulus. At $x = b$, Γ has a singularity so we improve upon Γ in this neighborhood as follows.

Consider again the ovals $\psi(x,y) = \frac{1}{2}(y-K)^2 + G(x)/\mu^2 = $ constant, where $\dot{\psi}(x,y) = -g(x)(F(x) - K)/\mu$. We will have $\dot{\psi} \leq 0$ wherever $F(x) \geq K$. Since $F(x) \geq F(b)$ everywhere in $x \geq 0$, we choose $K = F(b)$.

Then the contours $1/2(y - F(b))^2 + G(x)/\mu^2 = \text{constant}$ are such that solution trajectories may only cross them from without (since $\dot{\psi} \leq 0$). We choose the constant in the form $G(k)/\mu^2$ giving

$$\psi_k: \quad \frac{1}{2}(y - F(b))^2 + G(x)/\mu^2 = G(k)/\mu^2.$$

If we now select k so that the oval ψ_k is tangent to Γ, then we will have a smooth continuation of the outer bound (Figure 10).

The lower branch of ψ_k is $y = F(b) - (2(G(k) - G(x))^{1/2}/\mu$. In order to find the required value of k we add the requirements $y = F(x) - g(x)/\mu^2 f(x)$ and

$$dy/dx = g(x)/\mu(2(G(k) - G(x)))^{1/2} = f(x) - \frac{1}{\mu^2}\frac{d}{dx}(g(x)/f(x)).$$

We will find the point of tangency (x,y) and the appropriate k, by setting $x = b + \Delta$, $k = b + \delta$ and expanding the above equations. This yields

$$-(2g(b)(\delta - \Delta))^{\frac{1}{2}}/\mu = f'(b)\Delta^2/2 - g(b)/\mu^2 f'(b)\Delta + O(\mu^{-2})$$

from the or dinate equations, and

$$g(b)/\mu(2g(b)(\delta - \Delta))^{\frac{1}{2}} = f'(b)\Delta + g(b)/\mu^2 f'(b)\Delta^2 + O(\mu^{-4/3})$$

from the slope equation, where we have set $\Delta = O(\mu^{-2/3})$ and $\delta = O(\mu^{-2/3})$ in the "neglected" terms. Although we might have kept these terms in the form $O(\Delta^{\frac{1}{2}}/\mu)$, etc., and eventually determined that $\Delta = O(\mu^{-2/3})$, $\delta = O(\mu^{-2/3})$, we will assume this result immediately in order to simplify the algebra.

If we multiply the last two equations together, eliminating δ, a quadratic equation in the variable $S = (f'(b))^2\mu^2\Delta^3/g(b)$ results, namely: $S^2 + S - 2 = 0$ (or more precisely, $S^2 + S - 2 = O(\mu^{-4/3})$).

Choosing the positive root, S = 1 gives

$$\Delta = (g(b)/(f'(b))^2)^{1/3}\mu^{-2/3} + 0(\mu^{-4/3}).$$

Substituting to find δ gives

$$\delta = 9\Delta/8 = \frac{9}{8}(g(b)/(f'(b))^2)^{1/3}\mu^{-2/3} + 0(\mu^{-4/3}).$$

The appropriate ψ_k oval is then given by

$$\tfrac{1}{2}(y - F(b))^2 + G(x)/\mu^2 = G(k)/\mu^2$$

where

$$k = b + \frac{9}{8}(g(b)/(f'(b))^2)^{1/3}\mu^{-2/3} + 0(\mu^{-4/3}).$$

Although this contour will provide an outer bound to the negative y-axis we will only use it in the neighborhood of x = b. The reason for this is that it has a y-axis intercept of $y = F(b) - (2G(k))^{\frac{1}{2}}/\mu$. That is, $y = F(b) - 0(\mu^{-1})$, and this y-decrement of order $1/\mu$ is much larger than the y-decrement of the trajectories which we consider. In fact, we show below that trajectories "fall" by $0(\mu^{-4/3})$ at most, over the interval from x = b to x = 0.

Let us terminate ψ_k at $x = x_2 (x_2 < b)$ and continue from this point, which we call (x_2, y_2) with another outerbound as follows:

For a solution trajectory in this region we have

$$\mu^2 dy/dx = -g(x)/(y - F(x)) \leq -g(x)/(F(b) - F(x))$$

for $y < F(b) < F(x)$ and $0 \leq x < b$.

Now F(x) - F(b) has a zero of order two at x = b, so we put $F(x) - F(b) = H(x)(x - b)^2$ then

$$\mu^2 dy/dx \leq \frac{g(x)}{H(x)} \cdot \frac{1}{(x - b)^2} \leq M/(x-b)^2$$

where

$$M = \max(g(x)/H(x)), (0 \leq x \leq b).$$

We continue our outer bound with the solution to $dy/dx = M/\mu^2(x - b)^2$ which passes through (x_2, y_2). This gives

$$y = y_2 - \frac{M}{\mu^2}\left(\frac{1}{b - x_2} - \frac{1}{b - x}\right).$$

Our choice of x_2 will be such that this outer bound is tangent to ψ_k at $x = x_2$ (see Figure 11).

Equality of slopes at $x = x_2$ requires

$$\frac{M}{\mu^2}\cdot\frac{1}{(b - x_2)^2} = g(x_2)/\mu(2(G(k) - G(x_2)))^{\frac{1}{2}}$$

which determines x_2.

To fine x_2, we set $x_2 = b - \triangle$, $k = b + \delta$, (δ is given above) and expand about $x_2 = b$, $k = b$. This yields

$$\mu^2 g(b)\triangle^4/2M^2 = \triangle + \delta + 0(\mu^{-4/3})$$

where we have put $\triangle = 0(\mu^{-2/3})$ and $\delta = 0(\mu^{-4/3})$ in the higher order terms (the fact that $\triangle = 0(\mu^{-2/3})$ will appear presently).

We rewrite the equation for $\triangle$ in the form

$$\frac{\mu^2 g(b)\delta^3}{2M^2}(\triangle/\delta)^4 = (\triangle/\delta) + 1 + 0(\mu^{-2/3})$$

and substitute

$$\delta = \frac{9}{8}(g(b)/(f'(b))^2)^{1/3}\mu^{-2/3} + 0(\mu^{-4/3})$$

yielding

$$\frac{729}{1024}\cdot\frac{g^2(b)}{M^2(f'(b))^2}\ \alpha^4 = \alpha + 1$$

where $\triangle = \alpha\delta + 0(\mu^{-4/3})$ and $x_2 = b - \alpha\delta + 0(\mu^{-4/3})$.

We will leave x_2 in this form. For any particular differential

equation it will be necessary to solve this quartic equation for α. It is clear that the quartic has a single positive root. (Later we will do this for the van der Pol equation.) Then $x_2 = b - \Delta = b - 0(\mu^{-2/3})$ and $y = F(b) - (2(G(k) - G(x_2)))^{\frac{1}{2}}/\mu = F(b) - 0(\mu^{-4/3})$ from the equation for ψ_k.

At $x = 0$, our outer bound has a y-axis intercept of $y_o = y_2 - \frac{M}{\mu^2} \cdot \frac{1}{b - x_2} + \frac{M}{\mu^2}$ or $y_o = y_2 - M/\mu^2\Delta + 0(\mu^{-2}) = F(b) - 0(\mu^{-4/3})$, so that solution trajectories do not "fall" by more than $0(\mu^{-4/3})$ over this region, from $x = b$ to $x = 0$.

We must now continue into $x \leq 0$, from $(0,y_o)$. To do this consider the family of ovals defined by $\psi_a(x,y) = \frac{1}{2}(y - F(-a))^2 + G(x)/\mu^2 = \text{constant}$. Since $\dot{\psi}_a(x,y) = g(x)(F(-a) - F(x))/\mu \leq 0$ in $x \leq 0$, the member of this family which passes through $(0,y_o)$ will serve as an outer bound. This gives (choosing the lower branch of ψ_a):

$$y = F(-a) - ((y_o - F(-a))^2 - 2G(x)/\mu^2)^{\frac{1}{2}}.$$

If the radical is expanded we find that $y = y_o + 0(\mu^{-2})$. That is, ψ_a is simply a horizontal line to within $0(\mu^{-2})$.

The ψ_a oval we have chosen will intersect $y = F(x)$ very near $x = \bar{x}_o$ where $\bar{x}_o$ is defined to be the unique negative root of $F(x) = F(b)$ (Figure 12). This point of intersection will provide an upper bound on $|A^-|$, the magnitude of the maximum negative x-excursion attained by the periodic orbit.

Setting $y = F(x) = F(-a) - (y_o - F(-a))^2 - 2G(x)/\mu^2)^{\frac{1}{2}}$ $= y_o + 0(\mu^{-2})$ and solving for x gives

$$x = \bar{x}_o + \frac{f(b) - y_o}{f(\bar{x}_o)} + O(\mu^{-2}),$$

where we have expanded about $x = \bar{x}_o$.

We may now substitute for y_o and obtain

$$|A^-| \leq |\bar{x}_o| + (F(b) - y_2 + M/\mu^2\Delta)/f(\bar{x}_o) + O(\mu^{-2})$$

and finally

$$|A^-| \leq |\bar{x}_o| + (2(G(k) - G(x_2)))^{1/2} + M/\mu^2(b-x_2)/f(\bar{x}_o) + O(\mu^{-2})$$

where $k = b + \delta$, $x_2 = b - \Delta$, and $\Delta/\delta = \alpha$ satisfies

$$(729\ g^2(b)/1024M^2f'(b))^2\alpha^4 = \alpha + 1.$$

Let us compute this upper bound for the van der Pol equation. As mentioned previously we have $|A^-| = A^+ = A$, and $|\bar{x}_o| = x_o = 2$, due to symmetry where $\bar{x}_o = -2$ is a unique negative root of $F(x) = F(b)$ or $x^3/3 - x = -2/3$.

We determine $M = \max(g(x)/H(x)) = \max \frac{3x}{x+2} = 1$, $0 \leq x \leq 1$, so the equation for α becomes:

$$(729/4096)\alpha^4 = \alpha + 1.$$

The positive root is $\alpha = 2.032$, so that $x_2 = b - \alpha\delta + O(\mu^{-4/3}) = 1 - 2.032\delta + O(\mu^{-4/3})$ and since $\delta = \frac{9}{8}(g(b)/(f'(b))^{2\ 1/3}\mu^{-2/3} + O(\mu^{-4/3}) = (\frac{9}{8\cdot 4^{1/3}})\mu^{-2/3} + O(\mu^{-4/3})$ then $x_2 = 1 - 1.440\mu^{-2/3} + O(\mu^{-4/3})$

Substituting for $|A^-| = A$ gives

$$A \leq 2 + .922\mu^{-4/3} + O(\mu^{-2}).$$

Recalling that the exact asymptotic expansion of A is $A = 2 + .7794\mu^{-4/3} _ O(\log\mu/\mu^2)$, we see that the outer boundary of the annulus provides quite a good upper bound for the amplitude of the periodic solution, in the case of the van der Pol equation. Further we note that both the upper and lower amplitude bounds take the form $x_o + o(\mu^{-4/3})$

for the general van der Pol type of equation so that the confinement of the periodic solution by the annulus not only gives quite an accurate geometrical description of the orbit in the plane, but also yields the precise order of magnitude of the deviation of A^+ from x_o, or A^- from $\bar{x}_o$.

Figure 13 illustrates the complete annulus. We have joined the ψ_a contour to Γ with a short vertical line segment in order to complete the outer bound.

2.5 GENERALIZATIONS

The conditions assumed in section 2 may be relaxed somewhat. The function $g(x)$, for example, need not be continuously differentiable, but only Lipschitzian over the x-interval of interest. In order that the results of section 2 be valid, however, we retain the requirement of differentiability for $f(x)$, at least in the neighborhood of its zeros at $x = -a$ and $x = b$ (the amplitude bounds for the periodic orbit, for example involve $f'(-a)$ and $f'(b)$).

We may eliminate the condition of monotonicity for $g(x)/f(x)$ as follows. Recall that Γ is the zero-slope isocline in the scaled phase plane defined by $\dot{x} = \mu v$, $\dot{v} = -\mu f(x) v - g(x)/\mu$. That is $v = -g(x)/\mu^2 f(x)$ is obtained from $dv/dx = 0$. In $x > b$ then, we have $\dot{v} \geq 0$ for $v \leq -g(x)/\mu^2 f(x)$ and Γ may only be crossed from below wherever $g(x)/f(x)$ is monotone decreasing. (Figure 14 shows some typical trajectories.)

If Γ is not monotone over some range of x, as illustrated in Figure 14 for $x < -a$, then the required confining property is lacking.

However, we may construct a Γ^*, which provides the monotonicity, by inserting horizontal line segments between portions of Γ which are monotone. The dashed line in Figure 14 indicates the modification proposed. Note that Γ will be monotone near the zeros of $f(x)$ due to the singularity there. We will require however that Γ be monotone for large $|x|$. The modified contour Γ^* will then make up for any local lack of monotonicity in Γ, and will thus produce, in the scaled Lienard plane, an outer bound.

The damping function $f(x)$ may be generalized. We will require however that $f(x)$ be positive for large $|x|$, so that $F(\pm\infty) = \pm\infty$. The construction of an annulus for general $F(x)$ will proceed as indicated in the example for Figure 15.

In Figure 15, if the motion in "reverse" time is investigated by setting $t = -\tau$ in the equations of motion (2.2), and if we also put $y = -Y$ in order to preserve the form of the equations for reverse motion, we obtain

$$dx/d\tau = \mu(Y+F(x)), \quad dY/d\tau = -g(x)/\mu.$$

That is, the equation which governs the reverse motion may be obtained from (2.2), simply by replacing $F(x)$ by $-F(x)$. The geometry of the trajectories in reversed time will then depend upon the nature of the curve $Y = -F(x)$ as in Figure 16.

It is clear that an annulus may be constructed as indicated. The periodic orbit within this annulus is unique and stable (in reversed time τ).

Having located this periodic solution we see that it remains a periodic solution of the original equations of direction motion (2.2), except that it is unstable in direct time t. Then for a characteristic

curve $y = F(x)$ as illustrated in Figure 15, we conclude that there are two periodic orbits, the inner one being unstable and the outer one being stable (see appendix for uniqueness and stability of periodic orbits in an annulus). Amplitude estimates can be obtained for each.

Evidently the construction of annuli, as indicated above, will fail is $F(x)$ has maxima or minima of very nearly equal value. If this is the case however, any periodic solution which passes near these extrema will be structurally unstable.

2.6 SUMMARY

The geometric confinement of trajectories to a system $\dot{x} = \mu(y-F(x))$, $\dot{y} = -g(x)/\mu$ succeeds, in many cases, in generating an annulus for each periodic motion, stable or unstable. It should be noted however that such confinement as has been obtained in this chapter takes no regard to periodicity. That is, the confinement applies to all solutions in some region, regardless of whether or not they are periodic. We may expect good results only when there is strong convergence to a periodic orbit. Such is the case with the generalized Lienard equations we have considered, where the damping is strong and $g(x)$ is restoring.

The solutions for $\mu \ll 1$ differ greatly from the solutions for $\mu \gg 1$. In the small μ case it is more appropriate to work in the unscaled Lienard plane: $\dot{x} = y_1 - \mu F(x)$, $\dot{y} = -g(x)$. Here, confining contours of the form $y_1^2/2 + G(x) = \text{constant}$ are more natural. Indeed, for μ vanishingly small, these become precisely the solution trajectories. That is, a closed periodic orbit passes through every point in the plane.

It is the damping term which is responsible for the isolated periodic orbits, and generally speaking, the larger the damping coefficient, μ, the more rapid the convergence of any given trajectory to a periodic orbit.

For $\mu \gg 1$, the motion in the scaled Lienard plane consists of trajectory arcs which remain near the curve $y = F(x)$, at a distance $0(\mu^{-2})$, together with almost horizontal segments over which the y-deviation is $\leq 0(\log \mu/\mu^2)$. During the motion near $y = F(x)$ we have $\dot{x} = \mu(y-F(x)) = 0(\mu^{-1})$. Since $\dot{y} = -g(x)/\mu = 0(\mu^{-1})$ as well, the trajectory velocity is $0(\mu^{-1})$ in magnitude and a time of order μ is required to describe this portion of the trajectory. At an extemum of $y = F(x)$, where the orbit enters a region of negative damping, we have $|y-F(x)| = 0(\mu^{-4/3})$ so that $|\dot{x}| = 0(\mu^{-1/3})$. There then ensures a rapid, almost discontinuous motion from one positive going branch of $y = F(x)$ to another, with $|\dot{x}| = 0(\mu)$. During this switching the deviation of y from the value of $F(x)$ at the extremum is maintained at $0(\mu^{-4/3})$. Amplitude bounds on periodic orbits can be expected to take the form: $\bar{x}_o + 0(\mu^{-4/3})$.

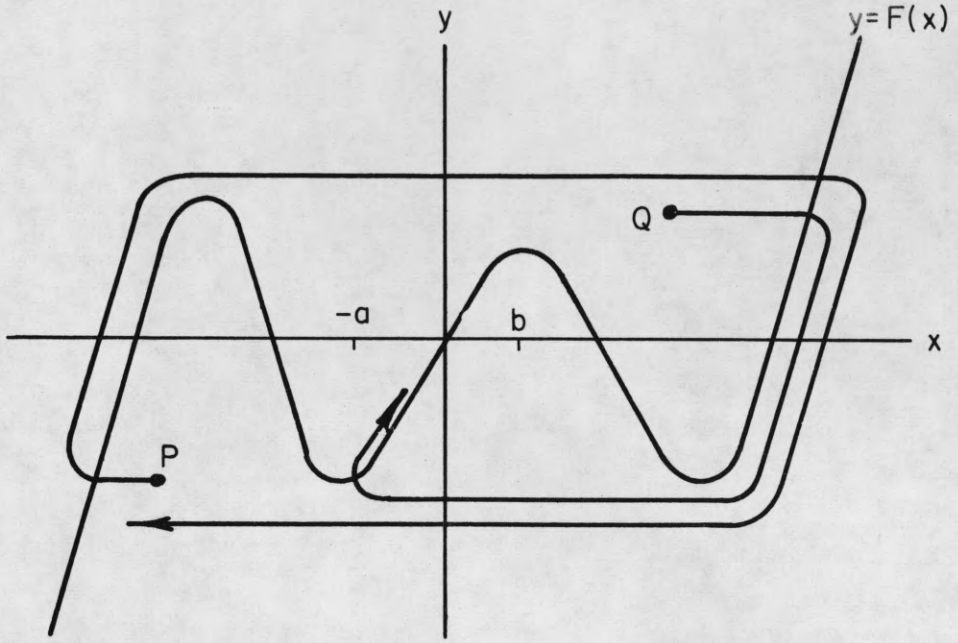

Figure 1

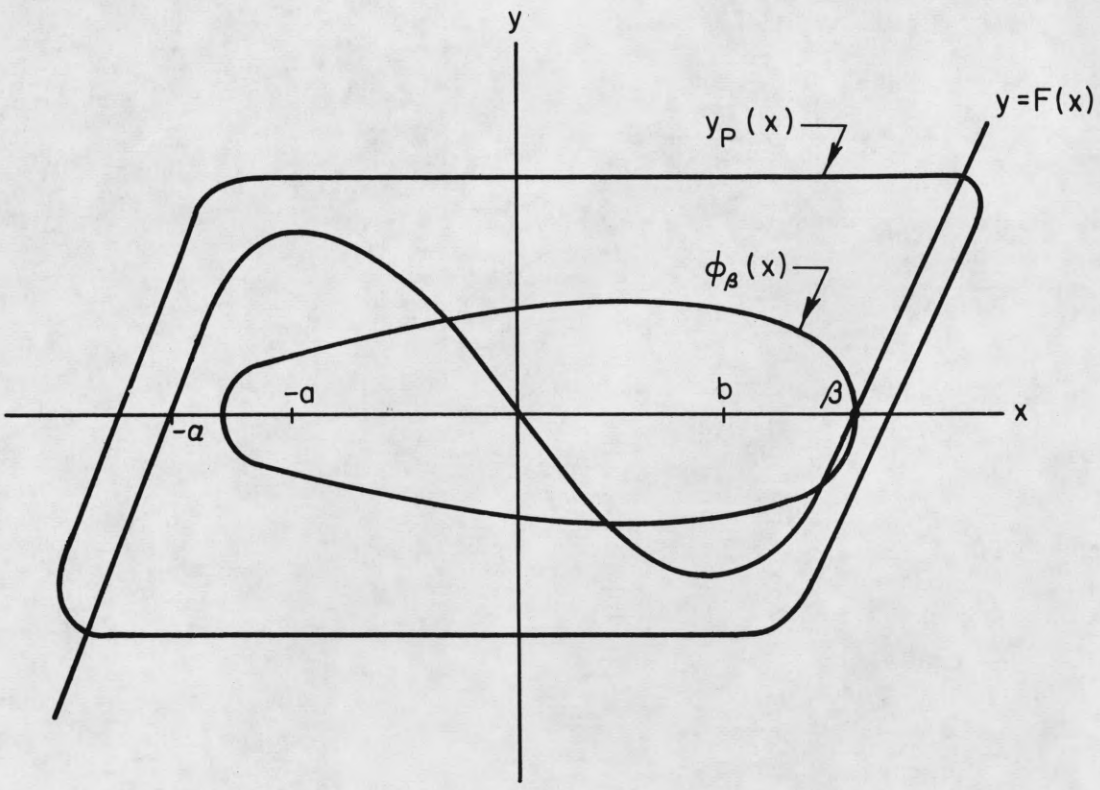

Figure 2

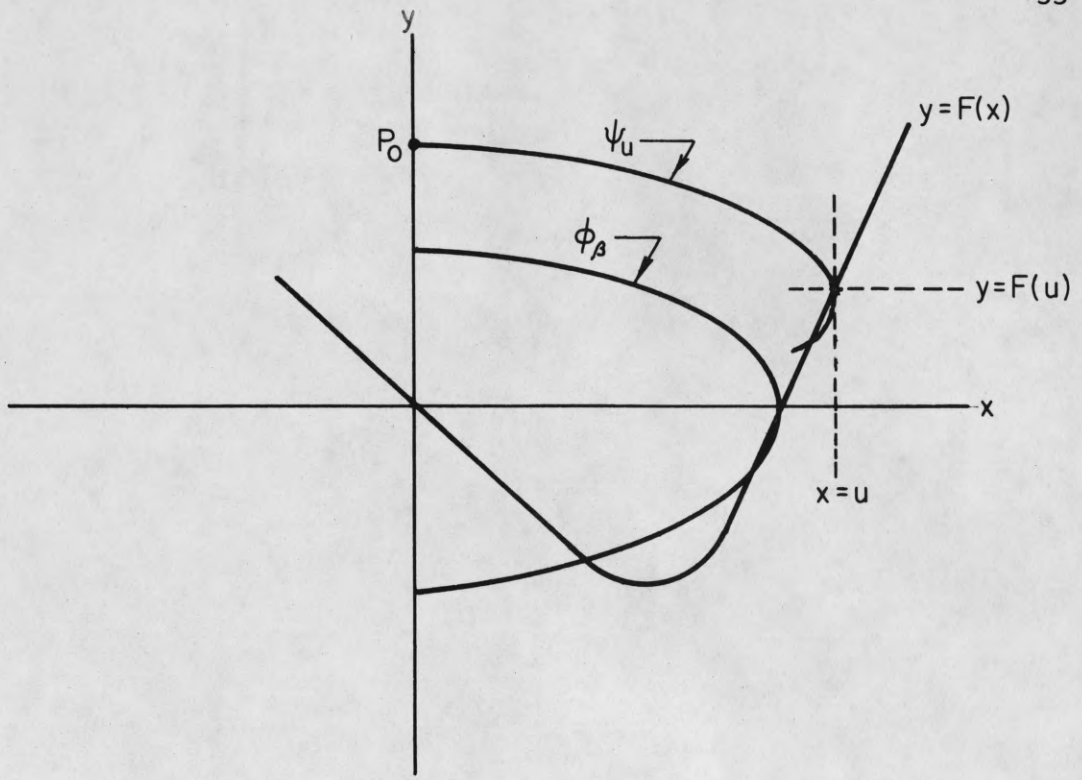

Figure 3

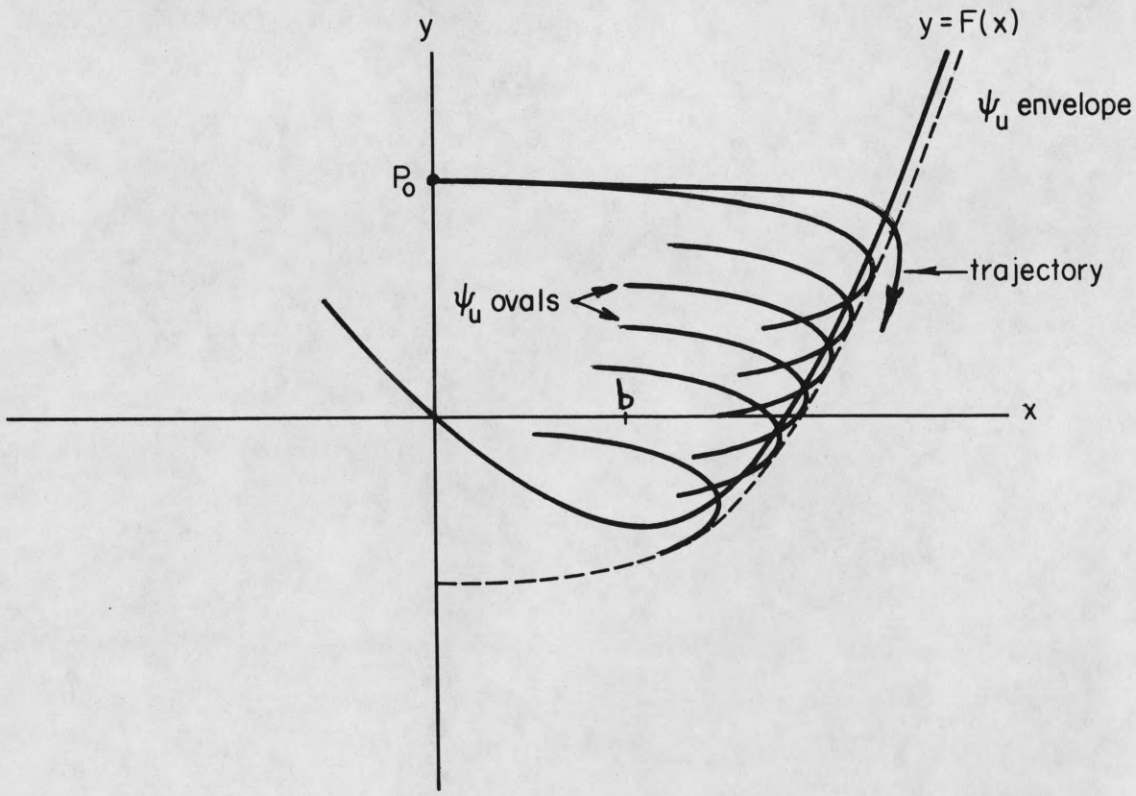

Figure 4

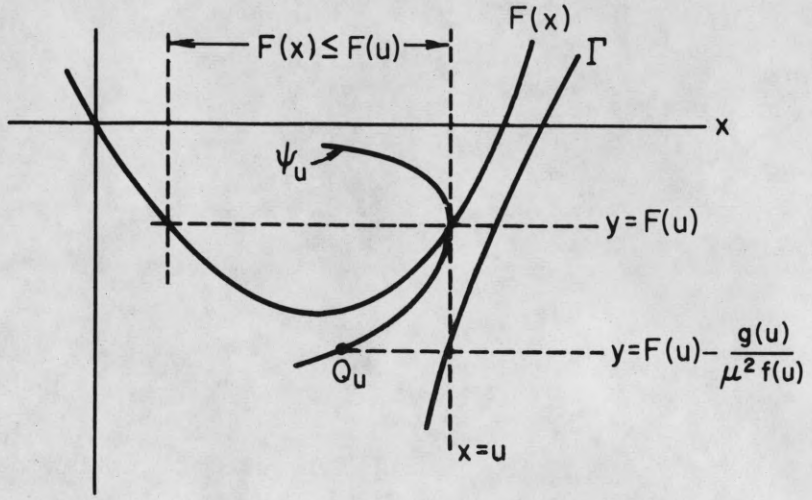

Figure 5

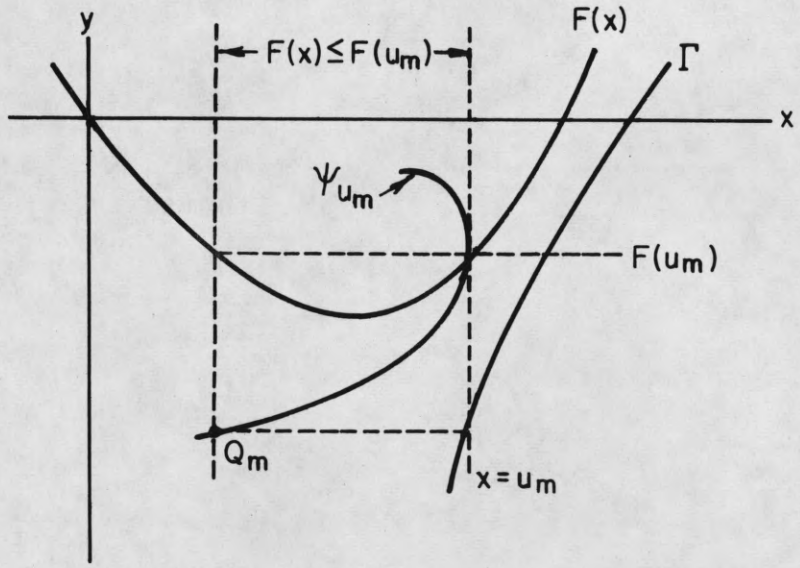

Figure 6

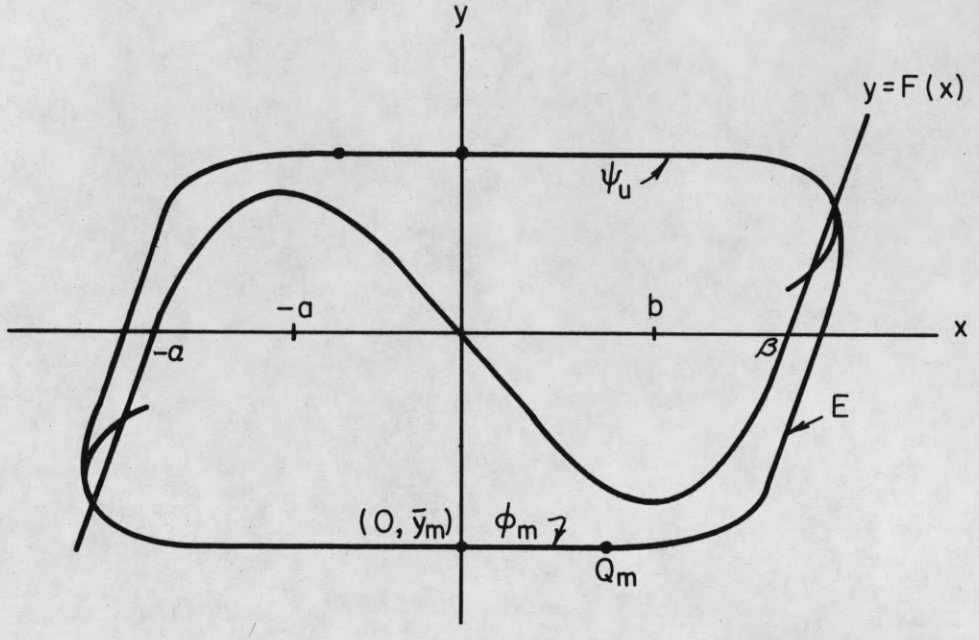

Figure 7

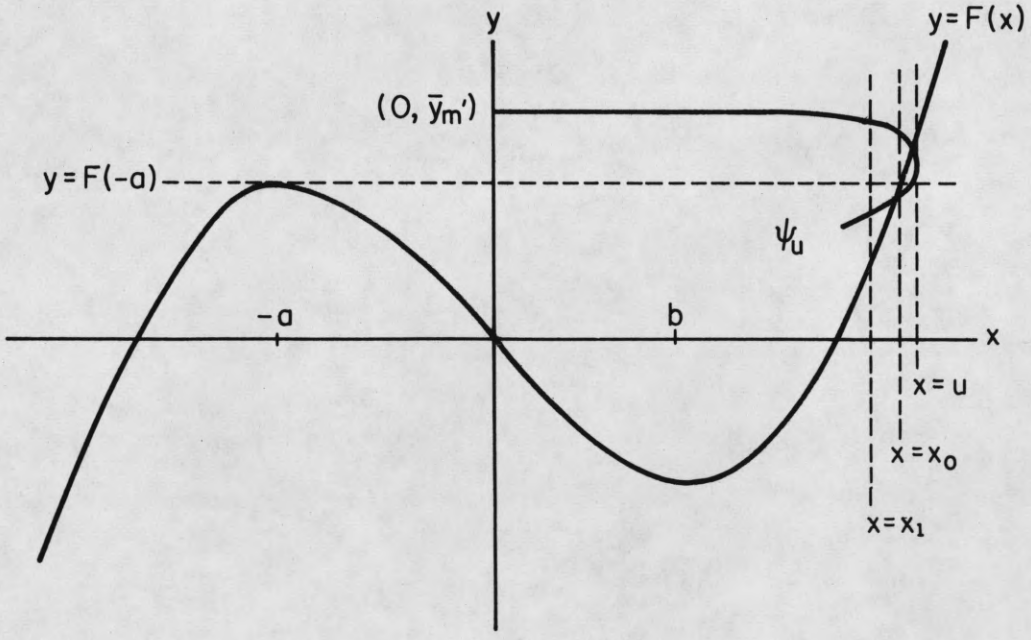

Figure 8

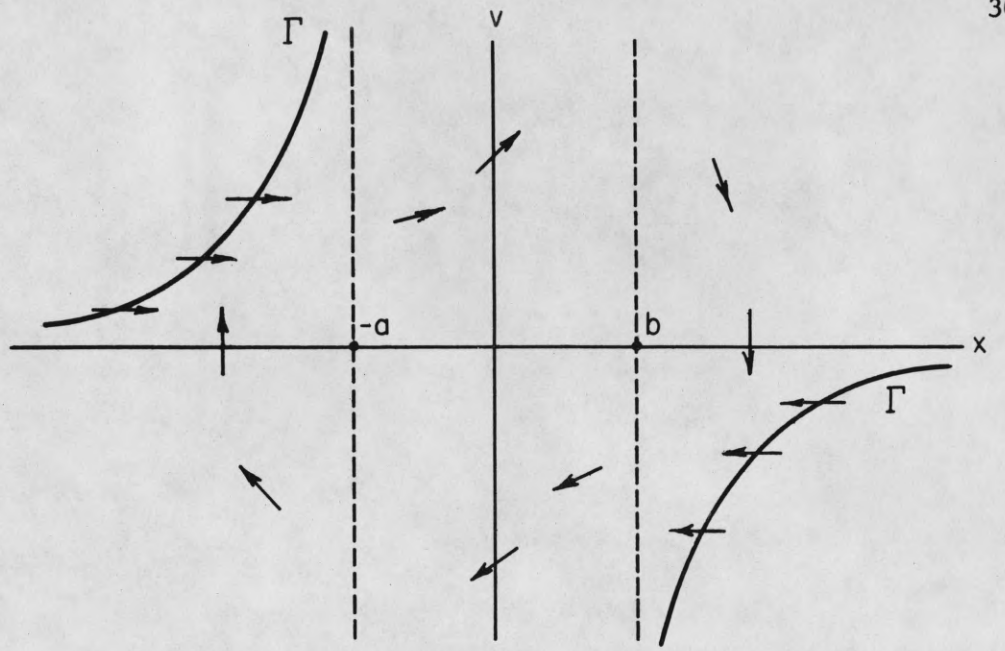

Figure 9(a)

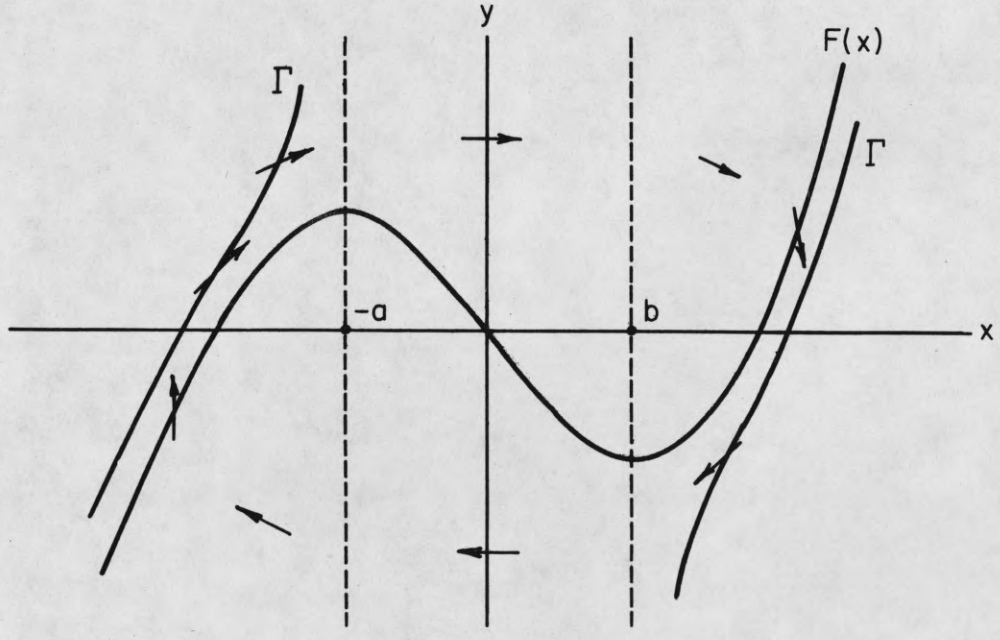

Figure 9(b)

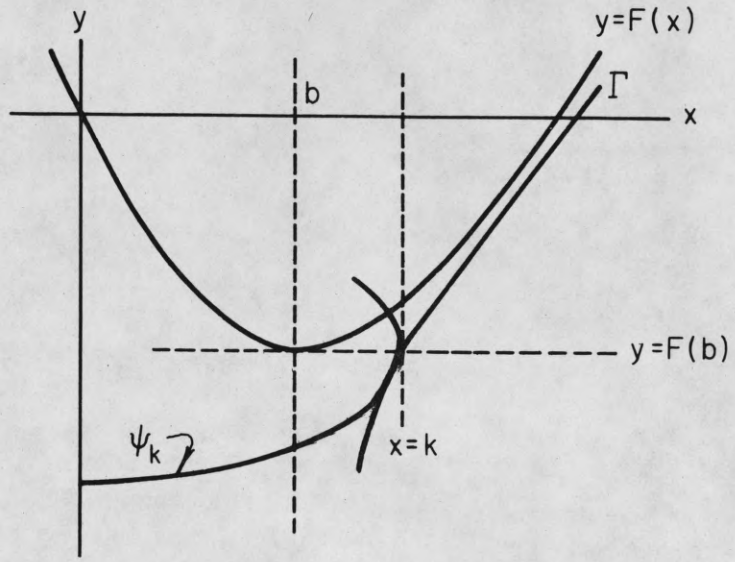

Figure 10

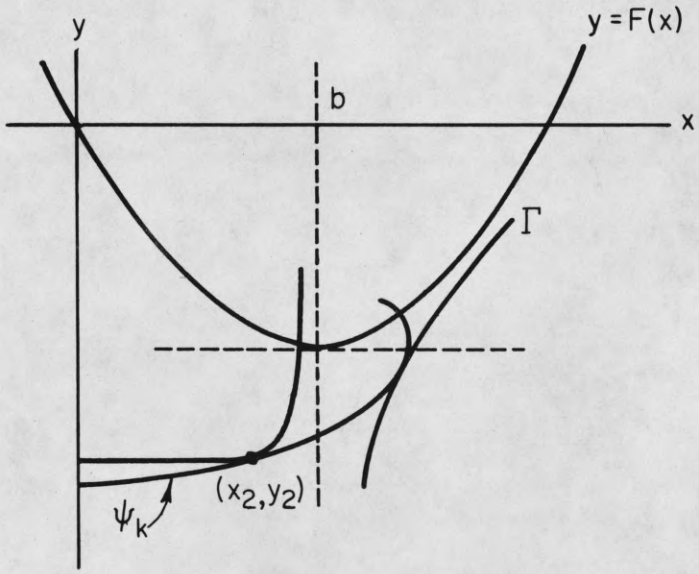

Figure 11

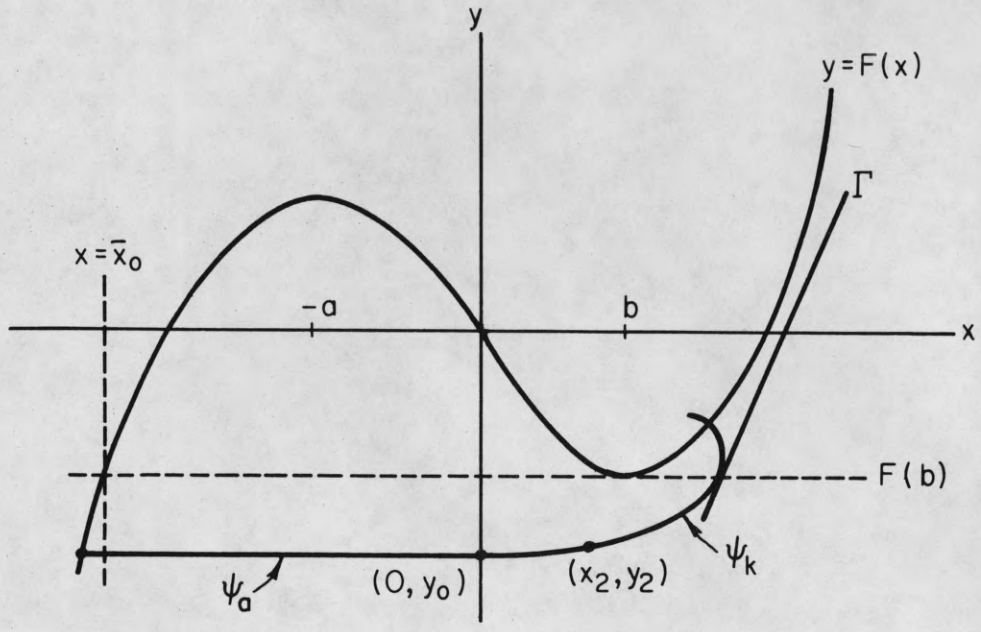

Figure 12

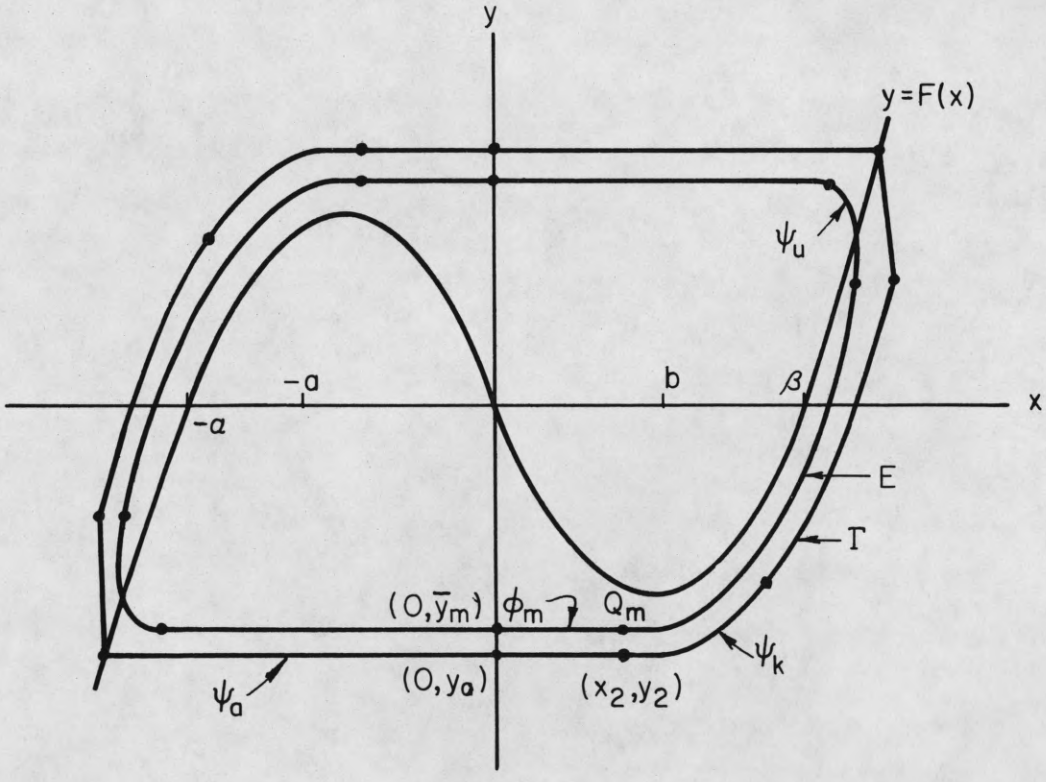

Figure 13

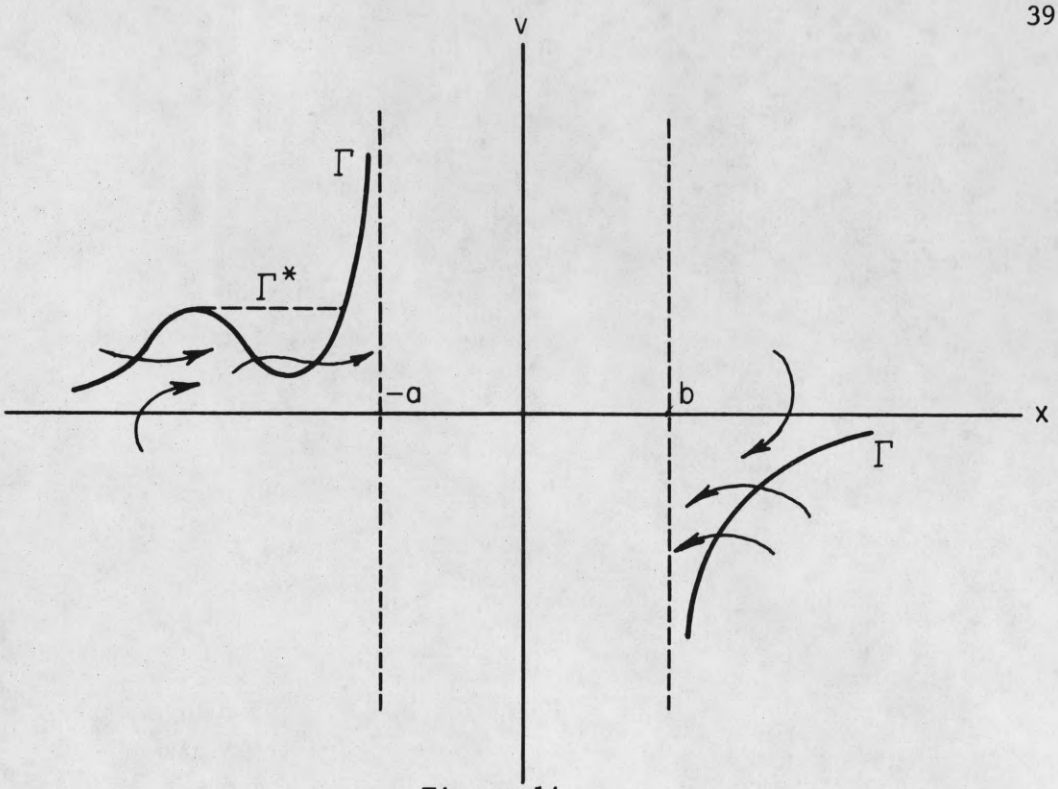

Figure 14

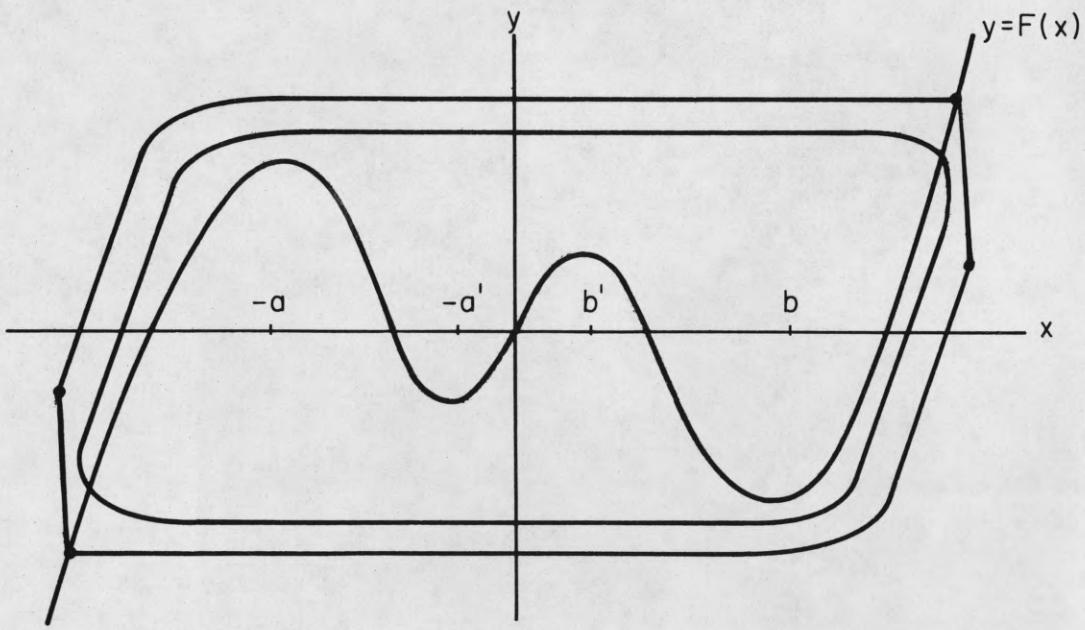

Figure 15

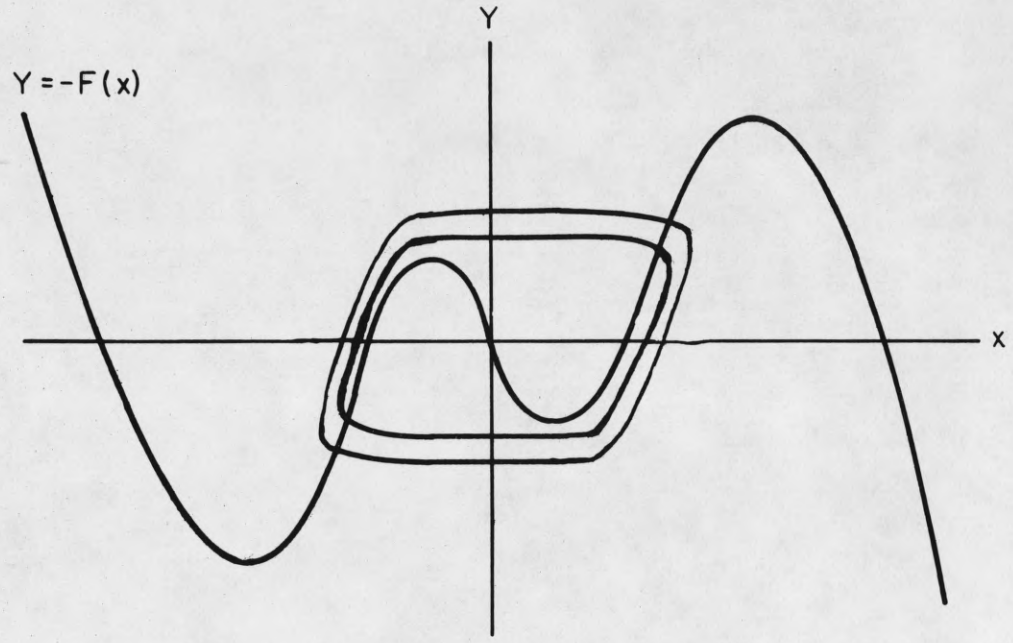

Figure 16

CHAPTER III

FORCED OSCILLATIONS IN A SECOND ORDER SYSTEM

3.1 INTRODUCTION

In this chapter we will consider the equation

$$\ddot{x} + \mu f(x)\,\dot{x} + g(x) = p(t) \tag{3.1}$$

where μ is a large positive parameter and

(a) $g(x)$ satisfies a Lipschitz condition, with $xg(x) > 0$ for $x \neq 0$. $G(x) = \int_0^x g(u)dU$ satisfies $G(\pm\infty) = \infty$,

(b) $F(x) = \int_0^x f(u)du$ satisfies a Lipschitz condition and $F(\pm\infty) = \pm\infty$,

(c) $p(t)$ and $P(t) = \int^t p(\tau)d\tau$ are bounded by all t, say $|p(t)| \leq 0(\mu)$, $|P(t)| \leq A \leq 0(\mu)$.

We will investigate the solution trajectories of the equivalent system:

$$\dot{x} = y_1 - \mu F(x) + P(t), \quad \dot{y}_1 = -g(x) \tag{3.2}$$

Note that the conditions of theorem 1 in the appendix are satisfield so that there exists a closed and bounded region R_0 in this plane such that all trajectories eventually enter and remain within R_0. Further we have $|x| \leq 0(1)$ within R_0, and $|y_1| \leq 0(\mu M+A)$ where $M = \max |F(x)|$ in R_0. For $M = 0(1)$ and $A \leq 0(\mu)$ we have $|y_1| \leq 0(\mu)$ in R_0, and consequently $|\dot{x}(t)| \leq 0(\mu)$ for all interior trajectories.

We state these remarks in a lemma.

LEMMA A:

All solutions to (3.2) eventually enter and remain in a closed and bounded region R_0 within which $|x(t)| \leq 0(1)$, $|\dot{x}(t)| \leq 0(\mu)$. From

(3.1) it is clear that $|\ddot{x}(t)| \leq 0(\mu^2)$ for solutions in R_0.

We will be concerned with the construction of annular regions in the plane with the property that solution trajectories, having entered such an annulus, must thereafter remain in the annulus. It will be convenient however to scale the coordinate y and consider, rather than (3.2), the plane defined by

$$\dot{x} = \mu(y - F(x) + P(t)/\mu), \quad \dot{y} = -g(x)/\mu \tag{3.3}$$

where we have set $y_1 = \mu y$.

Note that we have for this plane a region R_1 (the result of scaling R_0) within which $|x| \leq 0(1)$ and $|y| \leq 0(1)$. In (3.3) the term $P(t)/\mu$ is bounded by A/μ for all t, and we will write $\gamma = A/\mu$ so that $|P(t)/\mu| \leq \gamma$. If for example $p(t) = B \sin \omega t$ then we may take $P(t) = -B/\omega \sin \omega t$ so that $\gamma = B/\mu\omega$. Recall that this parameter had special significance for the forced van der Pol equation where Cartwright and Littlewood have determined that $\gamma = 2/3$ is a critical value. We will find below that the construction of annuli will succeed only for certain ranges of values for γ.

Observe now that the assumed conditions (a) - (c) assure the existence and uniqueness of solutions to (3.3) in x, y, t space, with $(\dot{x}, \dot{y}, 1)$ the unique velocity vector associated with each point of the space. The trajectories we consider, however, are the projections, onto the x, y plane, of motions in x, y, t space. For each point (x, y) in the plane then, the solution direction is not uniquely defined. Indeed the x component of the velocity in the plane may assume values in the range $\mu(y - F(x) - \gamma) \leq \dot{x} \leq \mu(y - F(x) + \gamma)$. The confinement of solution trajectories to the interior of same region must then be such that

all directions associated with a point on the boundary are directed toward the interior of the region. This can be achieved if we construct the region so that the direction limits, for which $\dot{x} = \mu(y - F(x) - \gamma)$ and $\dot{x} = \mu(y - F(x) + \gamma)$, satisfy this condition. This leads naturally to the investigation of a system, related to (3.3), where each point in the plane is assigned a velocity limit. That is, we set $\dot{x} = \mu(y - F(x) \pm \gamma)$ depending upon the type of solution confinement desired. There results an autonomous system of equations whose trajectories serve to bound the forced trajectories of (3.3) either away from or toward the origin. It is these autonomous trajectories which will provide the boundaries of our annuli.

3.2 THE FIRST AUXILIARY SYSTEM (FAS)

Figure 17 indicates the direction limits for some typical points in the plane, where $y = F(x)$ is a van der Pol type of characteristic curve. We note the following:

(i) $\dot{x} > 0$ for $y > F(x) + \gamma$ and $\dot{x} < 0$ for $y < F(x) - \gamma$.

(ii) On $y = F(x) + \gamma$ we have $\dot{x} \geq 0$ so that this curve is crossed only from the above in $x > b$, for example. Similarly, $\dot{x} \leq 0$ on $y = F(x) - \gamma$ so that this curve is crossed only from below in $x < -a$.

(iii) For $y > F(x) + \gamma + 0(1)$, then $\dot{x} = 0(\mu) > 0$ and solutions move rapidly to the right until $y = F(x) + \gamma$ is reached.

Similarly, for $y < F(x) - \gamma - 0(1)$ we have $-\dot{x} = 0(\mu) > 0$ and solutions move rapidly to the left until $y = F(x) - \gamma$ is reached. In general then, trajectories tend to move quickly toward the "strip": $F(x) - \gamma \leq y \leq F(x) + \gamma$.

Consider now the curve generated by starting at some point in $x > 0$ and "following" the rightmost direction limits. Such a curve will evidently intersect the negative y-axis. We now follow the leftmost directions in $x < 0$ until intersection with the positive y-axis occurs; we continue again into $x > 0$ along the rightmost directions. The curve so generated will then be such that no solution trajectory may cross this curve from within; that is, from the origin side of the curve. If it were possible to construct a closed curve in this manner, such a contour would provide confinement for interior trajectories. We show that such a closed curve does in fact exist.

A curve generated according to the above scheme will have a direction given by

$$\dot{x} = \mu(y - F(x) + \gamma), \quad \dot{y} = -g(x)/\mu \quad \text{in } x > 0$$

and

$$\dot{x} = \mu(y - F(x) - \gamma), \quad \dot{y} = -g(x)/\mu \quad \text{in } x < 0.$$

In other words, it will be a solution trajectory for the autonomous system:

$$\dot{x} = \mu(y - F_1(x)), \quad \dot{y} = -g(x)/\mu \tag{3.4}$$

where

$$F_1(x) = F(x) - \gamma \quad \text{in } x > 0$$

$$= F(x) + \gamma \quad \text{in } x < 0.$$

We will refer to this system as the First Auxiliary System (FAS).

If $F(x)$ is a van der Pol type of characteristic, then $y = F_1(x)$ will have the form indicated in Figure 18. A typical trajectory for the FAS equations (3.4) is illustrated in the figure. Several direction limits for the original forced system (3.3) are marked on this FAS trajectory. Note that the FAS trajectory will confine "interior", forced trajectories. It is also evident from the results of Chapter II that,

for the type of curve illustrated in Figure 18, the FAS equations admit a limit cycle. This limit cycle will then provide the outer boundary for an annulus which we will construct. Figure 19 illustrates the (unique) limit cycle C_0 of the FAS equations.

Observe that FAS trajectories suffer a discontinuity in $\dot{x}(t)$ of magnitude $2\mu\gamma$ upon crossing the y-axis. Note too, that the segment $-\gamma < y < \gamma$ on the y-axis is "singular" in the sense that all FAS trajectories move away from this segment (as indicated in Figure 19). Our interest however is in the geometry of FAS trajectories and, in particular, the location of the limit cycle C_0. Except for the singular segment on the y-axis, the direction of FAS trajectories is defined everywhere and this is sufficient to proceed with the geometrical determination of the limit cycle. Analytically, we imagine solutions in $x \geq 0$ as being terminated at $x = 0$ and a new solution generated in $x \leq 0$ using the terminal conditions for the $x \geq 0$ solution as initial conditions for the $x \leq 0$ solution. It is evident that all solutions will be continuous and piecewise differentiable.

Observe that the limit cycle C_0 will exist regardless of the precise nature of $P(t)$. We require only that $|P(t)| \leq A$. If, however, $P(t)$ is periodic with period τ, then the corollary to theorem 1(appendix) may be applied to the region interior to C_0 with the result that C_0 contains a periodic solution to (3.3) in its interior, and this solution has the period τ. In some cases however we may determine a closed curve interior to C_0, say C_1, such that C_1 will contain a periodic solution with period τ. We will investigate this possibility now.

Consider the solutions to (3.3) in reversed time. That is, we

set $t = -t'$ and $y = -Y$ to obtain the equations which govern the motion in reversed time t', namely:

$$\dot{x} = \mu(Y + F(x) - P(-t')/\mu), \quad \dot{Y} = -g(x)/\mu \tag{3.5}$$

The FAS associated with (3.5) is

$$\dot{x} = \mu(Y - \bar{F}_1(x)), \quad \dot{Y} = -g(x)/\mu \tag{3.6}$$

where $\bar{F}_1(x) = -F(x) - \gamma$ in $x > 0$

$= -F(x) + \gamma$ in $x < 0$, as in Figure 20.

Then the trajectories to (3.6) will serve to confine the reverse motions governed by (3.5). From Figure 20 it is evident that (3.6) possesses a limit cycle $\bar{C}_1$, provided $\gamma < -F(b) - \gamma$ and $-\gamma > -F(-a) + \gamma$; that is, provided $2\gamma < \min(F(-a), -F(b))$ and μ is sufficiently large.

The limit cycle $\bar{C}_1$ may only be crossed, by solutions to (3.5) toward its interior. That is, $\bar{C}_1$ will confine interior trajectories of the equations of reverse motion. If $P(t)$ hence $P(-t')$ is periodic with period τ, then $\bar{C}_1$ will contain a periodic solution to (3.5), with period τ. This follows from the application of the Brouwer fixed point theorem to the region of $\bar{C}_1$, as in the corollary to theorem 1 (appendix). If this periodic solution is $(x_o(t'), Y_o(t'))$ then $(x_o(-t), -Y_o(-t))$ is a periodic solution to the original equations (3.3) of direct motion, and is contained in the interior of C_1 (here C_1 is the result of changing back to the original time and ordinate variables).

Figure 20 illustrates the confining contour C_o, and for $2\gamma < \min(F(-a), -F(b))$, the contour C_1. We note however that although C_0 is confining C_1 is excluding. That is, C_1 excludes exterior trajectories from its interior. ($\bar{C}_1$ was confining for the reverse motions,

so C_1 is excluding for direction motions.) Nevertheless C_1 contains a closed periodic orbit. We may show however that this periodic solution is completely unstable for $\mu \gg 1$. To do this we will demonstrate that this solution is completely stable in reverse time t'. Indeed we will show that all reverse motions within $\bar{C}_1$ (Figure 20) converge to this periodic solution $(x_o(t'), Y_o(t'))$ as $t' \to \infty$.

Referring to the arguments used in the proof of theorem 2 (appendix) we have, for any two solutions $(x_1(t'), Y_1(t'))$ and $(x_2(t'), Y_2(t'))$ of (3.5) within $\bar{C}_1$, that $\xi(t') = x_2(t') - x_1(t')$ and $\eta(t') = Y_2(t') - Y_1(t')$ satisfy.

$$\dot{\xi} = \mu(\eta + f(\psi)\xi), \quad \mu\dot{\eta} = -g'(\Phi)\xi \quad \ldots(\cdot) = d/dt'$$

where $\psi(t') = x_1(t') + \theta_1 \xi(t')$ and $\Phi(t') = x_1(t') + \theta_2\xi(t')$, $0 < \theta_1, \theta_2 < 1$.

Then the quantity $\sigma^2 = g'(\Phi)\xi^2/2 + \eta^2$ satisfies $d\sigma^2/dt' = -(-2g'(\Phi)f(\psi) - \dot{g}'(\Phi)/\mu)\xi^2/\mu$.

Then for x in $\bar{C}_1$, and $B = \max |\dot{x}(t')|$ in $\bar{C}_1$, we have $f(x) \leq -\alpha < 0$, $g'(x) \geq \beta > 0$ and $\dot{g}'(x) \leq g''_{max}(x) \cdot B$ so that $d\sigma^2/dt' \leq -(2\alpha\beta - g''_{max} B/\mu)\xi^2/\mu$ (see theorem 2).

If μ is sufficiently large then $2\alpha\beta - g''_{max} B/\mu \geq L > 0$ say, so that $d\sigma^2/dt' \leq -L\xi^2/\mu$. As in theorem 2 (appendix) we conclude that $\sigma^2(t') \to 0$ as $t' \to \infty$ so that $\xi(t') \to 0$ and $\eta(t') \to 0$. That is, all reverse motions within $\bar{C}_1$ converge to a common solution, which is clearly the periodic solution which exists in $\bar{C}_1$. This periodic solution is then stable in reverse time t'. Returning again to direct motions, the periodic solution persists, in C_1, but is completely unstable. That is, all neighboring solutions to the periodic solutions, within C_1, diverge

from it as $t \to \infty$.

We have shown then, for an equation of the van der Pol type with P(t) periodic and $2\gamma < \min(F(-a),-F(b))$ that (i) a periodic solution exists within C_1 (Figure 21), (ii) it has the period of P(t), and (iii) it is completely unstable. This result is valid for μ sufficiently large. Further it is evident that this result applies to a wider class of equations than simply the van der Pol type. Indeed we need only require that $f(o) < 0$, that γ be sufficiently small, and μ sufficiently large. In the neighborhood of the origin, these requirements lead to the situation shown in Figure 22. In general then, for $f(o) < 0$ and the amplitude of the periodic forcing term sufficiently small, an unstable periodic solution exists in the neighborhood of the origin, with the same period as the forcing term.

In the introduction to this chapter we pointed out that in some cases, annular regions may be obtained for the system (3.3) such that solution trajectories within an annulus must remain therein. Referring to Figure 21 we may observe that such an annulus has already been obtained, namely the region between C_0 and C_1. The condition for its existence is $2\gamma < \min(F(-a),-F(b))$. If this inequality is satisfied however a third countour C_2 lying between C_0 and C_1 may be determined. This contour, which we obtain below, is excluding, as is C_1, so that an improved annular region between C_0 and C_2 exists. For this we introduce the "Second Auxiliary System" associated with equations (3.3).

3.3 THE SECOND AUXILIARY SYSTEM (SAS)

Referring to Figure 17, we may follow, in $x > 0$, the leftmost

trajectory directions, and in $x < 0$ the rightmost directions. Such a curve will evidently yield "inner bounds" on solutions to (3.3). That is, solution trajectories may not cross such a curve toward its origin side. If a curve generated in this manner were a simple, closed, convex curve then it would exclude exterior trajectories. We may show that such a closed curve does exist, in some cases.

Curves generated according to the above scheme are trajectories of the autonomous "Second Auxiliary System":

$$\dot{x} = \mu(y - F_2(x)), \ \dot{y} = -g(x)/\mu \tag{3.7}$$

where $F_2(x) = F(x) + \gamma$ in $x > 0$

$= F(x) - \gamma$ in $x < 0$.

For an equation of the van der Pol type the SAS characteristic $y = F_2(x)$ has the form indicated in Figure 23. If the SAS equations (3.7) admit a limit cycle C_2, as shown, then C_2 would exclude forced solution trajectories of (3.3) from its interior.

It is evident that C_2 will exist for $\gamma < F(-a) - \gamma$ and $-\gamma > F(b) + \gamma$, or $2\gamma < \min(F(-a), -F(b))$.

If we add C_2 to the diagram in Figure 21 we observe that C_2 lies interior to C_0, and C_1 lies interior to C_2, as in Figure 24. The annular region defined by C_0 and C_2 will confine solution trajectories in its interior. We now have the annulus we set out to obtain, at least for the van der Pol type of equation. Further, for P(t) periodic, not only does C_1 contain a periodic solution, but any other periodic solutions (if they exist at all) necessarily lie within this annulus. This is a consequence of the following remarks.

First, it is clear that C_1 contains a single periodic solution

since all solution trajectories in C_1 converge, in reverse time, to this periodic orbit. Any other periodic solution must then lie exterior to C_1. Next we observe that trajectories exterior to C_1 eventually enter the C_0-C_2 annulus, being guided as it were by FAS and SAS contours as indicated in Figure 25 (where three typical forced trajectories of (3.3) begin at points P, Q, R at some time t_o). Consequently all periodic orbits other than the unstable periodic solution within C_1 must lie in the C_0-C_2 annulus. In particular, all stable periodic solutions lie in this annulus.

3.4 GENERAL SYSTEMS

If we consider systems where F(x) has several maxima and minima, then the associated FAS and SAS equations may admit several limit cycles. Consider for example the situation illustrated in Figure 26.

There are two "stable" annular regions (shown hatched) which confine forced solution trajectories, and an "unstable" annulus (shown dotted) which excludes forced trajectories. There is also an unstable region about the origin which excludes exterior trajectories. If P(t) is periodic, this region (near the origin) will contain an unstable periodic orbit with the period of P(t).

In a physical system described by equations (3.3), with a characteristic curve F(x), as in Figure 26, one might expect two distinctly different types of motion, corresponding to the two stable annuli. If the system begins at rest ($x = y = 0$) then a motion within the inner stable annulus will eventually arise. If the system begins remote from the origin ($x(t_o)$ and/or $\dot{x}(t_o)$ large), then the eventual

motion will lie within the outer stable annulus. Because of the instability of motions within the simple closed region about the origin, one does not expect a physical system (subject to perturbations) to remain within this region. Nevertheless, from a mathematical point of view, there exist motions which remain here for arbitrary lengths of time -- due to the confinement of reverse motions within this region. Similarly, it is evident that the unstable annulus will contain motions which remain therein for arbitrary time intervals, due to the confinement afforded by this annulus to reverse motions. Except for these two "unstable" regions, all trajectories will enter one or the other of the two stable annuli.

For P(t) periodic, we have only been able to demonstrate the existence of one periodic orbit; namely the unstable periodic solution in the neighborhood of the origin. There is reason to suspect however that stable periodic motions exist within the stable annuli. This is certainly true, for example, if the function F(x) had a van der Pol character near the origin, and g(x) = x. In such a case the behavior of solutions within the inner stable annulus would satisfy a forced van der Pol equation, and the results of Cartwright and Littlewood show that, among the complexity of solutions which are possible in this annulus, there exist stable periodic motions (either one or two, depending upon the amplitude of P(t) = A sin ωt). Although we are not able to prove the existence of periodic solutions within the annuli, for general F(x) and P(t) periodic, we will mention a few general properties of annular solutions, in the next section.

Referring to Figure 26, it is to be observed that $F(x)$ was so constructed that no difficulty is encountered in defining the annular regions, according to the geometrical scheme outlined in Chapter II. In Figure 27, however, we indicate a situation where this scheme fails to produce an annulus due to our inability to produce a limit cycle for the associated SAS equations. Nevertheless we might expect that solution trajectories would be trapped within the "partial annulus", unless they crossed $x = b$ $(y > 0)$ at a time when $P(t)/\mu$ had a value very near $-\gamma$. If this were the case the equations of motion, $\dot{x} = \mu(y - F(x) + P(t)/\mu)$, $\dot{y} = -g(x)/\mu$ would take a form $\dot{x} = \mu(y - F(x) - \gamma)$, $\dot{y} = -g(x)/\mu$ very nearly. That is, the solution trajectory would satisfy at this time and place the SAS equations, and it is quite possible that such a solution would leave the partial annulus and in fact move toward, and be trapped within, the simple closed confining region about the origin. Figure 27 illustrates this possibility, as well as the case where the solution remains in the partial annulus. Whether one or the other happens, or some other possibility, will depend critically upon the "phase" of $P(t)$ when $x = b$ is reached. However, since $\dot{x} = \mu(y - F(x) + P(t)/\mu) \geq \mu(y - F(x) - \dot{\gamma})$ and $y > F(x) + \gamma$ over most of the range $-a < x < b$, then $\dot{x} = 0(\mu)$ and this portion of the upper, partial annulus is traversed in a very short time. Consequently the phase of $P(t)$ at $x = b$ is very nearly the same phase as at $x = -a$. We will show in the next section that $P(t)/\mu$ is very nearly $+\gamma$ at $x = -a$ (in the upper part of the partial annulus) for "most" trajectories in the partial annulus. Then "most" trajectories will not leave the partial annulus but rather they will continue past $x = b$ and remain confined. The

meaning of "most" will be made clear in the next section.

It is evident that a complete annulus would exist, for the situation in Figure 27, for a slightly smaller value of γ. It is also evident that if γ were increased, the region about the origin (which is "stable" since the damping function $f(x)$ is positive here) would cease to exist. Nevertheless, the outer boundary of our partial annulus would be present for all values of γ and so would confine interior solutions. Further, it would contain a periodic solution for $P(t)$ periodic.

3.5 SOME PROPERTIES OF SOLUTIONS WITHIN AN ANNULUS

In general, the stable annuli we consider consist of portions which are nearly horizontal, as well as portions which have the "shape" of $F(x)$. Regions of negative damping are traversed by solutions while they are in the nearly horizontal portions of the annulus. Here, too, we have $|\dot{x}| = 0(\mu)$ since $|y - F(x) \overset{+}{-} \gamma| = 0(1)$, and the nearly horizontal portions are traversed very rapidly. It is not until such a solution reaches a region of positive damping that $|\dot{x}(t)|$ is reduced. This occurs for example when the solution enters the portions of the annulus which "follow" $y = F(x)$. Lemma B below is concerned with this transition from rapid (almost discontinuous) motion to the slower motion in the regions of positive damping.

Lemma C, below, indicates that a great deal of time is taken to traverse the portions of the annulus which follow $F(x)$. Consequently, if any periodic motions exist within the annulus (for $P(t)$ periodic) they necessarily have long periods, of the order of magnitude of μ as shown below.

Finally we mention, in Lemma D, that trajectories leave the

regions of positive damping (where the annulus follows F(x)) at a time when $P(t)/\mu$ is very nearly an extremum. Here we assume that $P(t)/\mu$, although not necessarily periodic, is oscillatory in nature and assumes the values $\pm\gamma$ in time intervals of order 1.

LEMMA B:

If a solution remains in a region of positive damping, where $f(x) \geq \alpha > 0$, for a time $0(\log \mu/\mu)$, then $|\dot{x}| < 0(1)$ thereafter in this region.

PROOF:

We write the equation $\ddot{x} + \mu f(x)\dot{x} + g(x) = p(t)$ in the form

$$d/dt(\dot{x} \exp(\mu\int_{t_o}^{t} f(x)du)) = (p(t) - g(x)) \exp(\mu\int_{t_o}^{t} f(x)du)$$

Then

$$\dot{x}(t) = \dot{x}(t_o) \exp(-\mu\int_{t_o}^{t} f(x)du) + \int_{t_o}^{t} (p(\tau)-g(x)) \exp(-\mu\int_{\tau}^{t} f(x)du)d\tau$$

where t_o is arbitrary. If we choose t_o to be the time of entry into a region for which $f(x) \geq \alpha > 0$, then $|\dot{x}(t_o)| \leq 0(\mu)$, and $|p(t)| \leq 0(\mu)$ so that $|\dot{x}(t)| < 0(\mu) \exp(-\mu\alpha(t-t_o)) + 0(\mu) \int_{t_o}^{t} \exp(-\alpha(t-\tau)d\tau$

or $|\dot{x}(t)| \leq 0(\mu) \exp(-\mu\alpha(t-t_o)) + 0(1)$,

for as long as $f(x) \geq \alpha > 0$. Note then, that the first term is reduced to 0(1) in a time interval $(t-t_o)$ which is $0(\log \mu/\mu)$ so that $|\dot{x}(t)| \leq 0(1)$ thereafter in $f(x) \geq \alpha > 0$, which proves Lemma B.

Observe that $|\dot{x}| = \mu|y - F(x) + P(t)/\mu|$ implies $y = F(x) - P(t)/\mu + 0(\mu^{-1})$. In other words, the solution trajectory remains within $0(\mu^{-1})$ of the "moving" characteristic curve $y = F(x) - P(t)/\mu$. This is the situation in those portions of the annulus which have the shape of $y = F(x)$. Although $|\dot{x}| \leq 0(1)$ here, we have $|\dot{y}| = |-g(x)/\mu| = 0(\mu^{-1})$ so that the descent in $x > 0$, or ascent in $x < 0$, is very slow.

If this portion of the annulus occupies a y-interval of length 0(1) it will take a time $0(\mu)$ to traverse this portion. Lemma C gives a lower bound on this time interval.

LEMMA C:

We consider a solution $(x(t), y(t))$ which lies in $x > 0$ in a region of positive damping $f(x) \geq \alpha > 0$ during a time interval between $t = t_1$, and $t = t_2$. We assume that $|\dot{x}(t_1)| \leq 0(1)$ which is certainly true if the solution has been in this region for a time $\geq 0(\log \mu/\mu)$. Then $t_2 - t_1 \geq \frac{\mu}{c}(F(x_1) - F(x_2) - 2\hat{\gamma}) + 0(1)$ where $C = \max g(x(t))$ in $t_1 \leq t \leq t_2$. Thus, if $F(x_1) - F(x_2) \geq 2\gamma + 0(1)$ we have $t_2 - t_1 \geq 0(\mu)$.

PROOF:

For $t_1 \leq t \leq t_2$ we have $y = F(x) - P(t)/\mu + 0(\mu^{-1})$ since $|\dot{x}(t)| < 0(1)$. Then

$$y_1 - y_2 = F(x_1) - F(x_2) - P(t_1)/\mu + P(t_2)/\mu + 0(\mu^{-1}) \geq F(x_1) - F(x_2) - 2\hat{\gamma} + 0(\mu^{-1}).$$

Since $\dot{y} = -g(x)/\mu < 0$ in $x > 0$, then

$$y_1 - y_2 = \frac{1}{\mu}\int_{t_1}^{t_2} g(x)d\tau \leq c/\mu(t_2 - t_1) \text{ for } c = \max g(x),\ t_1 \leq t \leq t_2,$$

and $t_2 - t_1 \geq \mu/c(F(x_1) - F(x_2) - 2\gamma) + 0(1)$.

If the trajectory is such that $F(x_1) - F(x_2) \geq 2\gamma + 0(1)$ then a time $0(\mu)$ at least, is required to traverse this segment of the orbit, which proves Lemma C.

If Lemma C is applied to the van der Pol type of characteristic in Figure 28 we have that the time necessary to traverse the portion of the annulus in $x > b$ is greather than $\mu/c(F(-a) - F(b) - 2\gamma) + 0(1)$. In order that this be $0(\mu)$ we must have $2\gamma < F(-a) - F(b)$ or $\gamma < (F(-a) + |F(b)|)/2$, the average magnitude of the local maximum

and mimimum of $F(x)$. If $F(x) = x^3/3 - x$, so that the curve is precisely the van der Pol characteristic, then $F(-1) = -F(1) = 2/3$ and the condition becomes $\gamma < 2/3$ (recall that $\gamma = 2/3$ is a critical value). Note however, that the annulus as we have constructed it, does not exist unless $2\gamma < \min(F(-a), -F(b))$, which for $F(x) = x^3/3 - x$ becomes $\gamma < 1/3$. For $1/3 < \gamma < 2/3$ we are only able to construct a partial annulus since the associated SAS equations do not provide a limit cycle to be used for the inner boundary. The partial annulus (with inner boundary constructed of "partial" SAS trajectories) is shown in Figure 29. This also applies for the general van der Pol type of equation, with $\min(F(-a), -F(b)) < 2\gamma < F(-a) - F(b)$.

Note that this difficulty also arose in connection with the characteristic of Figure 27, where we explained that solutions may in fact leave the partial annulus through the "gaps" in the inner boundary. We mentioned however that this escape could only occur at certain phases of $P(t)$.

Consider the possibility of a trajectory leaving the annulus of Figure 29 through the upper gap (in $y > 0$). The exact nature of this gap is unspecified as yet, except that it begins on $x = 0$ and extends to just beyond $y = F(x) + \gamma$, where we again continue the inner boundary with a SAS trajectory. Let us close this gap with a trajectory to the automomous equations of free oscillation: $\dot{x} = \mu(y - F(x))$, $\dot{y} = -g(x)/\mu$.

The gap will appear as in Figure 30, where we show several solution directions associated with the original equations (3.3).

Observe that the free trajectory we chose to fill the gap

will not confine all forced solution trajectories (to (3.3)) but only those which reach the gap at a time when $P(t) > 0$.

To see this, we compare the slope of the gap, namely $dy/dx = -g(x)/\mu^2(y - F(x))$, to the slope of a solution trajectory on the gap, namely $dy/dx = -g(x)/\mu^2(y - F(x) + P(t)/\mu)$. If $P(t) > 0$, then forced solutions will not leave the partial annulus through this gap. We show, in Lemma D below, that solutions which leave the region $x < -a$ of positive damping do so when $P(t)/\mu$ is very nearly $+\gamma$. These solutions will reach the position of the gap with $P(t)/\mu$ still $+\gamma$, very nearly. That is, "most" solutions within the partial annulus (meaning those solutions which have been in a region of positive damping for a time 0(1)) will not leave. We turn then to Lemma D, which will refer to solutions in the region $x \geq b$.

LEMMA D:

Let a solution begin, at $t = t_o$, in $x > b$ at a point (x_o, y_o) where $y_o = F(x_o) - P(t_o)/\mu + 0(\mu^{-1})$.

Let this solution reach $x = b$ for the first time at $t = t_1$ where $y(t_1) = y_1 = F(b) - P(t_1)/\mu + 0(\mu^{-1})$. Then at $t = t_1$, $P(t)/\mu$ is very nearly a negative maximum.

PROOF:

We assume that $P(t)/\mu$, although not necessarily periodic, is oscillatory and atains the values γ and $-\gamma$ in time intervals of length 0(1).

Setting $y_o - y_1 = \frac{1}{\mu}\int_{t_o}^{t_1} g(x)dt$ we write

$$-(F(x_o) - F(b)) + \frac{1}{\mu}\int_{t_o}^{t_1} g(x)dt = P(t_1)/\mu - P(t_o)/\mu + O(\mu^{-1}) \quad (3.8)$$

and regard this as an equation to be solved for t_1, the time of first intersection with $x = b$.

The solution to this equation is shown graphically in Figure 31.

If $\gamma + P(t_o)/\mu \leq 2\gamma < F(x_o) - F(b)$, then the left-hand side of (3.8) is less than the right side for $t_o \leq t \leq t_1$. In Figure 31, the left side is represented by a curve which rises slowly from $-(F(x_o) - F(b))$ at $t = t_o$ with a slope $g(x)/\mu = O(\mu^{-1})$. Clearly, if $2\gamma + O(1) < F(x_o) - F(b)$ then the time of intersection, $t_1 - t_o$, is of the order of μ (as has been demonstrated in Lemma C). Further, it is clear that t_1 will occur very nearly at a minimum of $P(t)/\mu$.

At $t = t_1$ we evidently have $P(t_1)/\mu \leq -\gamma + O(\mu^{-1})$. If $P(t)/\mu$ has quadratic behavior near its minimum, say $P(t)/\mu = -\gamma + O(t - \bar{t}_1)^2)$ where $\bar{t}_1$ is the exact time at which the minimum is attained, then $|t_1 - \bar{t}_1| = O(\mu^{-1/2})$. That is, for a quadratic minimum, $x = b$ is reached at a time when $P(t)/\mu = -\gamma$ to within a time error $O(\mu^{-1/2})$.

In a similar way we may show that a solution in $x < -a$ will reach $x = -a$ at a time when $P(t)/\mu \geq \gamma - O(\mu^{-1})$.

Consider now a solution reaching $x = -a$ with $P(t)/\mu \doteq \gamma$. Such a solution may or may not decisively enter the region $-a < x < b$. It is quite likely that it will dip slightly into this region, then return to $x < -a$, "following the moving characteristic $y = F(x) - P(t)/\mu$. In a time $O(1)$ we will have $P(t)/\mu = \gamma$ again, and $x = -a$ will be crossed again. At each intersection with $x = -a$ however, the deviation of y from $F(x) - P(t)/\mu \doteq F(-a) - \gamma$ will increase by $O(\mu^{-1})$ since $\dot{y} = O(\mu^{-1})$ during the time $O(1)$ between intersections. Then $\dot{x} = \mu(y - F(-a) + \gamma)$

will increase by O(1) and consequently, after a few such oscillations and intersections with $x = -a$, the solution will quickly and decisively enter $-a < x < b$. When this occurs we will have $P(t)/\mu = \gamma + O(\mu^{-1})$ so that $\dot{x} = \mu(y - F(x) + \gamma) + O(1)$, $\dot{y} = -g(x)/\mu$. That is, the solution is approximately an autonomous trajectory for a short time. From Chapter II we see that such an autonomous trajectory will reach the gap of Figure 30 in a time $\leq O(\mu^{-1/3})$. (This follows from $dt = -\mu dy/g(x)$ and $|dy| \leq O(\mu^{-4/3})$ for autonomous trajectories over this region.) Then, at the gap, $P(t)/\mu = \gamma + o(1)$ where o(1), the deviation of $P(t)/\mu$ from γ, is a quantity which vanishes as $\mu \to \infty$. In order to leave the partial annulus through this gap (which we have closed with a free trajectory) we recall that P(t) must be negative. Consequently, "most" trajectories within the partial annulus will not leave it.

In a similar manner we may close the gap in $y < 0$ with a free trajectory. Normal annular trajectories will reach this lower gap with $P(t)/\mu = -\gamma$, very nearly, and will not leave the annulus.

We conclude that although a confining annulus exists only for $2\gamma < \min(F(-a), -F(b))$ a partial annulus will exist for $2\gamma < F(-a) - F(b)$ and will confine normal annular trajectories.

3.6 SUMMARY

We have described in this chapter how confining regions may be obtained in some cases, for solution trajectories satisfying $\dot{x} = \mu(y - F(x) + P(t)/\mu)$, $\dot{y} = -g(x)/\mu$. The construction of these regions depends upon the existence of limit cycles of associated autono-

mous systems, in which case the methods of Chapter II may be applied to locate the limit cycles.

It is to be noted that the annuli so obtained reduce to the limit cycles of the unforced system, as the forcing amplitude (measured by γ) goes to zero. That is, we expect annuli for a forced system, in the neighborhood of limit cycles for the unforced system (with $p(t) = 0$). Further, stable and unstable singularities at the origin, for the unforced system, give rise to stable and unstable (respectively) periodic motions of the forced system, for small amplitude, periodic forcing.

We have also mentioned some dominant analytic properties of the solutions. These properties have allowed us to construct a partial annulus, when γ is too large for the existence of a confining annulus, such that most solution trajectories will remain within this partial annulus. For γ larger than some critical value, neither a confining nor a partial annulus will exist.

It has been mentioned that Cartwright and Littlewood find that 2/3 is the critical value of γ for the harmonically forced equation of van der Pol. For $0 < \gamma < 2/3$ they describe in detail the nature of the solutions which, as we see, lie within the annulus we construct ("confining" for $0 < \gamma < 1/3$ and "partial" for $1/3 < \gamma < 2/3$). For $\gamma = 2/3$, very little can be said concerning the nature of solutions. We note however, the following interesting special case of the forced van der Pol equation:

$$\ddot{x} + \mu(x^2 - 1)\,\dot{x} + x = 2\mu \sin 3t$$

For this equation we evidently have $\gamma = 2/3$ (since $P(t) = -\frac{2}{3}\mu \cos 3t$ and $|P(t)/\mu| \leq \frac{2}{3} = \gamma$).

A solution to this equation is $x(t) = -2 \cos t$; a subharmonic of order three. We note that this solution possesses some of the properties common to all stable solutions within the annulus (for $\gamma < 2/3$). For example $|x(t)|_{max} = 2$ and it is clear from the geometry of the annulus that all solutions therein have a maximum amplitude which is very nearly 2. Further, $x(t)$ leaves the region $x < -1$ of positive damping at a time ($t = \pi/3 \bmod 2\pi$) when $P(t)/\mu = 2/3 \cos 3t$ has exactly the value 2/3. Perhaps the most remarkable property of this solution is its complete lack of dependence on μ.

We might also mention that exact solutions, such as the solution -2 cos t above, may be obtained for a variety of nonlinear differential equations. Indeed, $x = \cos(\omega t)$ is a subharmonic solution of order n for the equation

$$\ddot{x} + \mu/n\, T'_n(x)\dot{x} + \omega^2 x + \lambda T_n(x) = \lambda \cos(n\omega t) - \mu\omega \sin(n\omega t).$$

Here $T_n(x)$ is the Tschebychev polynomial of order n, and μ, ω, λ are arbitrary parameters. For $n = 3$, $\omega = 1$, $\lambda = 0$ this equation reduces to the van der Pol equation mentioned above (with the dependent variable scaled by 2).

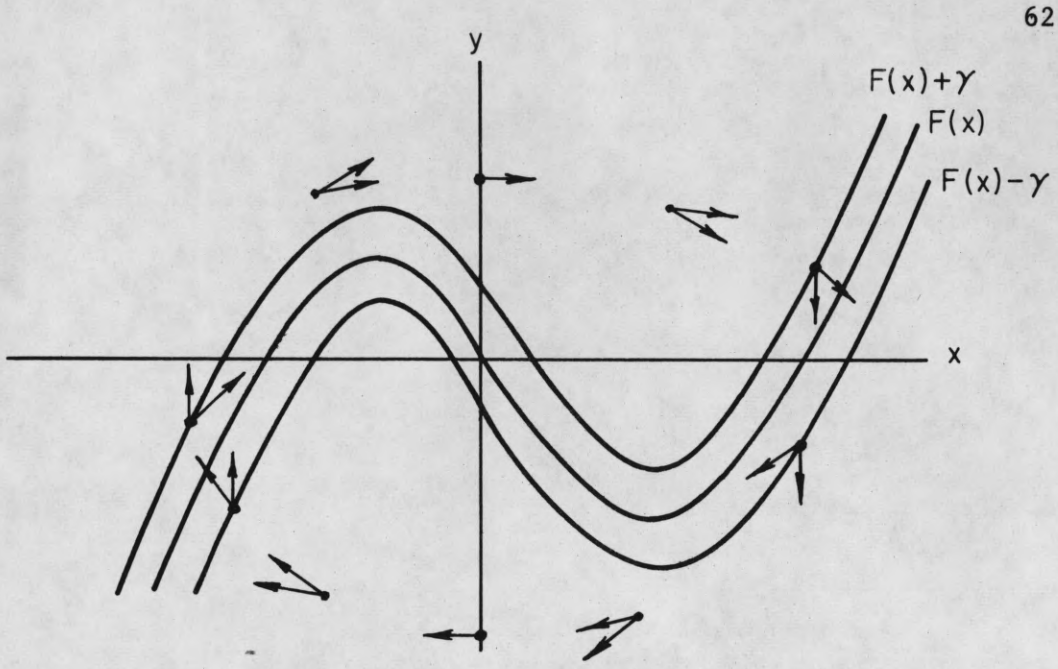

Figure 17

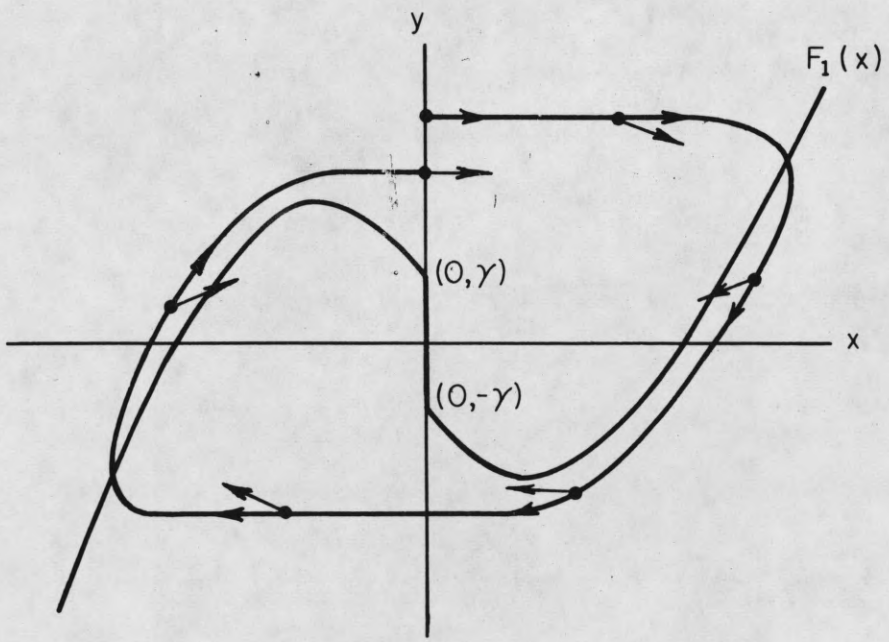

Figure 18

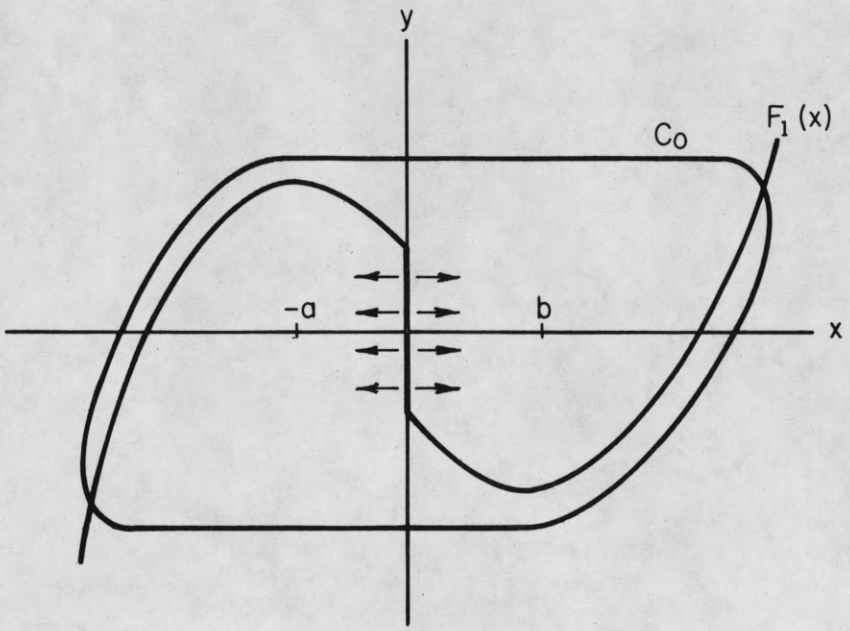

Figure 19

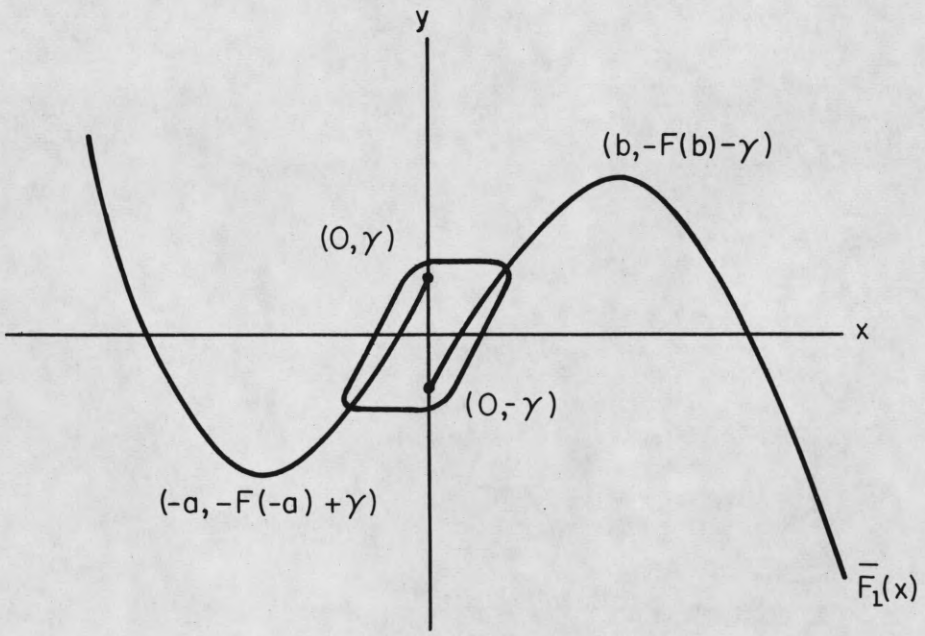

Figure 20

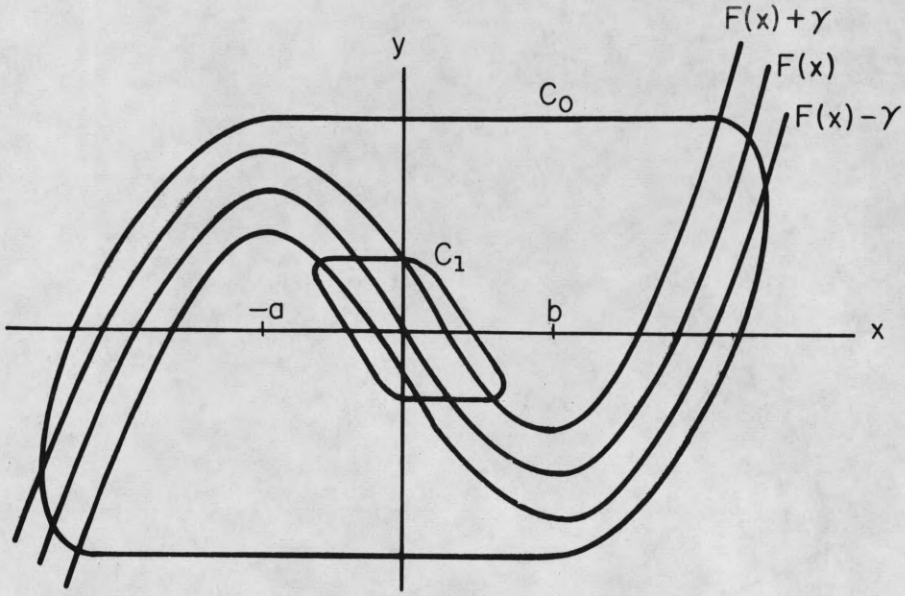

Figure 21

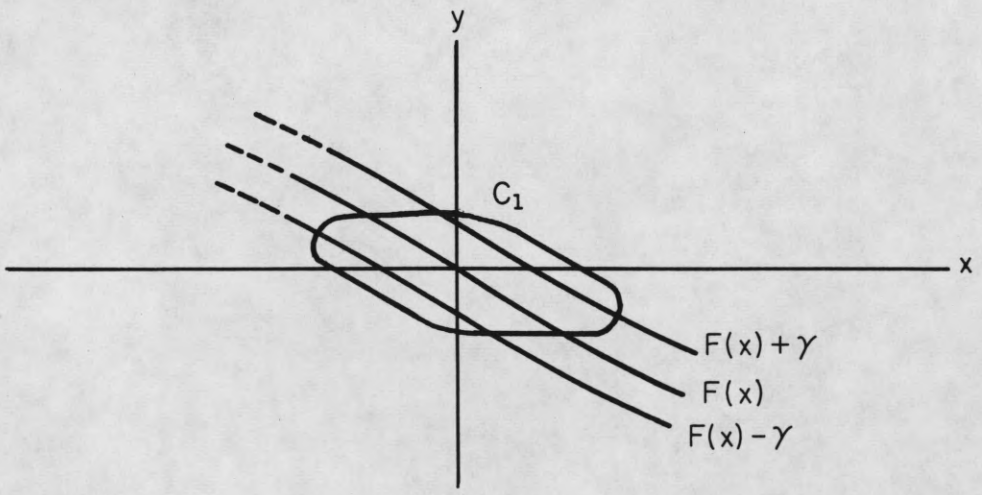

Figure 22

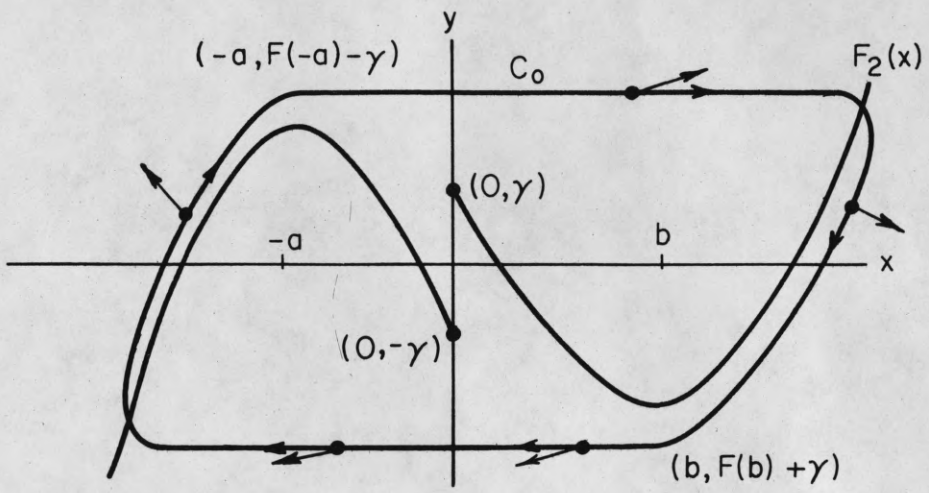

Figure 23

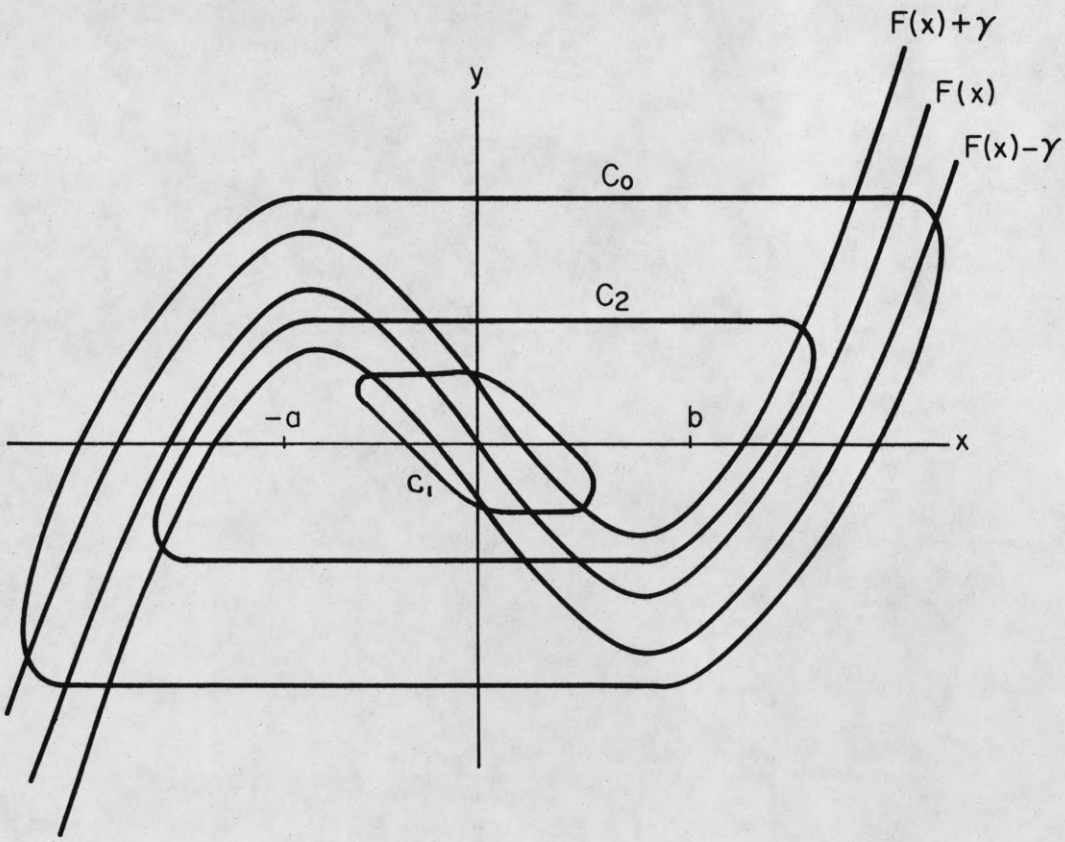

Figure 24

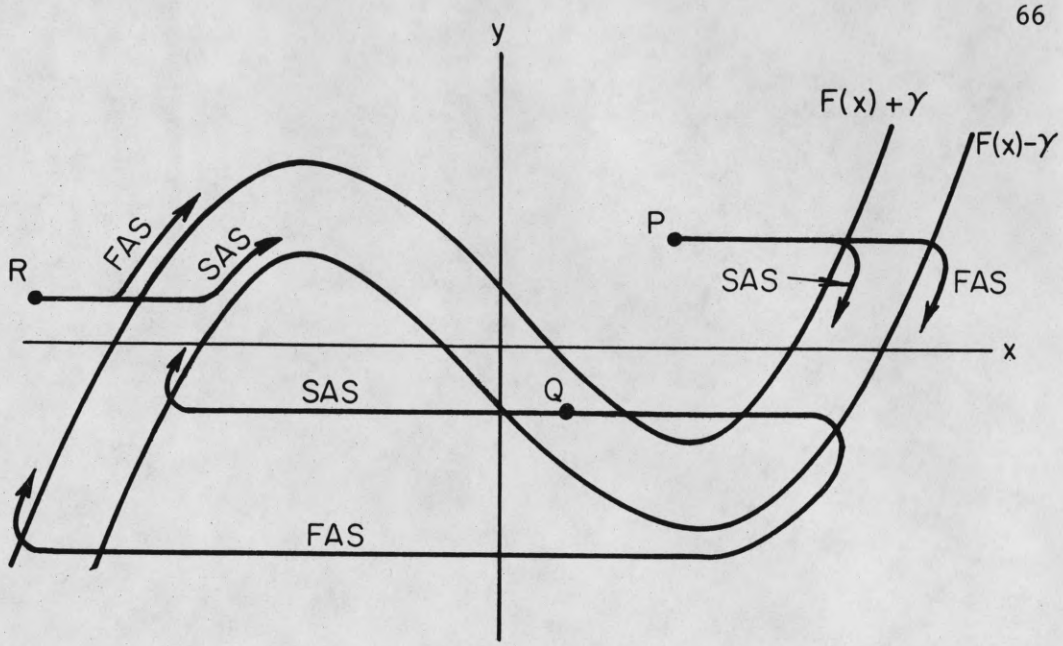

Figure 25

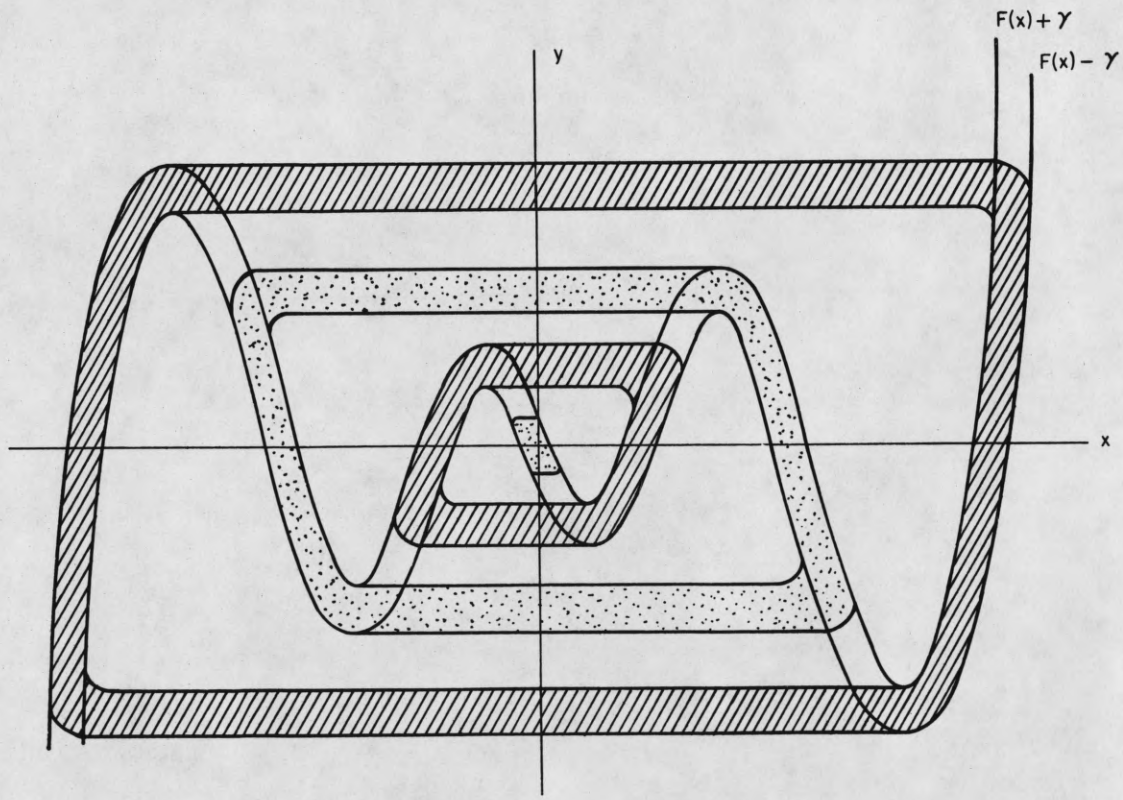

Figure 26

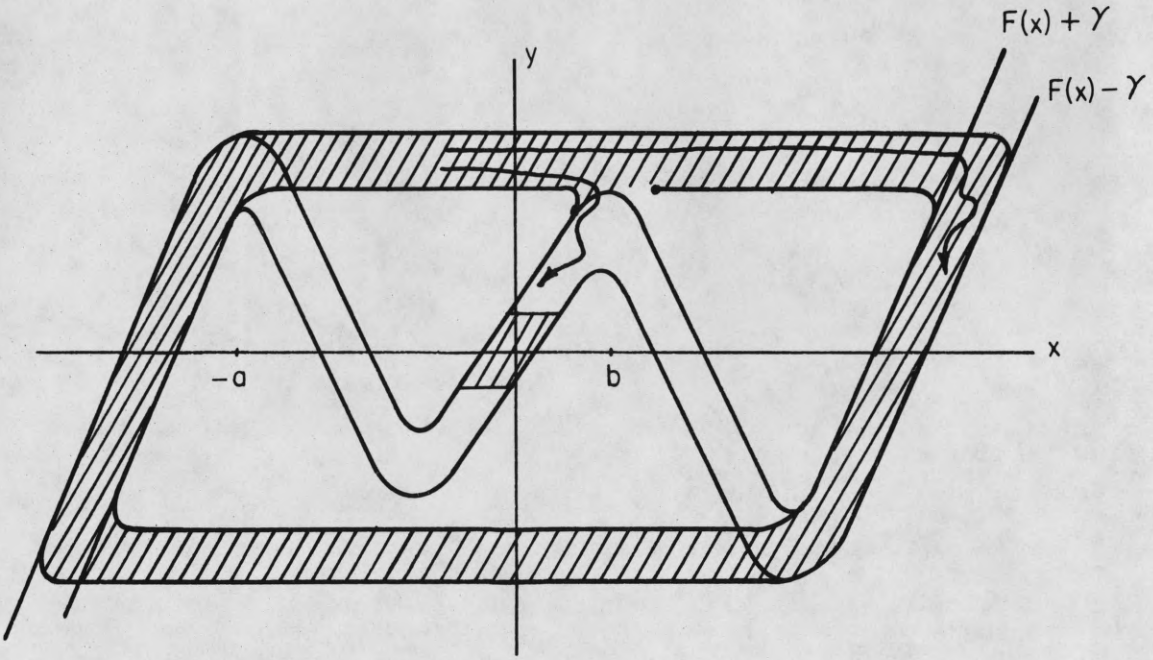

Figure 27

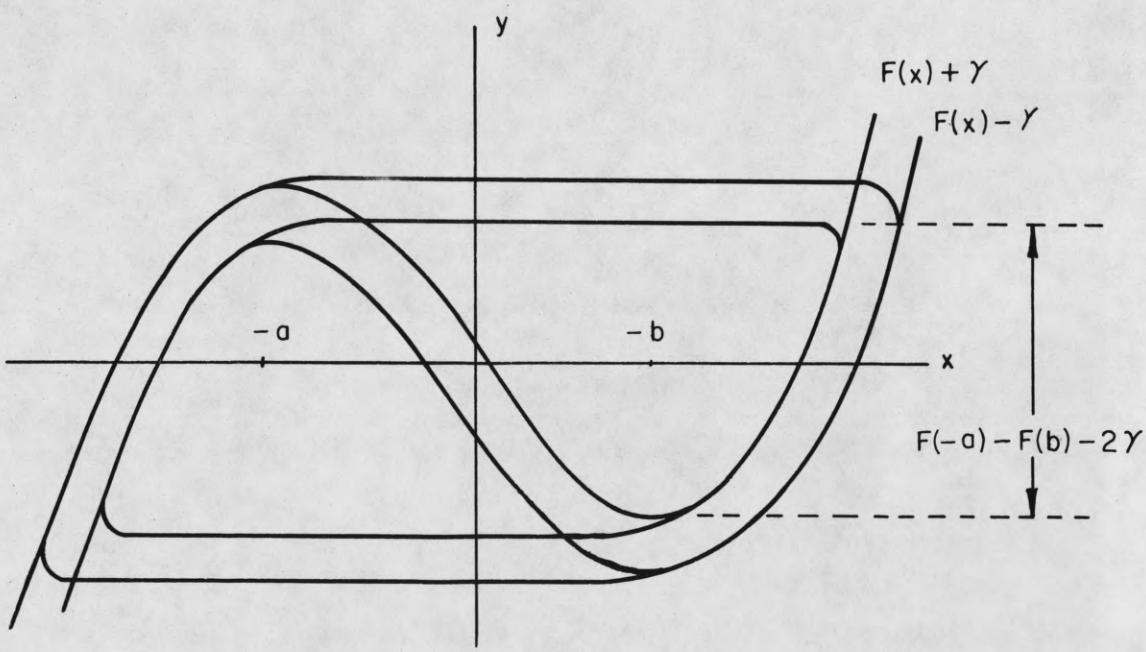

Figure 28

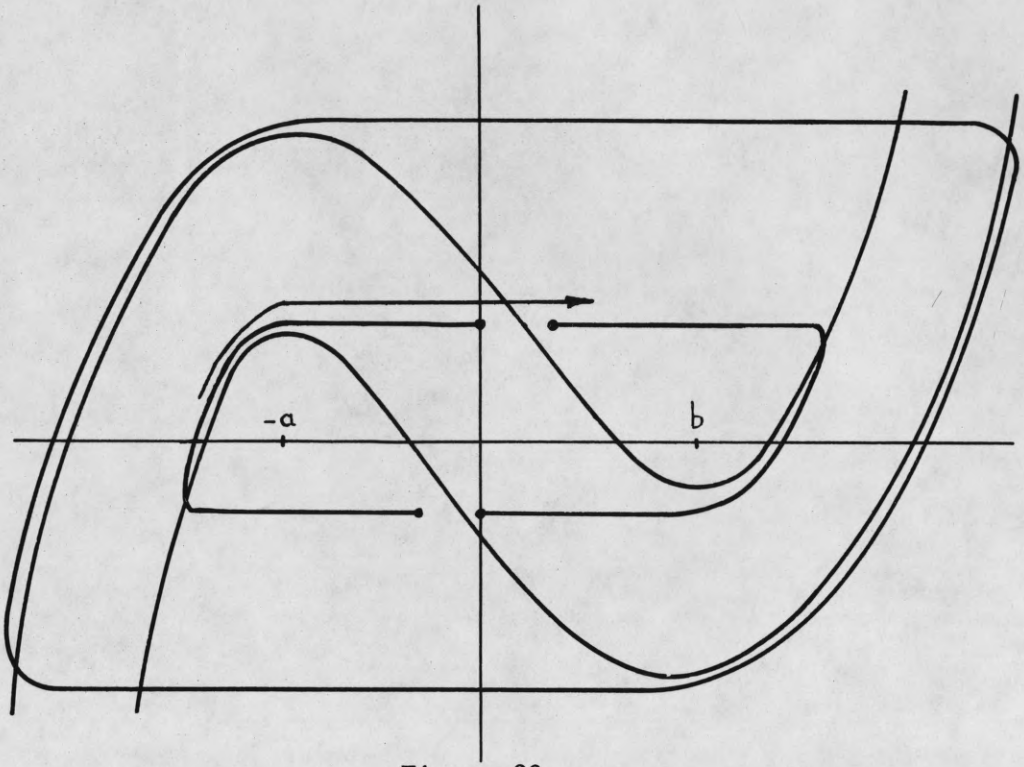

Figure 29

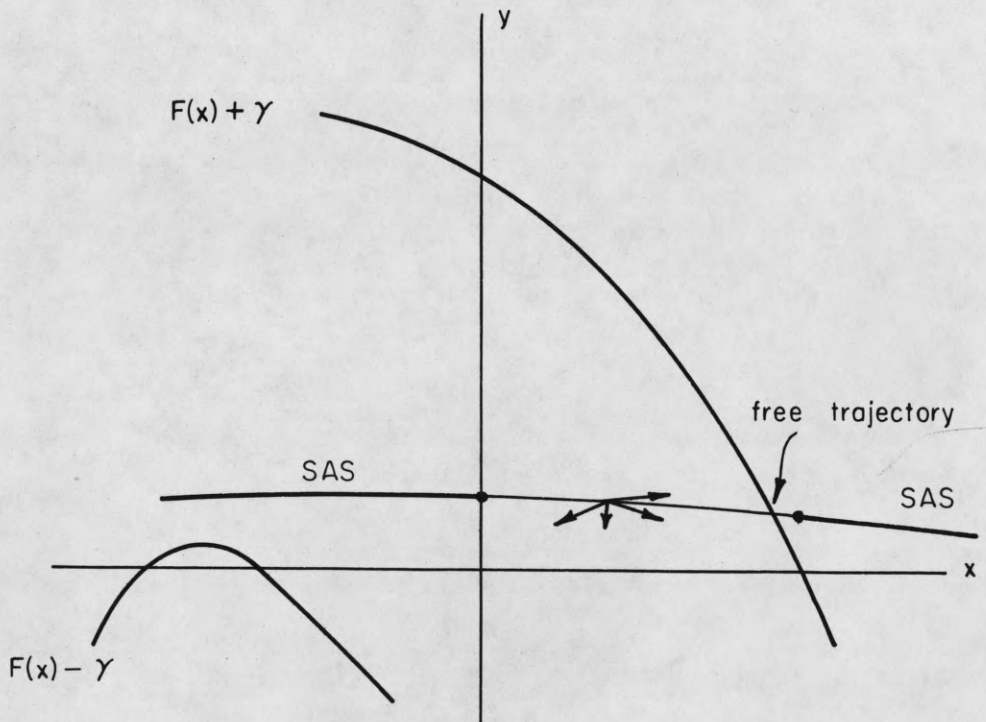

Figure 30

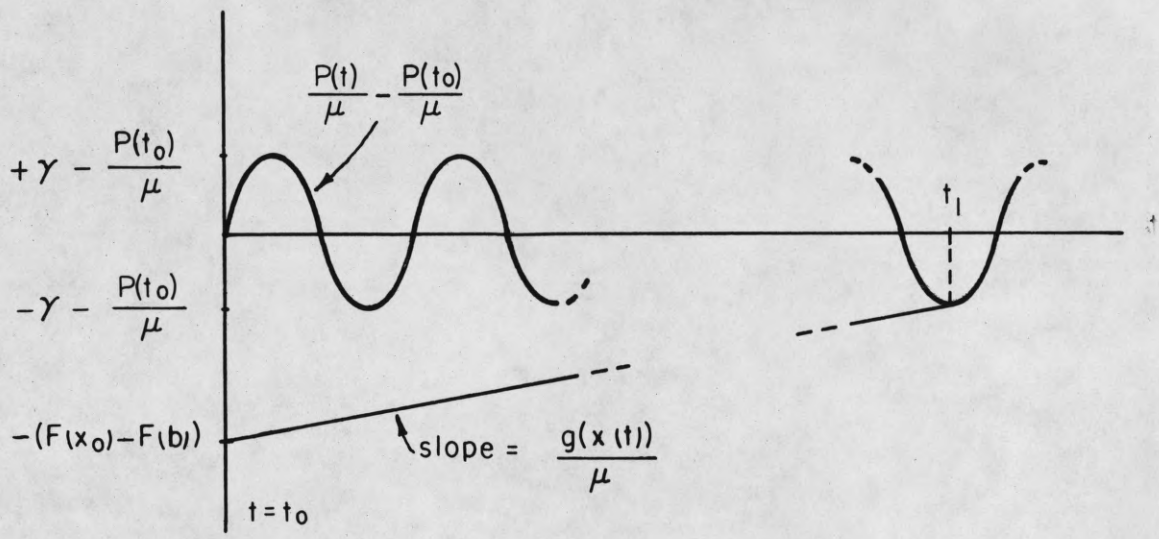
$\frac{P(t)}{\mu} - \frac{P(t_0)}{\mu}$
$+\gamma - \frac{P(t_0)}{\mu}$
$-\gamma - \frac{P(t_0)}{\mu}$
$-(F(x_0)-F(b))$
slope = $\frac{g(x(t))}{\mu}$
$t = t_0$
t_1

Figure 31

CHAPTER IV

NUMERICAL RESULTS

4.1 INTRODUCTION

In this chapter we will discuss briefly some numerical results, for equations of the form $\ddot{x} + \mu f(x)\dot{x} + g(x) = A \sin \omega t$ or the equivalent representation

$$\dot{x} = \mu(y - f(x) - \gamma \cos \omega t)$$

$$\dot{y} = -g(x)/\mu$$

where $F(x) = \int_0^x f(u)du$ and $\gamma = A/\mu\omega$.

Numerical integration was carried out on a Control Data 1604 digital computer with a Fortran coded version of the integration scheme devised by A. Nordsieck (Mathematics of Computation, Vol. XVI, no. 77, Jan. 1962).

The solution trajectories which follow are representative of the solutions to the second order systems discussed in Chapters II and III.

4.2 NUMERICAL SOLUTIONS

Figure 32 shows the limit cycle of the unforced van der Pol equation, with $\mu = 10$, as well as a typical forced periodic solution. Observe that the forced trajectory is a simple closed curve and in the regionof positive damping ($x^2 > 1$) the orbit lies effectively in the band defined by $F(x) - \gamma < y < F(x) + \gamma$. Note also that the forced trajectory has origin-symmetry and is a subharmonic of odd order.

Figure 33 illustrates several periodic solutions to the

equation

$$\ddot{x} + 10(x^4 - 3.5\,x^2 + 1)\dot{x} + x = 9 \sin 5t$$

as well as the annuli obtained according to the scheme outlined in Chapters II and III. The three orbits are symmetric, and odd subharmonics. The middle limit cycle is an unstable solution and was obtained numerically by integrating the equations in reverse time.

Figure 34 shows the solutions of Figure 33 in the x-t plane.

Figure 35 indicates two stable odd subharmonics for the harmonically forced van der Pol equation, as well as an unstable solution with the period of the forcing function. Note that this last solution lies entirely in $x^2 < 1$ where the damping is negative. All solutions converge to one or the other of the two stable subharmonics, and the figure indicates the regions in the plane, generating solutions (beginning at t = o) which converge to either the stable first or stable third subharmonic.

Figure 36 illustrates an even subharmonic solution for the system obtained by shifting the van der Pol characteristic curve $y = F(x) = x^3/3 - x$. In general it was found that periodic solutions to equations with symmetrical functions F(x), g(x) and P(t) (the kind of symmetry described in Theorem 4 of the appendix) were "more likely" (see Figure 37) to possess origin-symmetry and hence be odd subharmonics. However, even order subharmonics were easily obtained by introducing asymmetry into the equations.

Figure 37 shows a periodic orbit for the linearized type equation introduced by N. Levinson, namely

$$\ddot{x} + 20f(x)\dot{x} + x = \sin t,\ f(x) = 4/3 \text{ for } x^2 > 1,$$

$f(x) = -2/3$ for $x^2 < 1$. The curve $F(x) = \int_0^x f(u)du$ becomes a piecewise-linear approximation to the van der Pol characteristic $x^3/3 - x$. Note that the periodic solution shown is a subharmonic of <u>even</u> order and is asymmetric (with respect to the origin). Accordingly there is a second solution which is the reflection in the origin of the solution illustrated (see discussion following Theorem 4, Appendix).

Figure 38 illustrates the analytic solution $x = -2 \cos t$ for the equation $\ddot{x} + \mu(x^2 - 1)\dot{x} + x = 2\mu \sin 3t$ with $\mu = 10$. This solution is unstable and eventually converges to the stable fifth subharmonic shown. (The perturbation which disturbs the $-2 \cos t$ solution is furnished by the arithmetic errors inherent in the numerical integration on a computer.)

4.3 CONCLUSIONS

It has been shown, for strongly damped systems, that solutions exist which are confined to lie in the neighborhood of periodic orbits of the unforced system, provided the integral of the forcing term has a sufficiently small bound. In the physical situation described by the equations, the forcing term may be the result of external disturbances or noise. If however the forcing is intentionally applied and is periodic, there exists the possibility of periodic forced solutions within the annuli obtained by the methods described.

Whether or not such periodic orbits exist is not known except in some special cases, as for example the harmonically forced van der Pol equation discussed by Cartwright and Littlewood and the

linearized model described by N. Levinson. In both of these special cases the above authors find that either one or two stable subharmonic solutions may exist for some range of values of the forcing amplitude. Besides these, however, there exists a host of highly complex motions which may include periodic unstable, non-periodic and/or recurrent trajectories. It is clear then, that any attempt to prove the existence of stable periodic orbits within an annulus, for the general systems described in this thesis, must involve a good deal of mathematical sophistication. Indeed the above authors relied heavily upon the inherent symmetry of the equations involved (and in the linearized model, upon the integrability of the equation) and such symmetry is perhaps too great an idealization of the physical situation described.

The special cases mentioned above also include an unstable periodic solution with the period of the forcing term. However, the existence of such a solution, as well as its location, is easily demonstrated by the purely topological methods described in this thesis, where a simple fixed-point argument applied to a confining region suffices. From a physical standpoint, this solution is uninteresting.

One may observe, however, the similarity in the solution behavior for the special cases investigated by the above authors. One is led to conjecture that it is the geometrical similarity of the functions $F(x) = \int_0^x f(u)du$ in the Lienard plane, which is the basis for the solution similarity. In fact the two characteristic curves $y = F(x)$ are effectively symmetrical distortions, one of the other. The annuli obtained for both curves are very nearly coincident. It seems reasonable to suppose that the solution behavior described

by these authors can be extended to all systems which possess, in some sense, geometric similarity. Indeed there is a strong temptation to associate, at most, two stable subharmonic solutions with every annulus constructed about a stable limit cycle of the unforced system, and two unstable subharmonics with every annulus constructed about an unstable limit cycle of the unforced system. It is clear however that such a conjecture may not be verified by purely geometric means, due to the possible variety of complex motions within the annuli. Nevertheless, the confinement of solutions to the interior of an annular region suggests that the appropriate analytical investigation is one which is limited to solutions in an annulus. It is also reasonable to expect that the pertinent characteristics of the damping function $f(x)$ are the geometrical (rather than analytical) properties of $F(x) = \int_0^x f(u)du$. We may note for example that Cartwright and Littlewood arrive at their conclusions only after intensive analytic analysis of the solution behavior in the neighborhood of the zeros, $x^2 = 1$, of $f(x) = x^2 - 1$, where the quadratic behavior of $F(x)$ is evidenced. However, in the Levinson model $f(x) = \pm 1$ for $x^2 \gtrless 1$ and so is not defined at $x^2 = 1$. There is no analytical similarity in the functions $f(x)$, only the geometrical similarity in the curve $y = F(x)$.

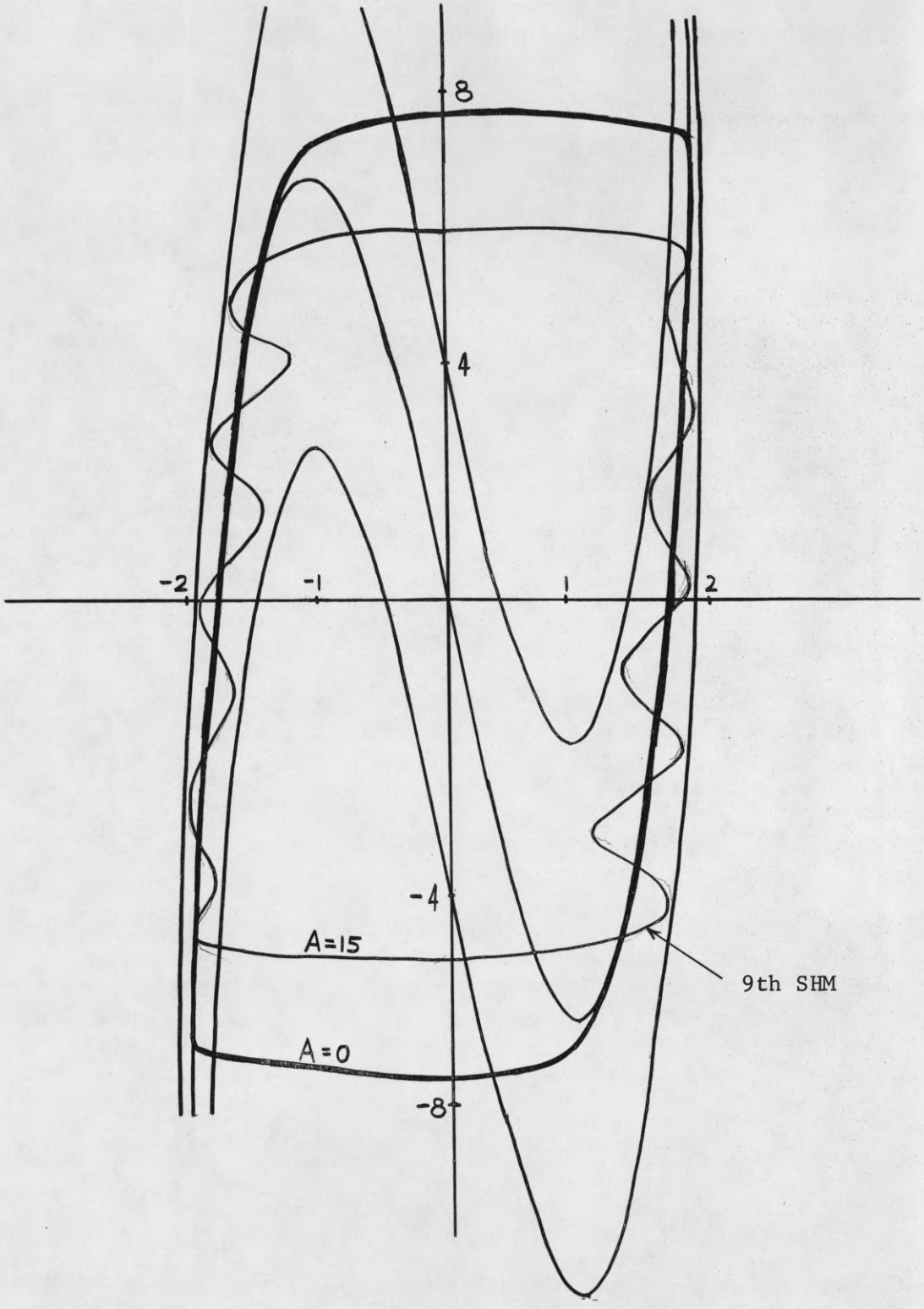

Figure 32

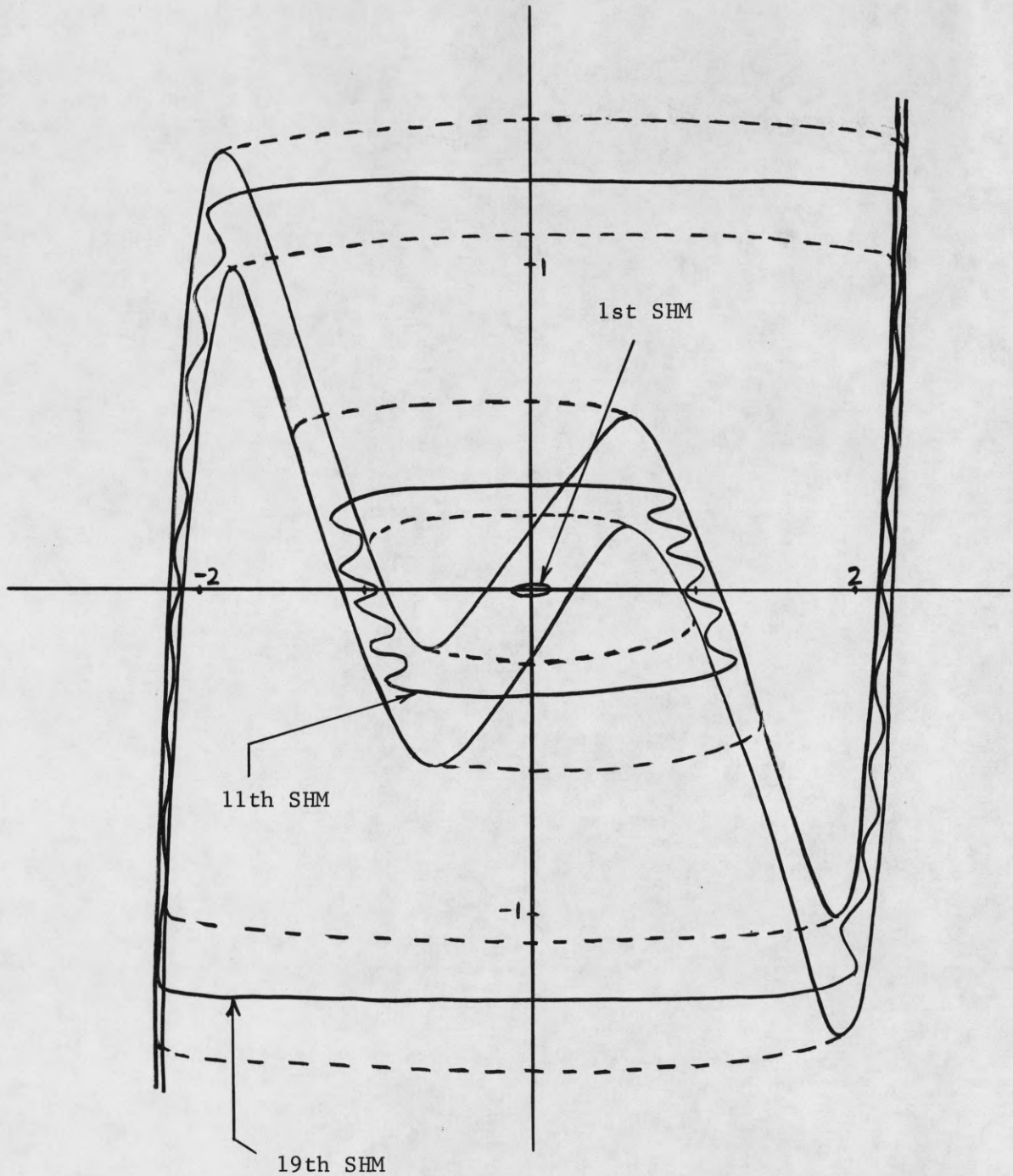

Figure 33

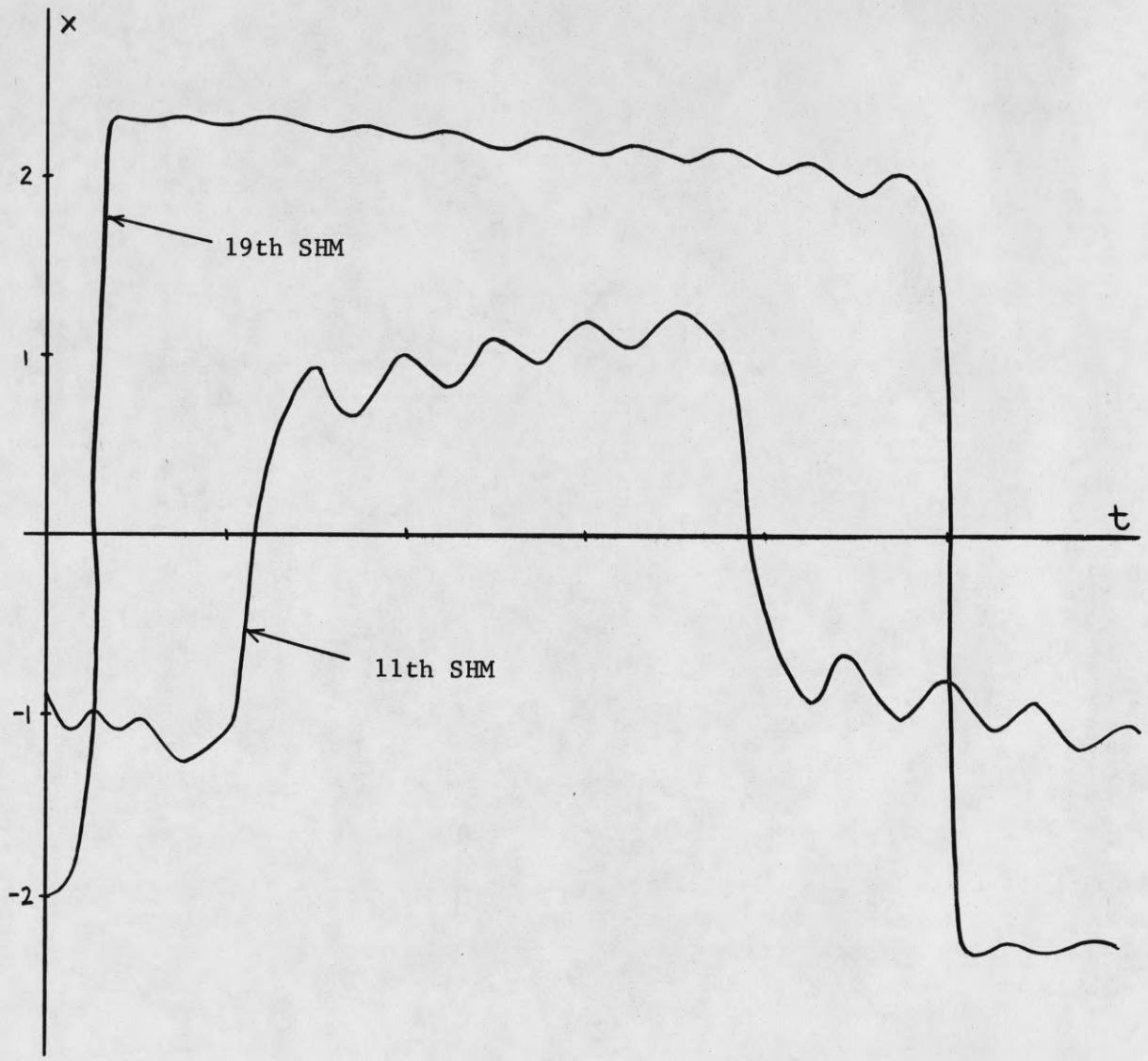

Figure 34

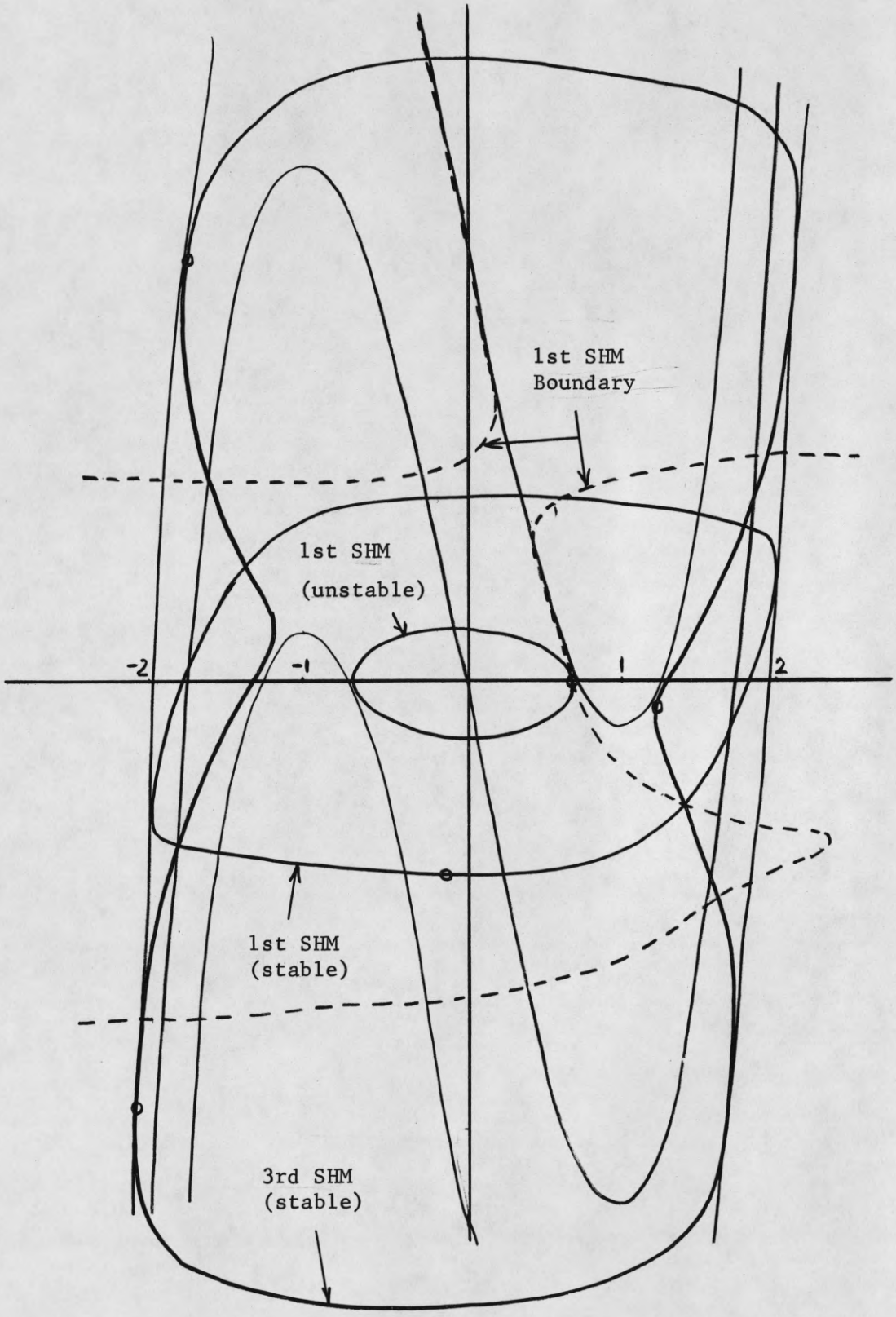
1st SHM
Boundary
1st SHM
(unstable)
-2
-1
1
2
1st SHM
(stable)
3rd SHM
(stable)

Figure 35

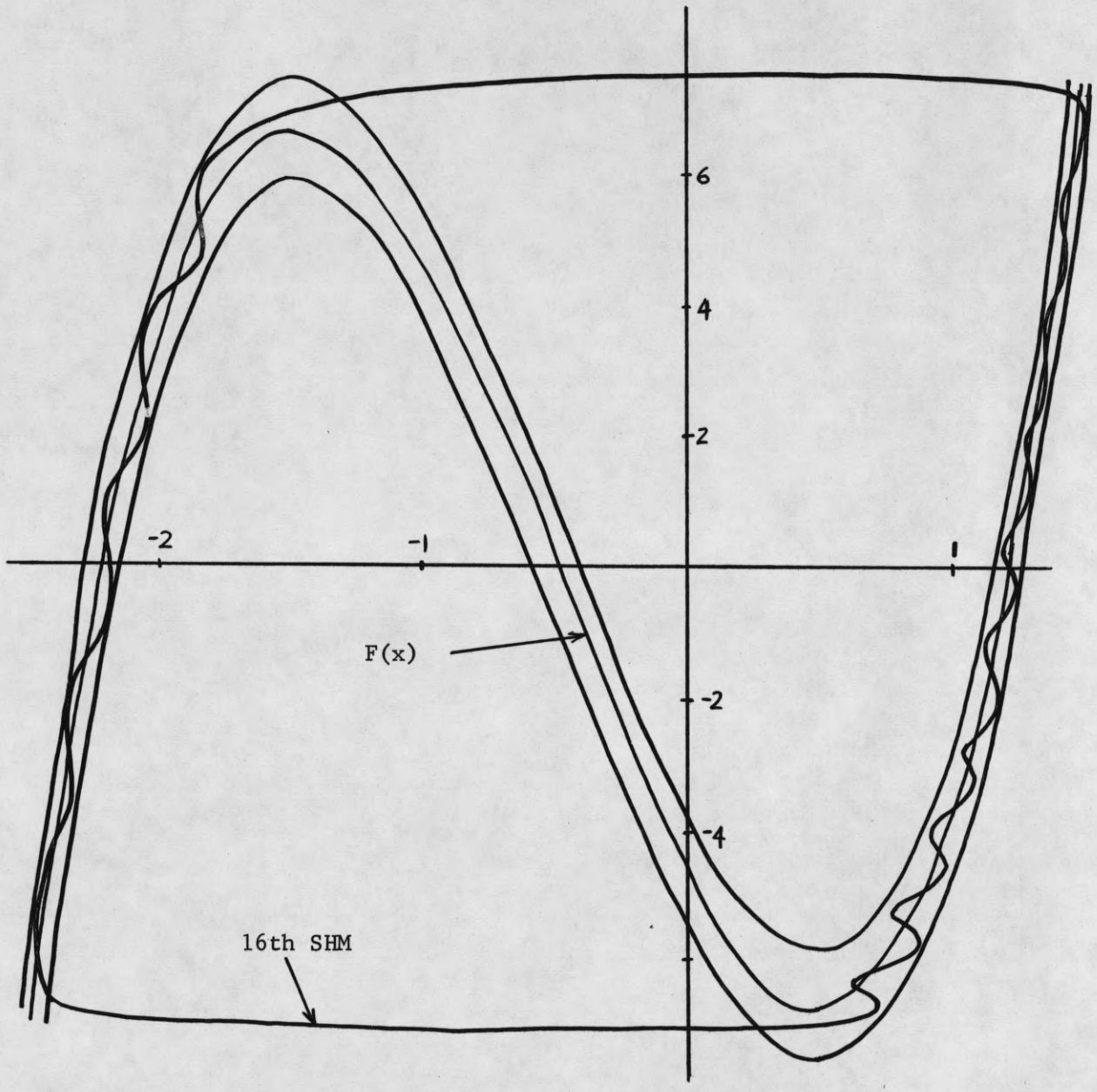

$\dot{x} = y - F(x) - 4/5 \cos 5t, \dot{y} = -x$

Figure 36

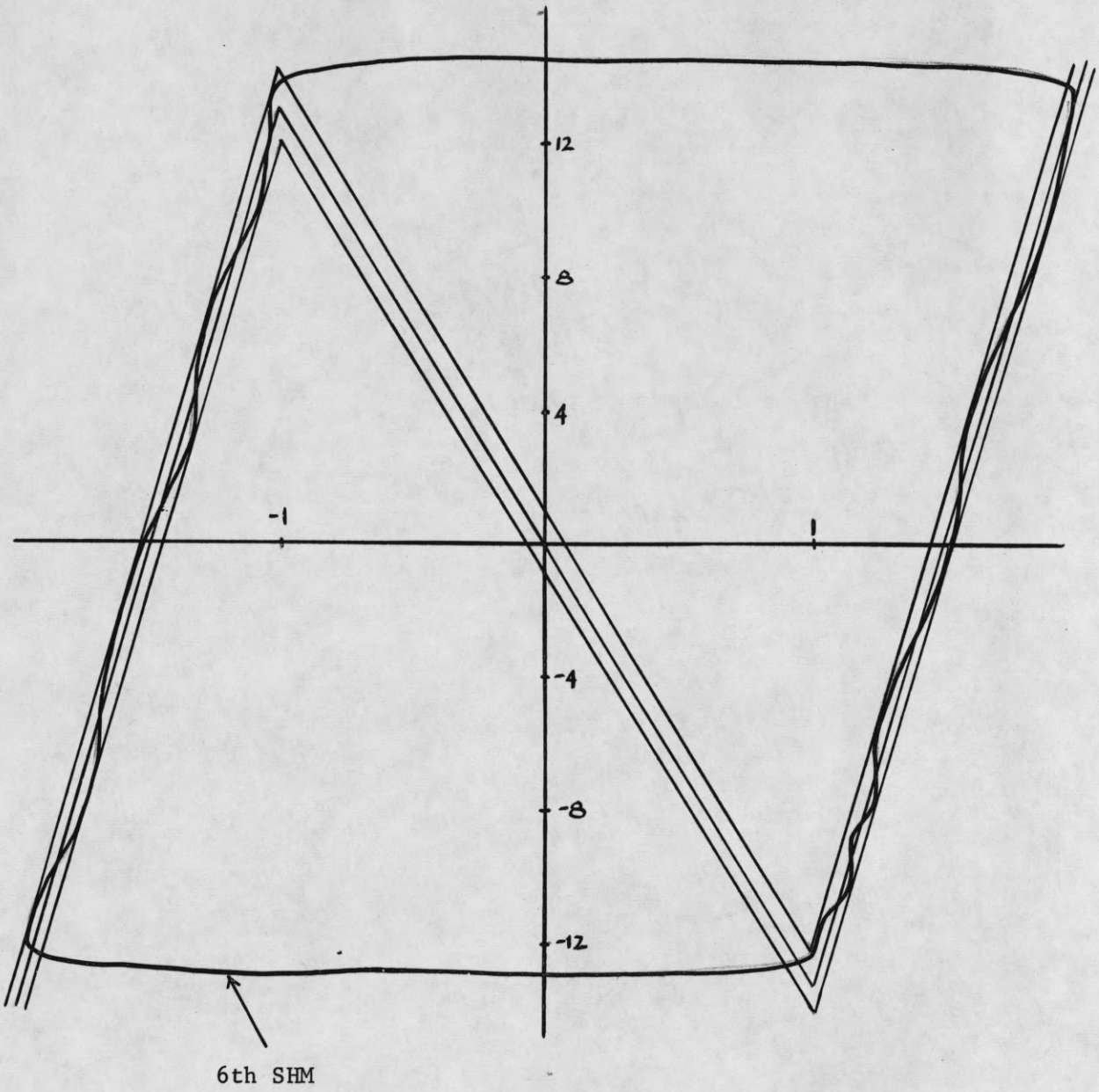

Figure 37

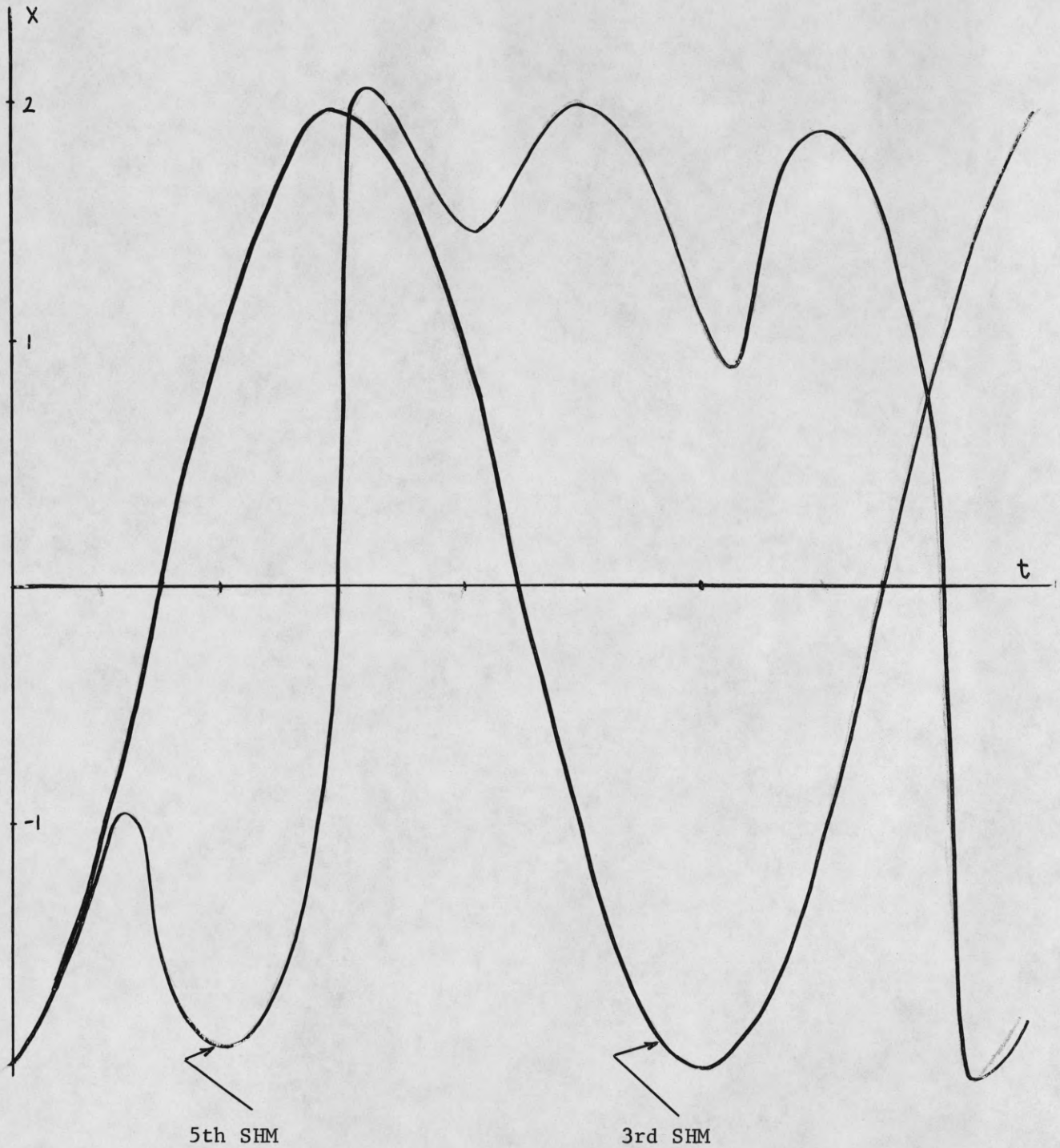

Figure 38

APPENDIX

THEOREM 1:

Consider the equation

$$\ddot{x} + f(x)\dot{x} + g(x) = p(t) \tag{1}$$

as represented by the system

$$\begin{aligned} \dot{x} &= y - F(x) + P(t) \\ \dot{y} &= -g(x) \end{aligned} \tag{2}$$

where $F(x) = \int_o^x f(u)du$

$P(t) = \int_o^t p(\tau)d\tau$

Equation (2) is considered with the following restrictions:

(a) $g(x)$ and $F(x)$ satisfy a Lipschitz condition, and $P(t)$ is continuous and bounded for all t, $|P(t)| \leq A$,

(b) $G(x) = \int_o^x g(u)du$ satisfies $G(\pm \infty) = \infty$,

(c) there exist positive constants a, b, c, K, M such that (i) $|g(x)| \leq C$, and $|F(x) \pm A| < M$, in $-a \leq x \leq b$, and (ii) $xg(x) > 0$, and $|F(x) \pm A| \geq K$, $xF(x) > 0$, outside the interval $(-a, b)$.

Then, every solution to (2) with finite initial conditions $x = x_o$, $y = y_o$ at $t = t_o$ is bounded for all $t \geq t_o$, the bound depending only upon (x_o, y_o). That is, $|x(t)| \leq B_1(x_o, y_o)$ and $|y(t)| \leq B_2(x_o, y_o)$ for $t \geq t_o$. Furthermore, there is a closed and bounded region R_o in the (x, y) plane, containing the origin, such that all solution trajectories enter R_o at some time $t_i(x_o, y_0)$ and thereafter remain in R_o for $t > t_1$.

Before proceeding to the proof of Theorem 1, we note that

condition (a) assures the existence and uniqueness of solutions with respect to an arbitrary set of initial conditions. Condition (b) associates infinite "potential energy" G(x) with infinite displacements. The conditions in (c) imply that g(x) is "restoring" for large $|x|$ (that is, g(x) has the sign of x) so that G(x) is monotone increasing as $|x| \to \infty$ outside (-a, b). Also, the conditions on F(x) imply that F(x) is sufficiently large and positive for x large and positive (so that $F(x) - A \geq K$ for $x \geq b$) and sufficiently negative for $x \leq -a$ ($F(x) + A \leq K$). These conditions on F(x) may be realized for example, if $f(x) \geq \alpha > 0$ for large $|x|$, so that $F(x) \to \pm \infty$, as $x \to \pm \infty$ (see Figure 39).

PROOF OF THEOREM 1:

The proof consists in constructing a simple closed bounded region R, containing (x_o, y_o) with the property that solution trajectories which cross the boundary of R do so from without. Thus the trajectory generated by (x_o, y_o) at $t = t_o$ is confined and bounded by R. Furthermore, the construction is such that a "minimal" region R_o may be obtained, into which all trajectories must enter eventually. We now proceed to the construction of R (Figure 40). We begin at a point P on X = b where $y_p > M + 4K$. Through P is passed a (unique) ψ-curve:

$$\frac{1}{2}(y - K)^2 + G(x) = \psi_p \qquad (3)$$

in $x > b$ so that ψ_p confines interior trajectories in $x \geq b$.

ψ_p reintersects x = b at a point Q where $y_Q = 2K - y_p$, due to symmetry of ψ_p about y = K. Note that $y_Q < -M - 2K$ for $y_p > M + 4K$.

ψ_P forms the boundary of R in $x > b$.

The boundary of R is continued, by passing through Q a line with slope $\frac{C}{-M-y_Q} > 0$ (since $y_Q < -M$).

The lines $y = \frac{-C}{M+y_Q} x + \ell$ (ℓ is a parameter) are crossed from below, in $-a \leq x \leq b$, $y \leq y_Q$ since $\dot{\ell} = \dot{y} + \frac{C}{M+y_Q} \dot{x} = -g(x) + \frac{C}{M+y_Q} (y - F(x) + P(t))$ and $\dot{\ell} \geq -C - \frac{C}{M+y_Q} ((F(x) - P(t))_{min} - y_{max}) \geq -C - \frac{C}{M+y_Q} (-M - Y_Q)$ so that $\dot{\ell} \geq 0$ in $(-a, b)$, for $y < M$.

The required line through Q is

$$y = \frac{C}{-M-y_Q} (x - b) + y_Q \tag{4}$$

The line (4) intersects $x = -a$ at a point S where

$$y_S = y_Q - \frac{(a+b)C}{-M-y_Q} < y_Q < -M - 2K.$$

Through S is passed a ψ-curve:

$$\frac{1}{2}(y + K)^2 + G(x) = \psi_S \tag{5}$$

Then $\dot{\psi} = g(x) (-K - F(x) + P(t)) < 0$ in $x \leq -a$ so that ψ_S confines interior trajectories in $x \leq -a$.

ψ_S reintersects $x = -a$ at T, where $y_T = -2K - Y_S > M$, since $y_S < -M - 2K$.

The boundary of R is continued by passing a line through T with slope $\frac{C}{y_T-M} > 0$. This gives

$$y = \frac{C}{y_T-M} (x + a) + y_T . \tag{6}$$

The line (6) is crossed from above in $(-a, b)$, (for the same reasons as were given for the line (4)) and intersects $x = b$ at P' where $y_{P'} = y_T + \frac{(a+b)C}{y_T-M} > y_T > M$.

If $y_{P'} < y_P$, the contour PQSTP'P defines a region R which will confine interior trajectories. Note that the line segment P'P is crossed from left to right, since $\dot{x} = y - (F(x) - P(t))$ and $\dot{x} \geq y_{P'} - M > 0$

along P'P. To show that $y_{P'} \leq y_P$ for sufficiently large y_P, we obtain the complete transformation from P to P' as:

$$y_{P'} = y_P - 4K + \frac{(a+b)c}{y_P - M - 2K} + \frac{(a+b)c}{y_P - M - 4K + \frac{(a+b)c}{y_P - M - 2K}} \tag{7}$$

Clearly $y_{P'} \sim y_P - 4K$ for $y_P \to \infty$, so that a confining region R always exists for sufficiently large y_P.

Given any initial point (x_o, y_o), R may be constructed (large perhaps, but bounded) so as to contain (x_o, y_o) and the solution trajectory which passes through (x_o, y_o) at $t = t_o$. Then R (and consequently the bounds on $x(t)$, $y(t)$) will depend solely on (x_o, y_o).

Note that the construction may be continued from P' thereby generating another, smaller region R', contained in R. We may repeat the construction obtaining a series of contracting regions R, R', R", etc. until either (i) the construction fails for some $y_P \not> M + 4K$ or (ii) the construction converges in the sense that the y_P approach a fixed point of the transformation (7), where $y_{P'} = y_P > M + 4K$.

Since there is a certain degree of latitude in the choice of constants a, b, c, K, M for any given system (2), we may expect that they can be chosen so that (ii) occurs. We show that this is in fact the case. That is, by choosing $4K^2 < (a+b)\,C$, we can guarantee the existence of a fixed point y_P of (7), satisfying $y_{P'} = y_P > M + 4K$, hence the convergence of the continued construction to a "minimal" region, R_o.

To show this, observe that $y_{P'} = y_P$ requires

$$4K = \frac{(a+b)C}{y_P - M - 2K} + \frac{(a+b)C}{y_P - M - 4K + \frac{(a+b)C}{y_P - M - 2K}}$$

For y_P sufficiently large, the right-hand expression is less than 4K. Since we want a fixed point $y_P > M + 4K$, we put $y_P = M + 4K$ and require the right-hand expression to be greater than 4K, ensuring equality for some $y_P > M + 4K$. We obtain $4K < \frac{(a+b)C}{2K} + 2K$ or $4K^2 < (a+b)\,C$ as a sufficient condition for the existence of a fixed point.

We will assume that K is chosen sufficiently small to ensure the existence of the minimal region R_o.

It is now evident that all solutions to (2) will eventually enter R_o, since solutions which begin exterior to R_o will be "forced" into R_o by the contracting, confining regions R, R', R", etc. (Note that solutions rotate in a clockwise sense about the origin, outside of $-a \leq x \leq b$, $|y| \leq M$, so that the "spiral" PQSTP'Q'S'T'P"..., which serves as an outer bound, will carry solution trajectories into R_o.) The time of entry into R_o will depend upon how remote (x_o, y_o) is.

This concludes the proof of Theorem 1.

COROLLARY TO THEOREM 1:

If in addition to the assumptions of Theorem 1 we have P(t) periodic, with period τ, then there is at least one periodic solution to (2), with period τ.

PROOF OF COROLLARY TO THEOREM 1:

We use Brouwer's Fixed Point Theorem which states that if a

continuous point transformation T maps a simple closed and bounded region R into itself, then there is at least one fixed point of the transformation T; that is, if for every point q in R, the transformed point Tq is also in R, then there is at least one point q_o in R such that $Tq_o = q_o$.

We take for the region, any R of Theorem 1, and in particular R_o. For the transformation T we take the period-transformation of points in the plane. That is, we consider the position at time $t_o + \tau$ of a solution point q(t) which starts at $q(t_o)$ at time t_o. Since solutions to (2) are continuous functions of their initial conditions, the transformation $T\, q(t_o) = q(t_o + \tau)$ is continuous (and in fact one to one).

By the fixed point theorem there exists a fixed point of T in the region R_o; a point (x_o, y_o) such that the solution to (2) satisfying $x(t_o) = x_o$, $y(t_o) = y_o$ also satisfies $x(t_o + \tau) = x_o$, $y(t_o + \tau) = y_o$. This solution is clearly periodic with the period τ of P(t).

This proves the corollary.

The above theorem says nothing about the stability or uniqueness of the periodic solution. There may be several periodic solutions with a variety of periods (all integral multiples of τ, however). In Theorem 2 we consider a special case of equation (1), for which a unique periodic solution exists to which all other solutions converge as $t \to \infty$. Theorem 2 includes the case of linear constant coefficient equations with periodic forcing, where $f(x) = \alpha$ = constant > 0 and $g(x) = \beta x$, $\beta > 0$, where all solutions converge to a unique periodic solution with the period of p(t).

THEOREM 2:

We consider the equation

$$\ddot{x} + f(x)\dot{x} + g(x) = p(t) \tag{1}$$

under the conditions

(a) $f(x) \geq \alpha > 0$ for all x,

(b) $g'(x) \geq \beta > 0$ for all x, and

(c) $g''(x) < 2\alpha\beta/3B$, where B is an upper bound on $|\dot{x}(t)|$, for solutions in the region R_o.

Then (1) has a unique solution to which all others converge.

Note that g(x) is to have continuous derivatives to second order. The upper bound on g''(x) implies that g(x) behaves much like a linear restoring spring.

The constant B in (c) may be determined once the differential equation is given, since R_o is then determined. (Since all solutions eventually enter R_o, B is an eventual upper bound on $|\dot{x}(t)|$, for all solutions).

Before proceeding to the proof of Theorem 2, we prove a lemma to which we will have occasion to refer.

LEMMA A:

$$\text{If } \begin{aligned} \dot{\xi} &= \eta - h(t)\xi \\ \dot{\eta} &= -k(t)\xi \end{aligned} \tag{8}$$

where $h(t) \geq \alpha > 0$ and $k(t) \geq \beta > 0$ and $\dot{k}(t) < 2\alpha\beta$, then all solutions $(\xi(t), \eta(t))$ to (8) converge to zero as $t \to \infty$.

PROOF:

Consider the function

$$\lambda(\xi,\eta,t) = k(t)\xi^2 + \eta^2$$

then $\lambda \geq \beta\xi^2 + \eta^2 > 0$ for $\xi^2 + \eta^2 \neq 0$

and $\dot{\lambda} = 2k(t)\xi\dot{\xi} + \eta\dot{\eta} + \dot{k}(t)\xi^2 = -(2k(t)h(t) - \dot{k}(t))\xi^2$. Then for $\dot{k}(t) < 2\alpha\beta \leq 2k(t)h(t)$ we have $\dot{\lambda} < 0$ for $\xi^2 \neq 0$. Then $\lambda(\xi,\eta,t) > 0$ is monotone decreasing. We show that $\lambda \to 0$ as $t \to \infty$ so that $\xi(t)$ and $\eta(t)$ converge to zero.

Let λ converge to a limit λ_∞ (since λ is monotone decreasing and bounded below, it must converge to some limiting value). Then $\dot{\lambda} \to 0$ as $t \to \infty$, so $\xi(t) \to 0$. We have for the limiting value of λ, $\lambda_\infty = \eta^2/2$ = constant, so that $\lim \xi(t) = 0$, $\lim \eta^2(t) = 2\lambda_\infty$. However the only constant solution to (8) is $\xi = \eta = 0$. Then $\lambda_\infty = 0$ and $\xi(t)$, $\eta(t)$ both converge to zero as $t \to \infty$, and Lemma A is proved.

We now proceed to the proof of Theorem 2.

PROOF OF THEOREM 2:

Let $x(t)$ and $w(t)$ be any two solutions to (1), where $f(x)$ and $g(x)$ satisfy the conditions of the theorem. Then

$$\ddot{x} + f(x)\dot{x} + g(x) = p(t)$$

and

$$\ddot{w} + f(w)\dot{w} + g(w) = p(t).$$

Substracting, and setting $w(t) - x(t) = z(t)$ gives

$$\ddot{z} + d/dt(F(w) - F(x)) + g(w) - g(x) = 0.$$

By the mean value theorem we may put $F(w) - F(x) = f(\psi)z$ where $\psi = x + \theta_1 z$, and $g(w) - g(x) = g'(\Phi)z$ where $\Phi = x + \theta_2 z$ and $0 < \theta_1, \theta_2 < 1$.

We have $\ddot{z} + d/dt(f(\psi)z) + g'(\Phi)z = 0$

or $\dot{z} = \eta - f(\psi)z$, $\dot{\eta} = -g'(\Phi)z$ as an equivalent representation.

The convergence of $z(t)$ and $\eta(t)$ to zero will follow from Lemma A provided

(i) $f(\psi(t)) \geq \alpha > 0$

(ii) $g'(\Phi(t)) \geq \beta > 0$, and

(iii) $\dot{g}'(\Phi) < 2\alpha\beta$.

Since (i) and (ii) are a consequence of conditions (a) and (b) of the theorem, we must now show that (iii) is a consequence of (c).

We have $zg'(\Phi) = g(w) - g(x)$ . . .

Differentiating gives

$$z\dot{g}'(\Phi) + \dot{z}g'(\Phi) = g'(w)\dot{w} - g'(x)\dot{x}$$

and putting $\dot{w} = \dot{x} + \dot{z}$ yields

$$z\dot{g}'(\Phi) = (g'(w) - g'(x))\dot{x} + (g'(w) - g'(\Phi))\dot{z}$$

or $$z\dot{g}'(\Phi) = g''(\Phi_1)z\dot{x} + g''(\Phi_2)(w - \Phi)\dot{z}$$

where we have again used the Mean Value theorem.

Putting $w - \Phi = w - (x + \theta_2 z) = (1 - \theta_2)z$ gives

$$\dot{g}'(\Phi) = g''(\Phi_1)\dot{x} + g''(\Phi_2)(1 - \theta_2)\dot{z}.$$

Now $\dot{x} \leq B$ and $\dot{z} \leq |\dot{x}| + |\dot{w}| \leq 2B$ and $0 < 1 - \theta_2 < 1$ so that $\dot{g}'(\Phi) \leq 3g''_{max}(x)B$.

Since $g''_{max}(x) < 2\alpha\beta/3B$ we obtain $\dot{g}'(\Phi) < 2\alpha\beta$ and by Lemma A, $|z(t)| = |w(t) - x(t)| \to 0$ as $t \to \infty$. Furthermore, $|\eta(t)| \to 0$ so that $|\dot{z}(t)| = |\dot{w}(t) - \dot{x}(t)| \leq |\eta(t)| + |f(\psi)z(t)| \to 0$ as $t \to \infty$.

We conclude that any two solutions to (1), with $f(x)$ and $g(x)$ satisfying the conditions of the theorem, approach each other and thus converge to a common solution. It follows that all solutions,

regardless of initial conditions, will converge to a common solution.

This completes the proof of Theorem 2.

Note that the conclusions reached above do not depend upon periodicity of $p(t)$. However, if $p(t)$ is periodic, period τ, then there is a periodic solution to (1), with period τ (corollary to Theorem 1). All solutions will then converge to this (unique) periodic solution with period τ.

Note also that for $p(t) = 0$, then $x = 0$ is the solution to which all others converge. This is clearly a special case of periodic $p(t)$. We may then add the corollary.

COROLLARY TO THEOREM 2:

If in addition to the conditions of Theorem 2 we have $p(t)$ periodic, period τ, then all solutions to (1) converge to a unique solution which is periodic with period τ.

We now turn to Theorem 3 to show that for the periodically forced second order equations which concern us, as well as for a more general class of forced equations, the only periodic solutions are subharmonics of integral order. Note that the periodic solutions referred to in the corollaries to Theorems 1 and 2 are subharmonics of order one.

THEOREM 3:

Periodic solutions to the system $\dot{\underline{x}} = \underline{F}(\underline{x}) + \underline{P}(t)$, where $\underline{F}(\underline{x})$ is single-valued, are necessarily subharmonic solutions of integral order. That is, it is necessary that $\underline{P}(t)$ be periodic and that the solution period be an integral multiple of the period of $\underline{P}(t)$ (we refer

here to the least period of $\underline{P}(t)$ and of the solution).

PROOF OF THEOREM 3:

If $\underline{z}(t)$ is a periodic solution with least period T, then

$$\underline{P}(t) = \dot{\underline{z}}(t) - \underline{F}(\underline{z}(t)).$$

Clearly $\underline{P}(t)$ must be periodic and have a period T. That is $\underline{P}(t + T) = \underline{P}(t)$.

If τ is the least period of $\underline{P}(t)$ then $T = m\tau$ for some $m = 1, 2, 3, \ldots$ so that periodic solutions are necessarily subharmonics of integral order.

It is interesting to observe that no statement such as Theorem 3 can be made for systems $\dot{\underline{x}} = \underline{F}(\underline{x},t)$. Indeed periodic solutions may exist for this type of equation regardless of whether or not $\underline{F}$ is periodic in t. If $\underline{F}(\underline{x},t)$ is periodic in t, the solution period (if any periodic solution exists) need bear no rational ratio to the period of $\underline{F}$.

Consider for example the system

$$\dot{x} = y$$

$$\dot{y} = -x + (1 - x^2 - y^2)H(t)$$

for which a periodic solution $x = \sin t$, $y = \cos t$ exists, regardless of the nature of H(t).

We now proceed to Theorem 4 which concerns periodic solutions to second order systems (1), where f(x), g(x), and p(t) have particular symmetries. Origin symmetry of the closed orbit in the plane is seen to imply the odd-subharmonic character of the solution.

THEOREM 4:

If, in the system

$$\dot{x} = y$$
$$\dot{y} = -g(x) - f(x)y + p(t), \tag{9}$$

we have (a) $f(x)$ an even function,

(b) $g(x)$ an odd function, and

(c) $p(t)$ odd-periodic, that is $p(t + \tau/2) = -p(t)$

where τ is the period of $p(t)$, then any periodic solution whose closed orbit is symmetrical about the origin will be an odd subharmonic. If T is the solution period, then $T = (2m + 1)\tau$ for some $m = 0, 1, 2, \ldots$

We note first that the time taken to describe any solution arc in the phase plane is dependent only upon the goemetry of the arc. From (9) $dt = dx/y$ and $t_1 - t_o = \int_{P_o}^{P_1} dx/y$, a line integral along the solution arc (see Figure 41. If P_o and P_1 are diametrically opposite points on the periodic orbit, and T is the solution period, then $T/2 = \int_{P_o}^{P_1} dx/y$ due to the assumed origin symmetry. Then for any origin-symmetric orbit we have $x(t + T/2) = -x(t)$ and $y(t + T/2) = -y(t)$ so that the solution is odd-periodic.

From (9) we have $\dot{y}(t + T/2) = -g(x(t + T/2)) - f(x(t+ T/2))\, y(t + T/2) + p(t + T/2)$.

Using the odd and even character of $g(x)$ and $f(x)$ respectively, and the odd-periodic nature of the solution $x(t)$, $y(t)$ we find that $p(t + T/2) = -p(t)$.

Since $T = m\tau$ for some integral m (Theorem 3) then $p(t + m\tau/2) = -p(t)$.

Clearly m cannot be an even integer (=2k) since $p(t + k\tau) = -p(t)$ contradicts the fact that τ is the period of $p(t)$.

We conclude that $m = 2k + 1$ and an origin-symmetric solution is both odd-periodic and an odd subharmonic, which proves the theorem.

The converse is not true. That is, an odd subharmonic need not possess origin-symmetry. It is interesting however to note some further consequences of the symmetry imposed on $f(x)$, $g(x)$, and $p(t)$.

If equations (9) are written in vector form

$$\dot{\underline{x}} = \underline{F}(\underline{x}) + \underline{p}(t),$$

then $\underline{F}(-\underline{x}) = -\underline{F}(\underline{x})$ and $\underline{p}(t + \tau/2) = -\underline{p}(t)$ due to the nature of $f(x)$, $g(x)$, and $-p(t)$.

Then if $\underline{z}(t)$ is any solution, $-\underline{z}(t + (2m + 1)\tau/2)$ will also be a solution for any integer m, as can be seen by direct substitution. In particular, if $\underline{z}(t)$ is a periodic solution then $-\underline{z}(t + (2m + 1)\tau/2)$ will be periodic with the same period, and the two closed orbits in the plane will be reflections of each other in the origin.

If $\underline{z}(t)$ has origin-symmetry then the limit cycles of $\underline{z}(t)$ and $-\underline{z}(t + (2m + 1)\tau/2)$ will be (geometrically) coincident. If however $\underline{z}(t)$ does not possess origin-symmetry the two solutions will be inherently different (the difference being more than just a time translation).

Note that an <u>even</u> subharmonic $\underline{z}(t)$ is necessarily asymmetric, so that the reflected solution $-\underline{z}(t + (2m + 1)\tau/2)$ is fundamentally different from $\underline{z}(t)$.

UNIQUENESS OF THE PERIODIC ORBIT WITHIN AN ANNULUS

We consider an annulus of the type generated by the methods of Chapter II, for the system:

$$\dot{x} = y - F(x), \quad \dot{y} = -g(x).$$

Figure 42 illustrates two solution trajectories, y_1 and y_2, within the annulus. We suppose that the inner trajectory intersects $y = F(x)$ at $x = x_o$ and we let $M = F(x_o)$. We make the following assumptions (in addition to those necessary for the construction of the annulus):

(a) $F(x) \leq M$ in $0 < x < x_o$,

(b) $F(x) \geq M$ in that part of the annulus for which $x \geq x_o$.

To demonstrate uniqueness we will show that the trajectories provide a contractional mapping of intervals on the positive y-axis onto intervals on the negative y-axis. That is, for any two trajectories BGJB' and AHA' within the annulus, we will have $y(A') - y(B') \leq y(B) - y(A)$. A similar statement holds for mapping of the negative y-axis onto the positive y-axis.

Consider the function $\Phi(x,y) = \frac{1}{2}(y - M)^2 + G(x)$.

Then

$$d\Phi = (y - M)dy + g(x)dx = (F(x) - M)dy = \frac{g(x)(M-F(x)dx}{y-F(x)} .$$

We have

$$\int_B^G d\Phi = \Phi(G) - \Phi(B) = \int_o^{x_o} \frac{g(x)(M-F(x))dx}{y_2-F(x)}$$

and

$$\int_A^H d\Phi = \Phi(H) - \Phi(A) = \int_o^{x_o} \frac{g(x)(M-F(x))dx}{y_1-F(x)} ,$$

but since $y_2 - F(x) > y_1 - F(x)$ over the portions BG and AH, then $\Phi(G) - \Phi(B) < \Phi(H) - \Phi(A)$.

We also have

$$\int_G^J d\Phi = \int_{y(G)}^{y(J)} (F(x) - M)dy$$

but since $F(x) \geq M$ and $dy < 0$ in this region, then $\Phi(J) - \Phi(G) < 0$. Finally, in a manner similar to that used for the first inequality above, we obtain $\Phi(B') - \Phi(J) < \Phi(A') - \Phi(H)$.

Adding the three inequalities gives $\Phi(B') - \Phi(B) < \Phi(A') - \Phi(A)$ or $(y(B') - M)^2 - (y(B) - M)^2 < (y(A') - M)^2 - (y(A) - M)^2$, which may be rearranged to read:

$$y^2(B') - y^2(A') < y^2(B) - y^2(A) - 2M(y(B) - y(A) + y(A') - y(B'))$$

so that $y^2(B') - y^2(A') < y^2(B) - y^2(A)$

and thus $y(A') - y(B') < y(B) - y(A)$ as required.

In exactly the same way, we may continue the trajectories into $x < 0$ and show that $y(B'') - y(A'') < y(B) - y(A)$ where A'' and B'' are the points on the positive y-axis to which the A and B trajectories (respectively) return, after making one revolution. Note that for a periodic orbit we would have $y(A'') = y(A)$. It is clear then, that there can be no more than one periodic orbit within the annulus, for if there were more than one, we must have $y(B'') - y(A'') = y(B) - y(A)$ for any two periodic trajectories, contradicting the above inequality.

Since there is at least one periodic orbit in a confining annulus (Bendixson's Theorem), it is unique. The stability of this unique orbit is evident.

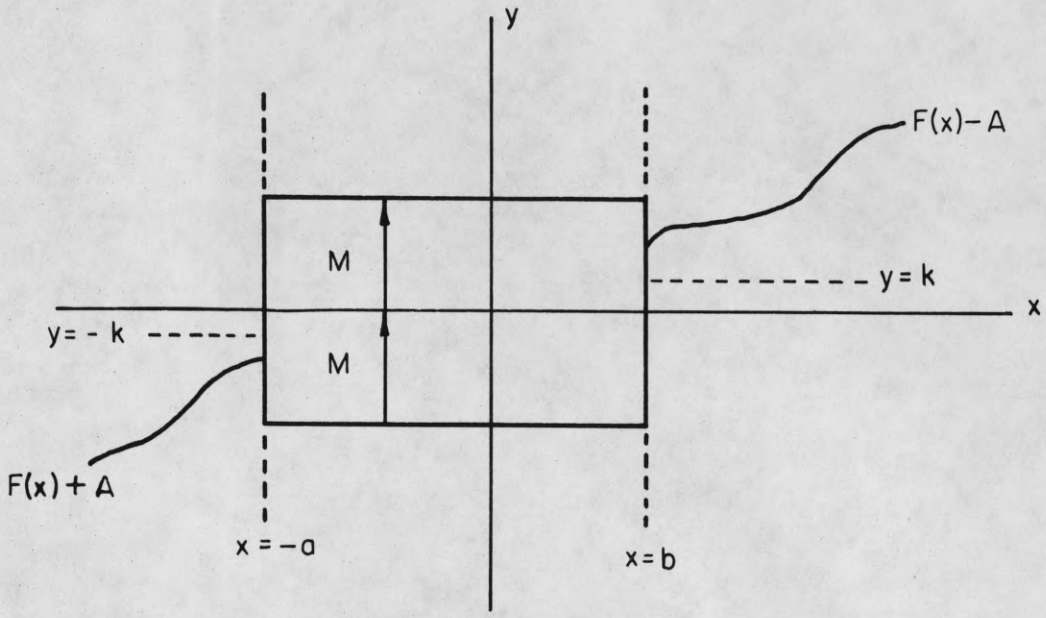

Figure 39

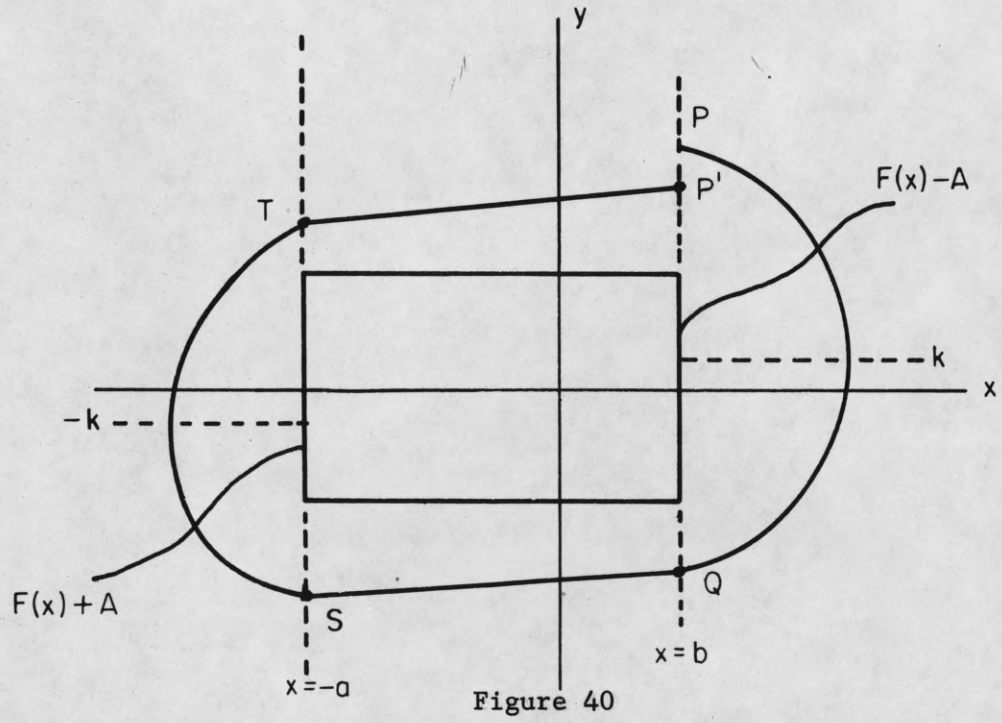

Figure 40

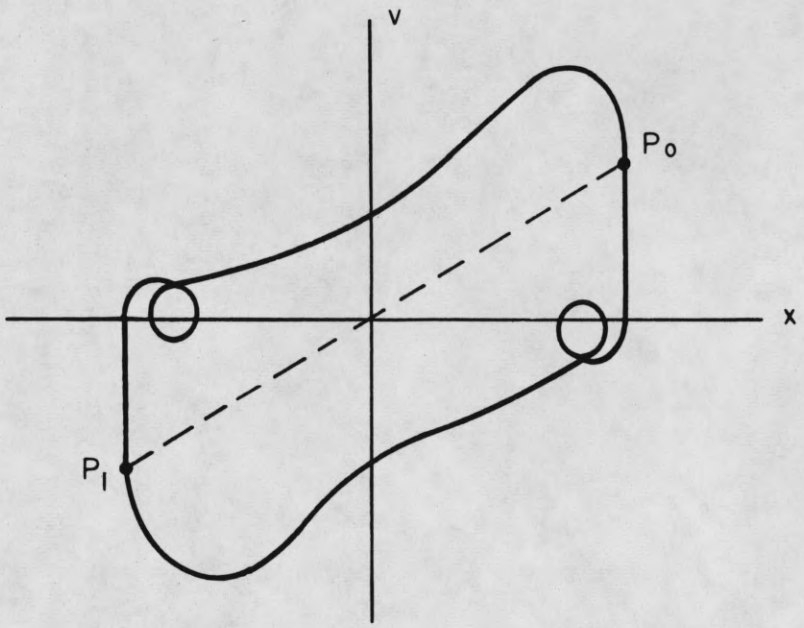

Figure 41

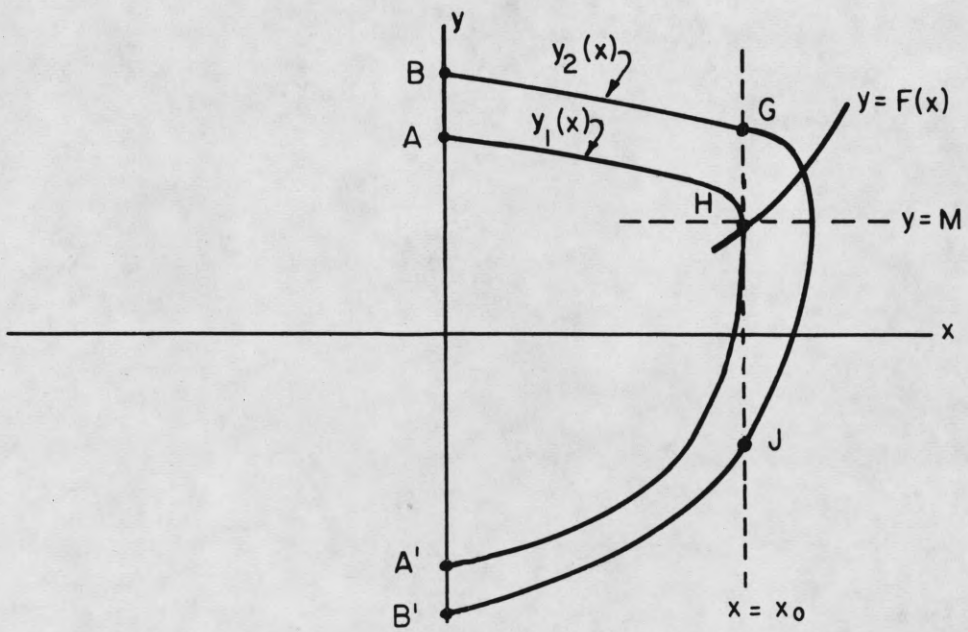

Figure 42

BIBLIOGRAPHY

1. Andronov, A. and Chaikin, C.E., Theory of Oscillations, Princeton Univ. Press, 1949.

2. Bogoliubov, N. and Krylov, N.M., "Introduction to Nonlinear Mechanics" (free translation by S. Lefschetz), Ann. of Math Studies 11, 1947.

3. Bogoliubov, N. and Mitropolsky, Yu. A., Asymptotic Methods in the Theory of Nonlinear Oscillations, Moscow, 1955. (2nd Ed.), 1958. Eng. transl.: Hindustan Publ. Corp, Delhi, 1961 (Gordon & Breach Sci. Publ., New York).

4. Cartwright, M.L., "Forced Oscillations in Nonlinear Systems," Contrib. to the theory of nonlinear oscillations, Ann. of Math. Studies 20, 1950.

5. Cartwright, M. L. and Littlewood, J. E., "The Equation $\ddot{y} - k(1 - y^2)\dot{y} + y = b\lambda k \cos(\lambda t + \alpha)$, k large," J. London Math. Soc. 20, 1945.

6. Cesari, L., "Asymptotic Behavior and Stability Problems in Ordinary Diff. Eqns.," Ergebnisse der Mathematik und Ihrer Grenzgebiete Series, vol. 16, publ. by Academic Press Inc., 1963 (2nd Ed.).

7. Dorodnytsin, A. A., "Asymptotic Solution of van der Pol's Eqn.," Prikl. Mat. Mech. sssr, 11, 1947. Am. Math. Soc. Transl. no. 88.

8. Langenhop, C. E. and Farnell, A. B., "The Existence of Forced Periodic Solns. of a Second Order Diff. Eqn. near Certain Eqm. Points of the Unforced Eqn.," Contrib. to the theory of nonlinear Osc., Ann. of Math. Studies 20.

9. LaSalle, J., "Relaxation Oscillations," Quart. of Appl. Math. 7, 1949.

10. Levinson, N., "A Second Order Diff. Eqn. with Singular Solns.," Ann. of Math. 50, 1949.

11. Minorsky, N., Introduction to Nonlinear Mechanics, Edwards, 1947.

12. Nemyckii, V. V. and Stepanov, V. V., Qualitative Theory of Diff. Eqns., GITL, Moscow (2nd Ed.), 1949.

13. Poincaré, H., Les Méthodes Nouvelles de la Méchanique Celeste, Paris, 3 vols., 1892, 1893, 1899.

14. van der Pol, B., "Forced Oscillations in a Circuit with Nonlinear Resistance," Phil. Magazine 3, 1927.

15. Stoker, J. J., "Nonlinear Vibrations in Mech. and Electr. Eng.," Interscience, 1950.

16. Wax, N., "On Amplitude Bounds for Certain Relaxation Oscillations," J. Appl. Phys., 22, 1951.

VITA

Peter J. Ponzo was born in Toronto, Canada, on November 6, 1934. He received the B.A.Sc. degree in Engineering Physics from the University of Toronto in 1957. In 1958 he was a lecturer in mathematics at the University of Waterloo, Ontario. He received the M.A. degree in applied mathematics from the University of Toronto in 1959 and returned to the Mathematics Department at the University of Waterloo until September, 1960, when he enrolled in the Graduate College of the University of Illinois.

DISTRIBUTION LIST AS OF JANUARY 29, 1964

1 Director
Air University Library
Maxwell Air Force Base, Alabama
Attn: CR-4803a

1 Redstone Scientific Information Center
U.S. Army Missile Command
Redstone Arsenal, Alabama

1 Electronics Research Laboratory
University of California
Berkeley 4, California

2 Hughes Aircraft Company
Florence and Teale
Culver City, California
Attn: N. E. Devereux
Technical Document Center

3 Autonetics
9150 East Imperial Highway
Downey, California
Attn: Tech. Library, 3041-11

1 Dr. Arnold T. Nordsieck
General Motors Corporation
Defense Research Laboratories
6767 Hollister Avenue
Goleta, California

1 University of California
Lawrence Radiation Laboratory
P. O. Box 808
Livermore, California

1 Mr. Thomas L. Hartwick
Aerospace Corporation
P. O. Box 95085
Los Angeles 45, California

1 Lt. Colonel Willard Levin
Aerospace Corporation
P. O. Box 95085
Los Angeles 45, California

1 Professor Zorab Kaprelian
University of Southern California
University Park
Los Angeles 7, California

1 Sylvania Electronic Systems - West
Electronic Defense Laboratories
P. O. Box 205
Mountain View, California
Attn: Documents Center

1 Varian Associates
611 Hansen Way
Palo Alto, California
Attn: Dr. Ira Weissman

1 Huston Denslow
Library Supervisor
Jet Propulsion Laboratory
California Institute of Technology
Pasadena, California

1 Professor Nicholas George
California Institute of Technology
Electrical Engineering Department
Pasadena, California

1 Space Technology Labs., Inc.
One Space Park
Redondo Beach, California
Attn: Acquisitions Group
STL Technical Library

2 Commanding Officer and Director
U.S. Naval Electronics Laboratory
San Diego 52, California
Attn: Code 2800, C. S. Manning

1 Commanding Officer and Director
U.S. Navy Electronics Laboratory
San Diego 52, California
Attn: Library

1 Office of Naval Research Branch Office
1000 Geary Street
San Francisco, California

1 The RAND Corporation
1700 Main Street
Santa Monica, California
Attn: Library

1 Stanford Electronics Laboratories
Stanford University
Stanford, California
Attn: SEL Documents Librarian

1 Dr. L. F. Carter
Chief Scientist Air Force
Room 4E-324, Pentagon
Washington 25, D. C.

1 Mr. Robert L. Feik
Associate Director for Research
Research and Technology Division
AFSC
Bolling Air Force Base 25, D. C.

1 Captain Paul Johnson (USN-Ret)
National Aeronautics and Space
Administration
1520 H Street, N. W.
Washington 25, D. C.

1 Major Edwin M. Myers
Headquarters USAF (AFRDR)
Washington 25, D. C.

1 Dr. James Ward
Office of Deputy Director
(Research and Info)
Department of Defense
Washington 25, D. C.

1 Dr. Alan T. Waterman
Director, National Science Foundation
Washington 25, D. C.

1 Mr. G. D. Watson
Defense Research Member
Canadian Joint Staff
2450 Massachusetts Ave., N. W.
Washington 8, D. C.

1 Mr. Arthur G. Wimer
Chief Scientist
Air Force Systems Command
Andrews Air Force Base
Washington 25, D. C.

1 Director, Advanced Research
Projects Agency
Washington 25, D. C.

1 Air Force Office of Scientific Branch
Directorate of Engineering Sciences
Washington 25, D. C.
Attn: Electronics Division

1 Director of Science and Technology
Headquarters, USAF
Washington 25, D. C.
Attn: AFRST-EL/GU

1 AFRST - SC
Headquarters, USAF
Washington 25, D. C.

1 Headquarters, R & T Division
Bolling Air Force Base
Washington 25, D. C.
Attn: RTHR

1 Headquarters, U. S. Army Material Cor
Research Division, R & D Directorate
Washington 25, D. C.
Attn: Physics & Electronics Branch
Electronics Section

1 Commanding Officer
Diamond Ordnance Fuze Laboratories
Washington 25, D. C.
Attn: Librarian, Room 211, Bldg. 92

1 Operation Evaluation Group
Chief of Naval Operations (OP-03EG)
Department of Navy
Washington, D. C. 20350

1 Chief of Naval Operations (Code OP-ONT)
Department of the Navy
Washington, D. C. 20350

1 Commanding Officer
U. S. Army Personnel Research Office
Washington 25, D. C.

1 Commanding Officer & Director
Code 142 Library
David W. Taylor Model Basin
Washington, D. C. 20007

1 Chief, Bureau of Ships (Code 686)
Department of the Navy
Washington, D. C. 20360

1 Chief, Bureau of Ships (Code 732)
Department of the Navy
Washington, D. C. 20360

1 Chief, Bureau of Naval Weapons
Technical Library, DLI-3
Department of the Navy
Washington, D. C. 20360

1 Director, (Code 5140)
U. S. Naval Research Laboratory
Washington, D. C. 20390

1 Chief of Naval Research (Code 437)
Department of the Navy
Washington, D. C. 20360

1 Dr. H. Wallace Sinaiko
Institute for Defense Analyses
Research & Engineering Support Division
1666 Connecticut Ave., N. W.
Washington 9, D. C.

1 Data Processing Systems Division
National Bureau of Standards
Conn. at Van Ness
Room 239, Bldg. 10
Washington 25, D. C.
Attn: A. K. Smilow

1 National Bureau of Standards
Research Information Center &
Advisory Service on Information
Processing
Data Processing Systems Division
Washington 25, D. C.

1 Exchange and Gift Division
The Library of Congress
Washington 25, D. C.

1 NASA Headquarters
Office of Applications
400 Maryland Avenue, S. W.
Washington 25, D. C.
Attn: Mr. A. M. Greg Andrus
Code FC

1 APGC (PGAPI)
Eglin Air Force Base
Florida

1 Martin Company
P. O. Box 5837
Orlando, Florida
Attn: Engineering Library
MP-30

1 Commanding Officer
Office of Naval Research, Chicago Branch
6th Floor, 230 North Michigan
Chicago 1, Illinois

1 Laboratories for Applied Sciences
University of Chicago
6220 South Drexel
Chicago 37, Illinois

1 Librarian
School of Electrical Engineering
Purdue University
Lafayette, Indiana

1 Donald L. Epley
Department of Electrical Engineering
State University of Iowa
Iowa City, Iowa

1 Commanding Officer
U. S. Army Medical Research Laboratory
Fort Knox, Kentucky

2 Keats A. Pullen, Jr.
Ballistic Research Laboratories
Aberdeen Proving Ground, Maryland

1 Director
U. S. Army Human Engineering Laboratories
Aberdeen Proving Ground, Maryland

1 Mr. James Tippett
National Security Agency
Fort Meade, Maryland

1 Commander
Air Force Cambridge Research Laboratories
Laurence G. Hanscom Field
Bedford, Massachusetts

1 Dr. Lloyd Hollingsworth
Director, ERD
AFCRL
L. G. Hanscom Field
Bedford, Massachusetts

1 Data Sciences Laboratory
Air Force Cambridge Research Lab
Office of Aerospace Research, USAF
L. G. Hanscom Field
Bedford, Massachusetts
Attn: Lt. Stephen J. Kahne - CRB

1 Instrumentation Laboratory
Massachusetts Institute of Technology
68 Albany Street
Cambridge 39, Massachusetts

1 Research Laboratory of Electronics
Massachusetts Institute of Technology
Cambridge 39, Massachusetts
Attn: Document Room 26-327

1 Dr. Robert Kingston
Lincoln Laboratories
Lexington, Massachusetts

1 Lincoln Laboratory
Massachusetts Institute of Technology
P. O. Box 73
Lexington 73, Massachusetts
Attn: Library, A-082

1 Sylvania Electric Products, Inc.
Electronic Systems
Waltham Labs. Library
100 First Avenue
Waltham 54, Massachusetts

1 Minneapolis-Honeywell Regulator Co.
Aeronautical Division
2600 Ridgeway Road
Minneapolis 13, Minnesota
Attn: Dr. D. F. Elwell
Main Station: 625

1 Inspector of Naval Material
Bureau of Ships Technical Representative
1902 West Minnehaha Avenue
St. Paul 4, Minnesota

20 Activity Supply Officer, USAELRDL
Building 2504, Charles Wood Area
Fort Monmouth, New Jersey
For: Accountable Property Officer
Marked: For Inst. for Exploratory Research
Inspect at Destination
Order No. 576-PM-63-91

1 Commanding General
U. S. Army Electronic Command
Fort Monmouth, New Jersey
Attn: AMSEL-RE

1 Mr. A. A. Lundstrom
Bell Telephone Laboratories
Room 2E-127
Whippany Road
Whippany, New Jersey

1 AFMDC (MDSGP/Capt. Wright)
Holloman Air Force Base
New Mexico

1 Commanding General
White Sands Missile Range
New Mexico

1 Microwave Research Institute
Polytechnic Institute of Brooklyn
55 John Street
Brooklyn 1, New York

1 Cornell Aeronautical Laboratory, Inc.
4455 Genesee Street
Buffalo 21, New York
Attn: J. P. Desmond, Librarian

1 Sperry Gyroscope Company
Marine Division Library
155 Glen Cove Road
Carle Place, L. I., New York
Attn: Mrs. Barbara Judd

1 Major William Harris
RADC (RAWI)
Griffiss Air Force Base
New York

1 Rome Air Development Center
Griffiss Air Force Base
New York
Attn: Documents Library
RAALD

1 Library
Light Military Electronics Department
General Electric Company
Armament & Control Products Section
Johnson City, New York

1 Columbia Radiation Laboratory
Columbia University
538 West 120th Street
New York 57, New York

1 Mr. Alan Barnum
Rome Air Development Center
Griffiss Air Force Base
Rome, New York

1 Dr. E. Howard Holt
Director
Plasma Research Laboratory
Rensselaer Polytechnic Institute
Troy, New York

3 Commanding Officer
U.S. Army Research Office (Durham)
Box CM, Duke Station
Durham, North Carolina
Attn: CRD-AA-IP, Mr. Ulsh

1 Battelle-DEFENDER
Battelle Memorial Institute
505 King Avenue
Columbus 1, Ohio

1 Aeronautical Systems Division
Navigation and Guidance Laboratory
Wright-Patterson Air Force Base
Ohio

1 Aeronautical Systems Division
Directorate of Systems Dynamic Analysis
Wright-Patterson Air Force Base
Ohio

1 Commander
Research & Technology Div.
Wright-Patterson Air Force Base
Ohio 45433
Attn: MAYT (Mr. Evans)

1 Commanding Officer (AD-5)
U.S. Naval Air Development Center
Johnsville, Pennsylvania
Attn: NADC Library

2 Commanding Officer
Frankford Arsenal
Philadelphia 37, Pennsylvania
Attn: SMUFA-1300

1 H. E. Cochran
Oak Ridge National Laboratory
P. O. Box X
Oak Ridge, Tennessee

1 U.S. Atomic Energy Commission
Office of Technical Information Extension
P. O. Box 62
Oak Ridge, Tennessee

1 President
U.S. Army Air Defense Board
Fort Bliss, Texas

1 U.S. Air Force Security Service
San Antonio, Texas
Attn: ODC-R

1 Director
Human Resources Research Office
The George Washington University
300 North Washington Street
Alexandria, Virginia

20 Defense Documentation Center
Cameron Station
Alexandria, Virginia
22314

1 Commander
U. S. Army Research Office
Highland Building
3045 Columbia Pike
Arlington 4, Virginia

1 U.S. Naval Weapons Laboratory
Computation and Analysis Laboratory
Dahlgren, Virginia
Attn: Mr. Ralph A. Niemann

2 Army Material Command
Research Division
R & D Directorate
Bldg. T-7
Gravelley Point, Virginia

1 Mr. Jose L. de Segovia
"Instituto L. Torres Quevedo"
Serrano 114
Madrid 6, Spain